Sound Transmission Loss of Composite Sandwich Panels

A thesis submitted in partial fulfilment of the requirements for the Degree of Master of Engineering at the University of Canterbury

Department of Mechanical Engineering

Christchurch, New Zealand

By

Andre Cowan

University of Canterbury

New Zealand

2013

Table of Contents

Table of Figures

List of Tables

Abstract

This thesis examines the sound transmission loss (STL) through composite sandwich panel systems commonly used in the marine industry. Experimental, predictive and optimisation methods are used to evaluate the acoustic performance of these systems and to improve their acoustic performance with noise treatment.

The complex nature of the material properties of composite sandwich panels was found to be dependent not only on the physical properties but also the frequency of incident noise. Young's modulus was found to reduce with increasing frequency as has been predicted in the literature which is due to the shear stiffness dominating over the bending stiffness. Two methods for measuring these properties were investigated; 'fixed-free' and 'free-free' beam boundary condition modal analyses. The disagreement between these methods was identified as the clamping fixed nature that increased flexibility of the beam.

Composite sandwich panels can be modelled as homogeneous isotopic materials when predicting their acoustic performance provided the dilatational resonance is above the frequency range of interest. Two such panels were modelled using this simple sound insulation prediction method, but the agreement between theory and experimental results was poor. A variable Young's modulus was included in the model but agreement remained relatively poor especially in the coincidence frequency region due to variation of Young's modulus with frequency.

A statistical method of optimisation of the parameter settings by fractional factorial design proved successful at identifying the important parameters that affect the sound transmission class (STC) of a noise treatment material applied to a panel. The decouple foam layer and attachment method were the most significant factors. The same method, with higher resolution was then used to identify the important parameters that affected the noise reduction class (NRC) finding that the outer foam thickness without a face sheet were the most significant factors. The independent optimisation studies performed for each of the STC and NRC produced conflicting results meaning that both could not be achieved simultaneously.

Acknowledgements

This Master's thesis was performed through the University of Canterbury Acoustics Research Group. I would like to acknowledge:

- Supervisor Dr John Pearse for his guidance, expertise and encouragement throughout the course of this project
- Industry partner Pyrotek Noise Control and Mike Latimer for their interest, support and direction
- Professor John Davy from RMIT for providing guidance, knowledge and enthusiasm throughout this project
- The support from the Ministry of Science and Innovation who funded this research through their Technology for Industry Fellowship (TIF) program
- My Great Grandma and Granddad, Vera and Leslie Cowan for funding all of my university fees throughout my six years of tertiary education. Education was very important to them despite having only received an education to the ages of thirteen years old. They will be missed

Chapter 1

1 Introduction and Literature Review

Summary

The background and objectives of the project are presented. An introduction to the theory of sound, transmission loss and noise control are described. A literature review identified current and previous work in tuned panels, optimisation studies and acoustics in the marine industry.

1.1 Introduction

Composite sandwich panels are increasingly used in the automobile, marine and aircraft industies (see Figure 1.1) because of their high strength to weight ratio. However these materials are also often required to perform well acoustically.

Figure 1.1 Applications for composite sandwich constructions

1.1.1 Project scope

The scope of this thesis is the sound transmission loss (STL) of composite panel systems as typically used by the marine industry. Experimental and theoretical methods are used to evaluate the acoustic performance of typical panels (see Figure 1.2) and strategies for increasing their STL. The construction of these panels is described in chapter 2.

Figure 1.2 Composite sandwich panels

Homogeneous, isotropic single leaf STL prediction models by Davy [1] were evaluated and modified to accurately predict the acoustic performance of composite sandwich panels. Prediction modelling can be an effective means of determining how these constructions perform acoustically. Modal analysis methods were used to determine Young's modulus and loss factors of these materials and then these properties were entered into acoustic modelling software to verify various models and develop them.

To meet acoustic regulations and comfort levels composite constructions are often required to be treated with acoustic products. Sorberbarrier® is a noise control product produced by the Pyrotek Noise Control and used for increasing airborne STL. This product has no structural properties and is a limp material. Sorberbarrier® is a treatment that can be applied to wall constructions that have poor acoustic performance or require increased performance. In addition to favourable noise control properties, noise control products must also be flame resistant to meet the requirements in the industry.

Identification of the key parameters that affect the STL of Sorberbarrier® was achieved using Design of Experiments (DOE) fractional factorial design. DOE is a statistical optimisation technique used in a wide range of applications. Optimal parameter settings that produce the highest Sound Transmission Class (STC) were determined and the effectiveness of fractional factorial design as an acoustic optimisation technique was evaluated. An in depth study of composite sandwich constructions was conducted to produce an improved STL and sound absorption system with the addition of acoustic treatment material. The effect of covering open pores of foam with a thin aluminium foil and a thicker mass loaded barrier on STL and sound absorption was investigated.

1.1.2 Deliverables

The primary aim was to deliver a comprehensive analysis of the acoustic performance of composite sandwich panels together with treatments to improve the STL. This was broken down as follows-

1. Experimentally determine the material properties of composite sandwich panels
2. Predict the STL of composite sandwich panels and compare to experimental measurements
3. Identify Sorberbarrier®'s significant performance parameters and optimal settings for best STL

4. Identify Sorberbarrier®'s significant parameters and optimal settings for sound absorption
5. Develop composite panel systems with increased STL for marine industry application

1.1.3 Sound pressure levels, decibels, octave bands and intensity

Table 1.1 Sound pressure level chart

Example	Sound Pressure (Pa)	Sound Pressure Level (dB)
Jet take off (25m distance)	200	140
Rock concert	20	120
Pneumatic chipper	2	100
Average street traffic	0.2	80
Conversational speech	0.02	60
Living room	0.002	40
Bedroom	0.0002	20
Threshold of hearing	0.00002	0

Sound is measured in decibels (dB) which is a logarithmic unit that indicates a ratio, typically pressure or intensity relative to a reference level. The relationships between sound pressure, sound pressure level and sounds from everyday examples help show the nature of the logarithmic scale (see Table 1.1). The logarithmic dB scale was adopted to show the magnitude of sound strength. This was thought to be appropriate because it was considered that our hearing obeyed the Weber Fechner law as shown in equation 1.2. This was later found to be incorrect due to its inability to provide values for objective sound strength that correlated with subjective sound loudness.

$$Sensation \propto Log(stimulus\ magnitude) \quad (1.1)$$

Human hearing is very complex and Steven's power law was subsequently developed to better match our wideband hearing than the Weber Fechner's law. Steven's power law (see equation 1.3) is used for expressing the objective sound stimulus magnitude. Generally the value of N is set to 0.6.

$$Sensation \propto (Stimulus\ magnitude)^N \quad (1.2)$$

The reference level most commonly used to define 0 dB is the human threshold of hearing (20µPa or 10^{-12}W/m²). The human ear has a wide range of hearing from 20µPa (p_{ref}) to the

threshold of pain at ~200Pa Sound pressure and Sound Pressure Level (SPL) are related by equation 1.3. p_{rms} is the root, mean square of the pressure used to calculate SPL.

$$SPL = 20 \log \left(\frac{p_{rms}}{p_{ref}} \right) \tag{1.3}$$

Sound intensity is the power per unit area transmitted by the sound wave (see equation 1.4)

$$Power\ per\ unit\ area = pressure\ \times velocity \tag{1.4}$$

An octave band is a frequency range where each subsequent band represents is a doubling of frequency. When higher frequency resolution is required, one third octave bands may be used.

1.2 Literature Review

A comprehensive survey of conference and journal papers, national and international standards was conducted to provide direction and background to this research. This section summarises previous research and acoustic theory as background to this thesis.

1.2.1 Sound transmission loss in single panels

This section describes the theory of sound transmission loss (STL) through a single panel. The theory of STL has been separated into sections depending on frequency (see Figure 1.3). STL is defined as a means to divert or dissipate acoustic energy. STL occurs when there is an impedance mismatch and sound is reflected or absorbed where the greater the sound reflected, the higher the STL.

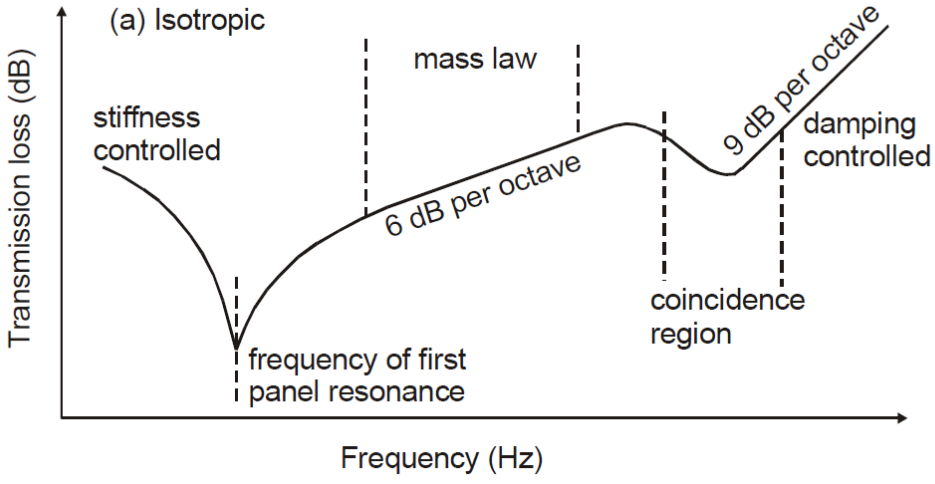

Figure 1.3 Typical single panel sound transmission loss curve [2]

1.2.2 Stiffness controlled region

At frequencies below the first panel resonance, the STL is controlled by the bending stiffness of the panel. For a panel to transmit sound energy, the panel must vibrate. A high bending stiffness leads to high STL in this region as more energy is required to vibrate the panel [3].

1.2.3 Panel resonance

The panel resonance region is characterised by a number of dips in the STL curve which coincide with the first natural frequencies of the panel. At these frequencies (see equation 1.5) incident acoustic waves excite structural modes which lead to a significant vibration and therefore to an increase in transmitted sound power or reduced STL respectively. The resonant frequency depends on the size and geometry of the panel. The size of the panel is often fixed for structural reasons, but it is important to know the values of the resonant frequency.

$$f_{i,n} = \frac{\pi}{2}\sqrt{\frac{D}{m}}\left[\frac{i^2}{a^2}+\frac{n^2}{b^2}\right] \quad i,n = 1,2,3 \ldots \tag{1.5}$$

where D is bending stiffness, m is the mass per unit area, a and b are the panel dimensions and i,n are integers.

1.2.4 Mass Law

The mass law states that for any given frequency the STL of a panel increases with increasing mass per unit area at a rate of 6dB per octave. The mass law is effective over the entire frequency range but is the dominant factor in the mass law region. For a thin panel, neglecting stiffness and damping, the STL in this region is governed by equation 1.6.

$$STL = 10\,log\left[\frac{\omega^2 m^2}{4(\rho c)^2/cos^2\,\theta}\right] \tag{1.6}$$

where θ is the angle of incidence, ρ is the density of air, c is the speed of sound, m is the mass surface area and ω is the angular frequency.

1.2.5 Coincidence region

The coincidence region is often the most important range when constructing panel systems. See Figure 1.3 where there is a prominent dip in the STL curve. This dip often occurs in the frequency range where noise is an issue that can be modified by changing the mass or bending stiffness. The phenomenon of coincidence is well documented by Cremer [4] and Bies and Hansen [2].

When the wavelength of sound in air is shorter than the wavelength of transverse waves propagating along a plate, the plate becomes an efficient sound radiator (see Figure 1.4). This phenomenon is called coincidence because the trace wavelength of the radiated sound is equal to the transverse wavelength of the plate. At coincidence sound travels through the plate more easily for a particular angle of incidence and transmission. The critical frequency is the lowest frequency at which coincidence occurs. This happens when the longitudinal wavelength in air is equal to the bending wavelength in a finite plate ($\lambda_B = \lambda$). It is well known that the sound transmission through panels is primarily by bending waves [3]. These waves are dependent on both the material and geometric properties.

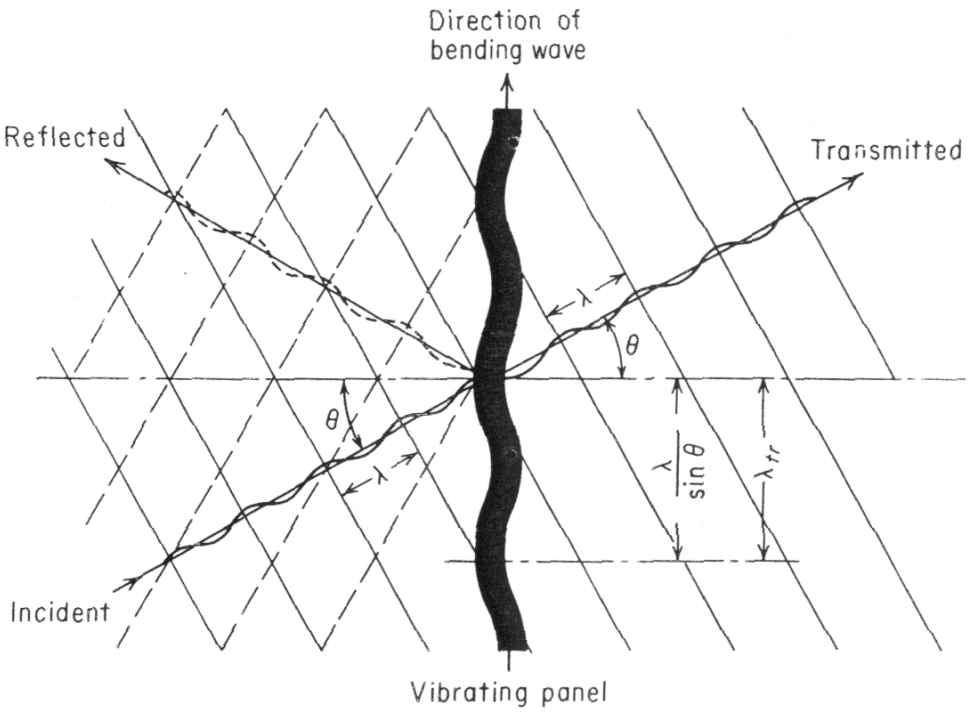

Figure 1.4 Single panel sound propagation model [5]

The governing equations of bending waves in isotropic panels are provided below.

The bending wave equation is

$$B\left(\frac{\partial^4\eta(x,y,t)}{\partial x^4}+2\frac{\partial^4\eta(x,y,t)}{\partial x^2\partial y^2}+\frac{\partial^4\eta(x,y,t)}{\partial y^4}\right)=-m\frac{\partial^2\eta(x,y,t)}{\partial t^2} \quad (1.7)$$

The panels bending stiffness is

$$B=\frac{Eh^3}{12(1-v^2)} \quad (1.8)$$

The bending wavelength is

$$\lambda_B(\omega) = 2\pi \left(\frac{B}{\omega^2 \rho h}\right)^2 \tag{1.9}$$

The speed of the bending waves is

$$C_B(\omega) = \left(\frac{B\omega^2}{\rho h}\right)^{1/4} \tag{1.10}$$

Sound propagates through all materials but is faster through materials with high stiffness and low density. The sound energy vibrates particles doing work on the material.

1.2.6 Damping controlled region

Frequencies above the coincidence region are dominated by damping. The STL increases by 9dB per octave.

1.2.7 Dilatational resonance

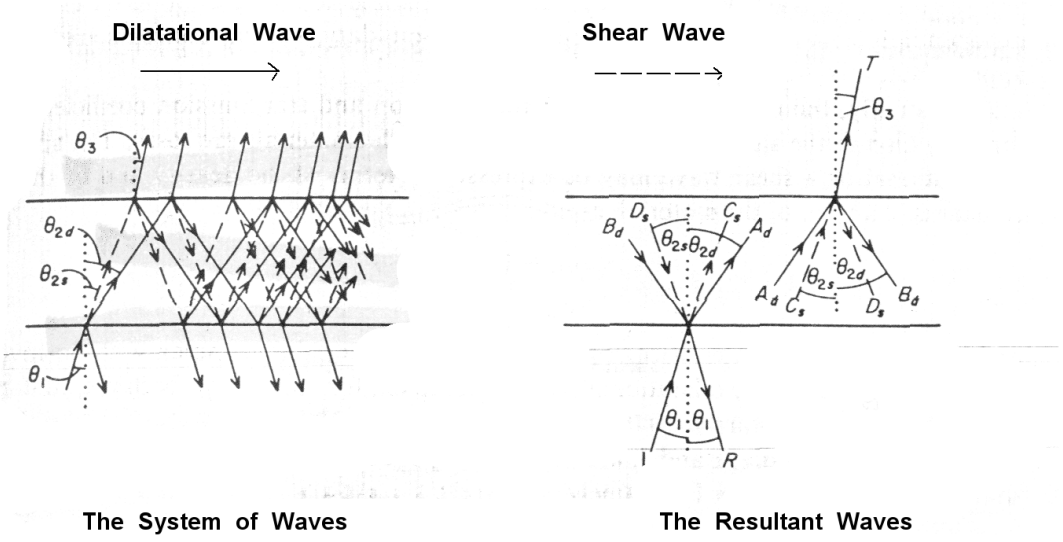

Figure 1.5 Wave propagation in a thick plate

Dilatational resonance was not shown in Figure 1.4 as it is specific to sandwich panels or thicker panels. This is relevant in this research. The dilatational resonance frequency relates to the thickness resonance of a sandwich plate or thick plate (see Figure 1.6). Ballagh [6] adapted simple prediction methods to sound transmission of lightweight foam cored panels. Most isotropic panels such as gypsum board contain a critical frequency dip. The dip that appears in

the STL curve for lightweight foam cored panels does not correspond to the thickness of the panel. This due is due to the dilatational resonance, or mass-spring-mass resonance where the outer skins are the masses and the core is the spring. Dilatational resonance frequency is given by equation 1.11.

$$f_0 = \frac{1}{2\pi}\sqrt{\frac{E(m_1 + m_2)}{Tm_1m_2}} \tag{1.11}$$

where E is the Young's modulus, m_1 and m_2 are the surface densities of the skins and T is the thickness of the core.

To move a dip outside an acoustic frequency range of interest of 100Hz – 5kHz typically requires a very large change in the parameters. The core thickness would need to increase by a factor of 100 or decrease by a factor of 20. A similar magnitude of change would be required for the skin [6]. However the sandwich panels considered in this thesis do have their dilatational resonance frequencies above the frequency range of interest.

1.2.8 STC ratings

The sound transmission class (STC) is a single number acoustic rating given to wall constructions where a higher number indicates better sound insulation. STC uses a curve fitting technique between 125Hz and 4000Hz. STL values are rounded to the nearest whole number where the sum of deviations should be less than or equal to 32dB. The measurement results may not be more than 8dB from the reference curve in any one third octave band.

1.2.9 Frequency and wavelength

Frequency is measured in hertz (Hz) and is the number of pressure fluctuations per second. The frequency(ies) of a sound produce a certain tone or combination of tones that make up distinct sounds [2]. For example a person whistling would typically contain one dominant frequency where speech would contain a combination of frequencies between 300Hz and 3kHz. Wavenumber is equal to 2π divided by the wavelength and is defined as the phase change in radians per unit distance. The wavelength of a sinusoidal wave is the spatial period between consecutive points of the same phase. Equation 1.12 describes the relationship between wavelength and frequency.

$$Wavelength\ (\lambda) = Speed\ of\ sound\ (c) / Frequency\ (f) \tag{1.12}$$

Sound waves are mechanical vibrations that travel as longitudinal wave forms and require a medium to transmit. Longitudinal waves transfer sound energy by oscillation of converting the potential energy of compression to kinetic energy. The speed of sound depends on the medium the waves pass through. The speed of sound is proportional to the square root of the ratio of the elastic modulus or stiffness to density of the medium. The speed of sound in air, at sea level, at room temperature is approximately 343m/s.

1.2.10 Wave equation

The derivation of the wave equation brings together the fundamental components of acoustics. It is important to understand each of these components before further experimental and prediction modelling. There are three fundamental premises to the wave equation; Euler's equation (equation of motion), conservation of mass and the equation of state. The wave equation is a second order linear partial differential equation which can be used to describe all types of waves including; sound waves, light waves and water waves. This thesis is concerned with the application of the wave equation 1.13 to sound waves [2].

$$\nabla^2 \varphi = (1/c^2)\, \partial\varphi^2/\partial t^2 \tag{1.13}$$

where ∇ is the Laplacian operator, φ is the acoustic potential function, c is the speed of sound and t is time.

Euler's equation is the equation of motion for a fluid derived from Newton's first law of motion, if an object experiences no net force the object will either remain at rest or at a constant velocity. Euler's equation states that the mass of particle fluid multiplied by its acceleration is equal to the sum of external forces acting on it (i.e. $F = ma$).

Conservation of mass states that the rate of mass entering or leaving the volume must equal the rate of change of mass in the volume.

$$\int_A \rho_{tot}\, U_{tot}\, n\ dA = -\frac{d}{dt}\int_V \rho_{tot}\, dV \tag{1.14}$$

where A is the area of the surface enclosing the volume, V and n is the unit vector normal to the surface A, at location dA. The equation of state is defined for very small perturbations to the ambient state of a fluid and is assumed to be adiabatic. The total pressure p_{tot} is related to the total density, ρ_{tot} as shown in equation 1.15.

$$p_{tot} = f(\rho_{tot}) \tag{1.15}$$

In the case of acoustics since pressure perturbations are small, and p and ρ are constant, $dp = dp_{tot}$, $d\sigma = d\rho$ and equation 1.17 below can be expanded by a Taylor series.

$$dp = \frac{\partial f}{\partial p} d\sigma + \frac{1}{2}\frac{\partial f}{\partial \rho}(d\sigma)^2 + (higher\ order\ terms) \tag{1-16}$$

1.2.11 Noise Control

Composite sandwich panels are used in a wide range of applications because of their low weight, high strength and thermal insulation properties. In these applications it is often necessary to provide additional sound attenuation due to the poor acoustic properties of these composite sandwich constructions. When designing a composite sandwich structure to maximise sound reduction important variables must be identified.

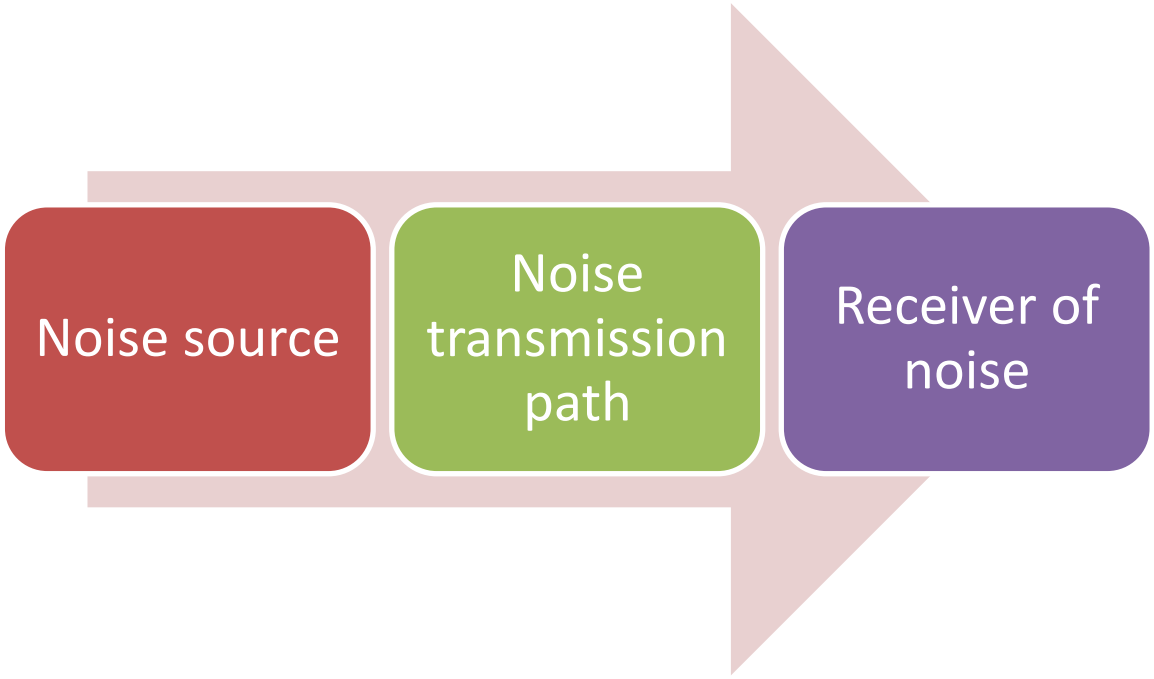

Figure 1.6 Noise control strategy "adopted from [2]"

When designing and implementing acoustic solutions it is important to understand the process that will provide the best outcome. Figure 1.7 shows the three main areas for intervention in which these should be investigated for a solution [2].

First the noise source must be identified and it must be determined if the noise is coming from the machinery attached to the structure or the structure itself. Isolating the source is always the

first step. The frequencies produced by the source must also be investigated as they may be found to represent rattling or tonal noise which can be subjectively annoying out of proportion to the sound pressure level (SPL). These can often be mitigated by a muffler or the balancing of machinery.

If sound attenuation of the source alone is insufficient to meet the noise regulations or desired comfort levels, it is important to identify whether the path of noise is airborne, structural or a combination of both. Vibrations from machinery can travel through a structure and propagate noise from vibrating panels that act as sound boards [2]. Incorporating damping into the system will reduce vibration levels through viscous energy dissipation. If airborne noise is the most significant path then an enclosure or wall system may be built around the source. When building enclosure or wall systems a number of considerations must be taken into account. When noise transmitted through air reaches a wall it is reflected, absorbed or transmitted through the wall. For attenuation of low frequencies (below 500Hz) a stiff, thick panel should be used. At frequencies above 1kHz less stiff material should be used and/or viscoelastic material should be added to the panel.

The resonant frequency depends on the size of the panel. The size of the panel can often not be changed but it is important to know what the resonant frequency is. This is shown by equation 1-9.

There are a range of methods recognised in literature for increasing the STL through panels. A very effective and simple way to do this is by increasing mass, although applications such as the aircraft and marine industries often have weight restrictions constrained by efficiency and running costs. Adding mass raises the STL curve in the mass law region extending from the resonance controlled region to the coincidence controlled region. Decreasing the bending stiffness of a panel shifts the coincidence effects to higher frequencies, there by extending the mass law region [7]. Increasing the internal damping reduces the effect of coincidence therefore increasing the STL. This is achieved by the addition of layers to the core that are highly viscous but unfortunately are often too expensive to be economic to implement [8].

Increasing or adding air space between two panels is known as a double wall construction and is a cost effective and lighter option than a single thick wall. For best results, the two panels must be isolated from one another to avoid structurally transmitted noise. Structurally transmitted noise is a mechanical bridge that noise can readily travel through. Structural born noise is often unavoidable but can be minimised by isolating the facing panels in the system.

The mass-air-mass resonance frequency f_0 shown in equation 1.18 is a problem with double wall constructions where the air acts as a spring between the two wall masses. To reduce noise peaks of the resonant frequency absorption material is applied in the cavity to provide damping [9].

$$f_0 = \frac{1}{2\pi}\left(\frac{1.8\rho c^2(m_1 + m_2)}{d m_1 m_2}\right)^{1/2} \tag{1.17}$$

where m_1 and m_2 are the surface densities of each panel and d is the gap width.

1.2.12 Optimisation studies

Lang and Dym [10] studied optimisation of composite sandwich panels by considering three variables- Young's modulus and the thickness of the skin and core. Using the search pattern method, a range of design variables were evaluated to improve the sound insulation. The results showed that increasing the total mass raised the STL in the mass law region. Decreasing the stiffness of the core material increased the coincidence frequency and an overall improvement in the sound insulation was obtained.

Wang [11] used genetic algorithms in aerospace applications where mass is considered the most important design constraint due to its impact on running costs for aircraft. Mass was therefore chosen as the objective function for this optimisation and both mechanical and acoustical properties were considered. For the mechanical properties, the sandwich beam was required to meet sufficient stiffness while undergoing a deflection test with simply supported boundary conditions. An acoustical STL performance constraint was then applied in the frequency range from 1kHz to 4kHz. The optimisation was applied using a prediction model based on Kurtze and Watters [12]. Eight face sheet materials and sixteen core materials were investigated. The optimisation displayed STL values above the mass law at frequencies between symmetric and antisymmetric coincidence frequencies. This was attributed to the cancellation of the symmetric and antisymmetric impedances.

Wennhage [13] studied the optimisation of large scale composite sandwich constructions in railway car bodies. The optimisation technique method of moving asymptotes (MMA) used to minimise weight while meeting structural requirements. This analysis was performed with and without acoustical constraints as it was found that a heavier design was required when considering acoustical STL performance. This technique was used for large scale structural-acoustic optimisation and is shown in Figure 1.8.

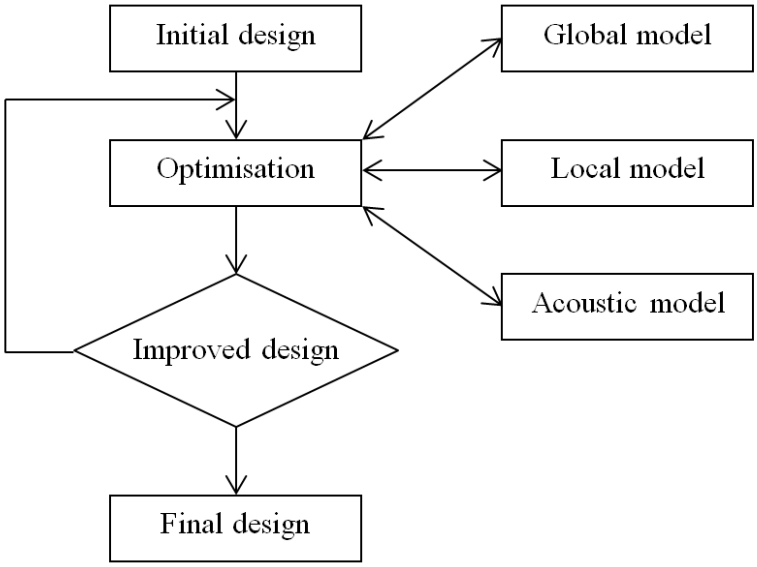

Figure 1.7 Optimisation process with global, local and acoustic models "adopted from [13]"

The face sheet of the sandwich material remained unchanged as a quasi-isotropic carbon fibre reinforced polymer laminate throughout the optimisation. One core material was used; Divinycell H-grade solid foam where density was a variable.

The finite element analysis contained two separate models; structural and acoustical. The global model was a structural analysis of an entire generic railway carriage and the local model was a structural analysis of various individual components. The acoustic model used the sound reduction index *R* as the constraint which was specified as the level considered acceptable in railway carriages. This study showed that a significant 23% increase in mass resulted from the inclusion of the acoustic constraints.

1.2.13 Acoustics in the marine industry

Acoustic treatment in the marine industry is categorised depending on the size of marine craft; small, medium or large. No acoustic treatment is currently applied to small marine craft due to a much greater emphasis being placed on the power to weight ratio (these marine craft often don't have a fly bridge or will have a large cockpit). Power to weight ratio is also important in medium sized composite marine craft where there is a reluctance to add acoustic material, but there is an opportunity for improving the acoustic performance of their composite sandwich panels. In large marine craft where people spend months aboard, composite sandwich panels are treated with acoustic material to increase the acoustic performance to a level comfortable for passengers [14].

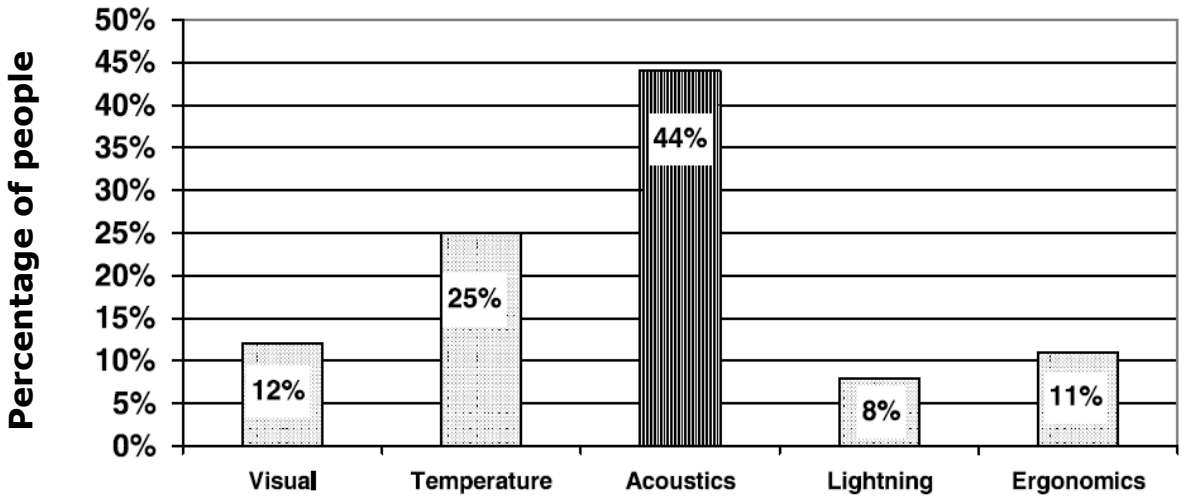

Figure 1.8 Survey on areas of comfort that need improvement on board large marine craft [15]

Goujard [15] investigated comfort on board large marine craft where the stay on board for passengers ranged from several hours to several weeks (see Figure 1.9). The study surveyed 100 people during two sea trials and it identified that acoustics was the area that required the greatest improvement. The marine craft was divided into sections where it was found that cabins were the most uncomfortable place acoustically and therefore required the most improvement. Sources of noise that provided the most discomfort fell into the three categories of engine noise, ventilation and whistles, and squeaking, clattering, clattering, cracking and creaking. Goujard investigated the natural phenomenon of sea noise and found it was not universally unpleasant to passengers with some people considering it should not be attenuated.

An interview with the chief engineer at Yachting Developments Limited (personal correspondence) highlighted the issues facing the acoustical design of one hundred foot marine craft they manufacture. Primary noise sources aboard these marine crafts were identified as engines, air conditioning, wave slap and winch systems. Primary noise paths were identified as ducts and sound transmission through composite wall constructions.

Air gaps can have a significant effect in acoustics. Surfaces inside marine craft contain protrusions and cavities from structural supports, electrical wiring and variations in building tolerances from behind the finishing panel [14]. This introduces issues with cavity resonances and undesired structural connections between rooms.

Important factors for boat builders are cost, space and weight and these factors must be considered when designing and applying acoustic treatments. Bootten [14] identified space as

the most important factor, closely followed by cost and then weight. Space inside large marine craft is at a premium, especially in catamarans where two narrow hulls must contain engines, all living quarters, ventilation ducts, cooking and washing facilities etc.

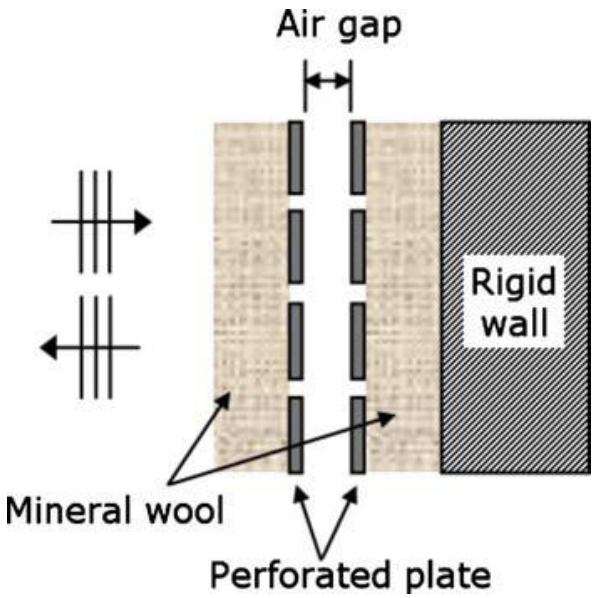

Figure 1.9 Double leaf sandwich construction [16]

Sound attenuation through double leaf sandwich panels was examined in large marine craft, cabin to cabin and cabin to corridor by Kim and Hong [16]. The effect of perforated plates and the air gap between panels were measured experimentally. The material used in the double leaf panel comprised 0.6mm steel plate either side of a 25mm thick 140kg/m³ density mineral wool with 2mm diameter holes and porosity of 6.08% (see Figure 1.10). Air gaps of 10, 15, 25 and 50mm spaces were measured and it was found that a gap of 15mm produced the best results through the mid-range frequencies. The 15mm air gap double leaf panel was then filled with four different absorbing materials and compared. It was found that having an absorption material increased the STL and the best material was found to be a perforated plate (thickness 10mm, hole diameter of 2mm, porosity 6.08%, weight 31.33kg/m²).

Naify [17] investigated lightweight noise treatments to already lightweight composite sandwich panels by the use of Helium and Argon filled bladders. This improved the acoustic performance by as much a 17dB at frequencies above 1kHz due to the change in density and the associated change in impedance.

Sargianis [18] investigated the STL performance of carbon-fibre sandwich composite structures. The core thicknesses were varied to obtain the best STL performance. It was found that the thickest core did not necessarily produce the highest STL curve over the frequency range 100Hz

to 5kHz and reducing the core thickness from 10.7mm to 8.4mm resulted in a significant improvement in STL performance. There was a non-linear relationship between core thickness and coincidence frequency. By coupling core thickness and specific shear modulus, further improvement can be achieved in STL performance.

1.2.14 Tuned panel resonators

Noise control of low revving diesel engines, high frequency whistles and rattles of various sections of marine craft is important. To attenuate these specific frequencies a tuned construction should be implemented.

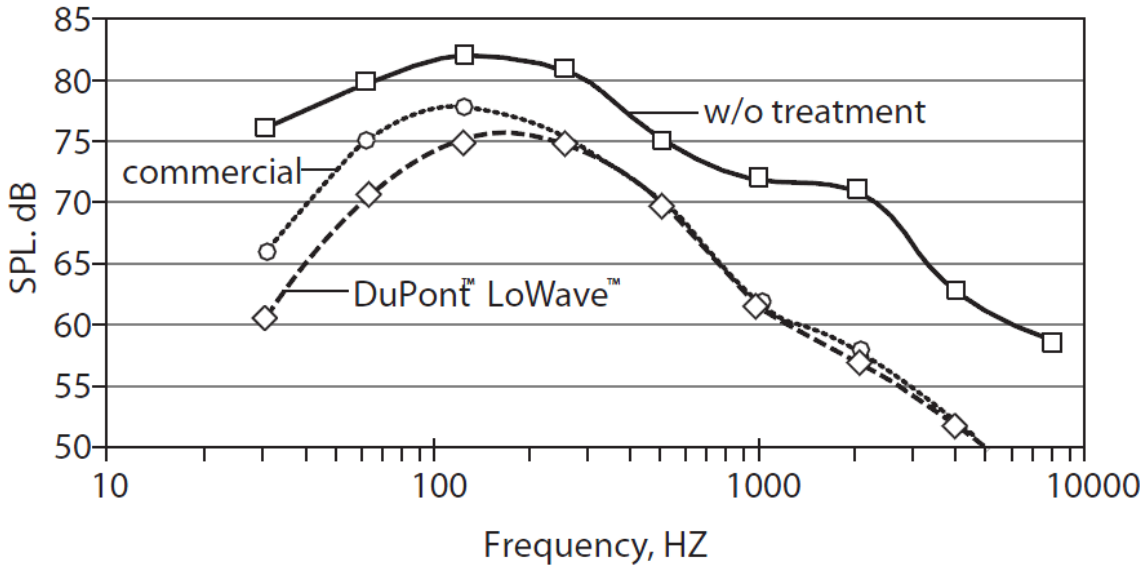

Figure 1.10 Test results comparing SPL from a structure with and without acoustic treatment [19]

Fuller and Cambou [19] [20] investigated both available tuned panels and those they developed themselves. They found that a distributed vibration absorber (DVA) was more effective at reducing a plate's vibration than a single tuned vibration damper. DVA's attenuate low frequency (<200Hz) structural noise. The combination of the mass and stiffness of the poroelastic material created a matrix of vibration absorbers with natural frequencies tuned to the low frequency region. System simulation is better by a freely suspended plate than a single degree of freedom system. Figure 1.11 shows a 10dB improvement at frequencies less than 200Hz.

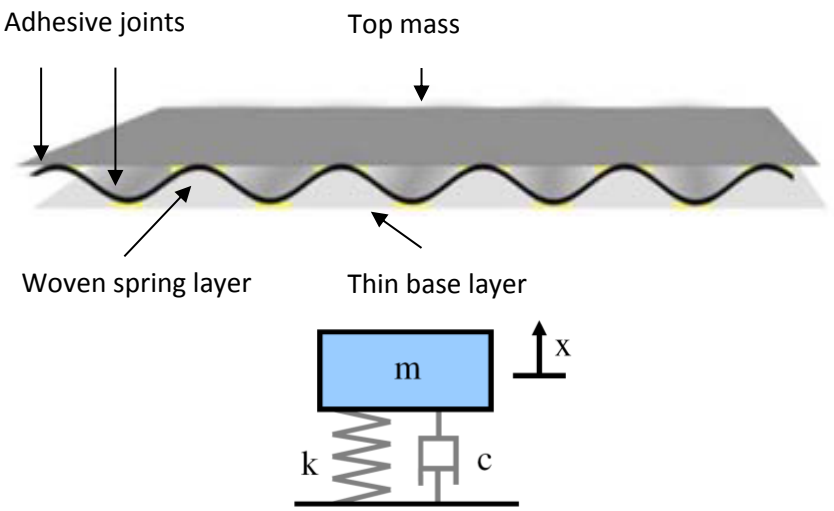

Figure 1.11 Components of a DVA with woven spring layer [19]

Figure 1.12 displays each of the factors that can be used to tune a DVA. Analogies with a simple mass-spring-damper system are listed below and the natural frequency is given in equation 1.18.

1. Top mass fabric (m)
2. Woven wavelength or thickness of weave material (k)
3. Adhesive method (c)

$$f_n = \frac{1}{2\pi}\sqrt{\frac{k}{m}} \tag{1.18}$$

Rajaram, Wang and Nutt [21] considered improving the acoustic design of a sandwich composite panel with a honeycomb core based on the theory for floor panel applications. The behaviour of these panels was complex and mechanical properties were dependent on both core shear motion and bending stiffness. The performance of these panels throughout the frequency range of interest (100Hz-5kHz) depended on the wave motions in relation to the speed of sound. Kurtze and Watters [12] separate their model into three regions; the first is dominated by the total panel bending, the second by the core shear and the third by the bending of the skins.

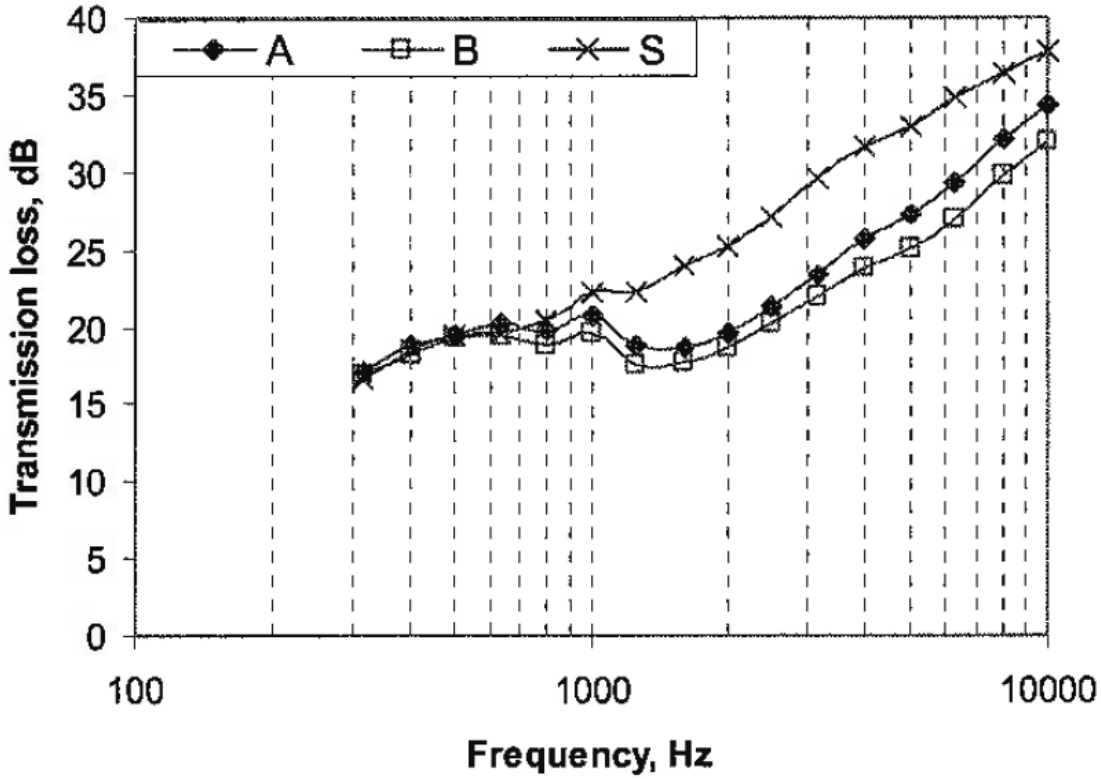

Figure 1.12 Sound transmission loss of aircraft floors [21]

A study performed by Rajaram [21] investigated commercial grade aircraft floor panels (see Figure 1.13). The design for panel S was to meet the subsonic criteria that the core shear speed is two thirds of the speed of sound and no dip at 1kHz is evident in panel S. The improvement in STL for panel S was due to the supersonic core shear wave speeds in panels A and B, and a subsonic wave speed in panel S. To achieve a subsonic wave speed the stiffness of panel S is twice the stiffness of panels A and B. The increase in stiffness was achieved by thicker skins on panel S which represented a weight gain of 10%.

1.3 Summary

Three stages in noise control were identified as first attenuating the noise source before applying noise control to the transmission path then the receiver of noise.

It was identified that acoustics was the area that required the greatest improvement on board marine craft. Cabins required the greatest acoustic improvement over all areas on board these marine craft.

In optimisation studies where acoustic STL performance is added as a constraint, additional mass is required. Other improvements in STL in composite sandwich panels were due to the subsonic core shear wave speeds.

Chapter 2

2 Material Properties of Composite Sandwich Constructions

Summary

A literature review of the dynamic material properties of sandwich composite constructions is presented including methodologies for their analysis. Descriptions of the facilities, equipment, and materials used in this thesis are provided. An important finding is that composite sandwich constructions exhibit can frequency dependent material properties.

2.1 Introduction

Analytical STL single leaf prediction models require the input of material properties. Commonly available models in Insul (Ballagh [6]) and ENC (based on theory described in Engineering Noise Control [2] by Davy [1] and Sharp [22]) contain a database of mechanical material properties for common existing materials but when new materials or combinations of materials are constructed the properties of these must be measured.

There are a range of methods used to obtain material properties and two of these are investigated in this study: fixed-free and free-free constrained impulse response modal analyses. A test rig was purpose built to enable the fixed-free (cantilever) method to be implemented. The method used is based on standard ASTM E756 [23].

Composite sandwich panels are typically used in the marine industry. Sandwich panels are composed of two face sheets which are thin relative to the panel and are high in strength and stiffness. The inner core material is thick relative to the panel but lightweight. The core material does not carry much load bearing stress which this is carried by the high strength of the skins. Materials used in the skins often contain laminates that contain reinforced fibres of various weaves. The material properties can differ considerably between sandwich constructions as the bonding techniques, laminates and core materials can be customised to produce material properties suitable. for specific applications. There is also a very large number of cores available, differing in shear modulus and many options for laminates with a large range of stitched fabrics in both E-glass and carbon fibre. Skins in sandwich constructions are typically laminates 3-6mm thick and are treated as thin isotropic plates. In some cases the weave of the fibres in the skins can have anisotropic properties. Core materials are treated as thick plates and are generally between 25mm and 75mm thick. Core materials are often isotropic. The Young's Modulus for the skin laminates is much higher than the core material.

2.1.1 Objectives

1. Use experimental modal analysis to determine the material properties of composite sandwich materials
2. Predict the Young's modulus and compare this with back calculated STL measurements and the experimental Young's modulus
3. Compare the fixed-free and free-free boundary methods using a beam modal analysis

2.2 Background

2.2.1 Fixed-free boundary condition

The Young's modulus (E_n) of a fixed-free (cantilever) beam can be calculated using equation 2.1 for the resonant frequency (f_n) of each mode obtained. This is a fixed-free condition excited by an excitation force.

$$E_n = \frac{48\pi^2 l^4 f_n^2 \rho}{\lambda_n^4 t^3 w} \tag{2.1}$$

where l is the unsupported length, f_n is the frequency of each mode, ρ is the mass per unit area, w is the width of the beam, t is the beam thickness and λ_n are the modal coefficients where the first five are: $\lambda_n = 1.875, 4.694, 7.854, 10.995, 14.137$.

2.2.2 Free-free boundary condition

Equation 2.1 is also used to calculate the Young's modulus for a free-free condition. The first five modal coefficients are: $\lambda_n = 4.694, 7.854, 10.995, 14.137, 17.278$.

2.2.3 Loss factor

The loss factor for each mode (η_n) is defined as-

$$\eta_n = \frac{\Delta f_n}{f_n} \tag{2.2}$$

where f_n is the resonant frequency of the nth mode in Hz, and Δf_n is the half power bandwidth for each mode, n at the 3dB down points.

2.2.4 Frequency dependent materials

In 1921 Timoshenko [24] first identified shear effects in straight uniform cross sectional area beam when investigating transverse vibrations. The shear coefficient K was introduced to allow for the fact that shear stress is not uniform over the cross section of a beam and can be defined by equation 2.3.

$$K = \tilde{\tau}(G\gamma_{eff}) \tag{2.3}$$

where $\tilde{\tau}$ is the average shear stress on a cross section, G is the shear modulus and γ_{eff} is the effective transverse shear strain.

The correction for shear, K was found to be four times greater than the correction for rotational inertia. It was found that the correction increases with increasing of frequency. Later research performed by Timoshenko [25] the following year found that if the wavelengths of the transverse vibrations were much larger than the cross sectional dimensions of the beam, the corrections do not apply.

Kaneko [26] reviewed Timoshenko's studies of the shear coefficient, K for circular and rectangular uniform beams. Timoshenko's differential equation for flexural vibrations for a beam is shown in equation 2-3.

$$\frac{\partial^4 \xi}{\partial x^4} + \frac{1}{a^2 r^2}\frac{\partial^2 \xi}{\partial t^2} - \frac{1}{a^2}\left(1 + \frac{2(1+\sigma)}{K}\right)\frac{\partial^4 \xi}{\partial t^2 \partial x^2} + \frac{\rho}{K a^2 G}\frac{\partial^4 \xi}{\partial t^4} = 0 \qquad (2.4)$$

where x is the distance along the beam, t the time, ξ the lateral deflection, $a = (E/\rho)^{1/2}$ the transmission of longitudinal waves, where E is Young's modulus and ρ the density, r the radius of gyration of the cross section, σ Poisson's ratio, and G the shear modulus.

Kaneko also reviewed twenty two other models in existence prior to 1975 to determine of K for rectangular and circular sections and compared these with experimental results. His work showed that the best theoretical expression to experimental results for a rectangular uniform section was Timoshenko's expression (see equation 2.4).

$$K = (5 + 5\sigma)/(6 + 5\sigma) \qquad (2.5)$$

The frequency dependent dynamic material properties of sandwich constructions with stiff laminate skins and lightweight foam cores were first studied by Kurtze and Watters [12]. It was found that the bending stiffnesses of sandwich panels were not only dependent on material parameters and panel geometries but was also highly dependent on frequency. As the frequency increased in sandwich plates the lateral motion was no longer solely dependent on bending alone. Shear and rotation in the core material influenced the deflection as frequency increased (see Figure 2.1). This phenomenon limits the applicability of current single panel STL models from the literature.

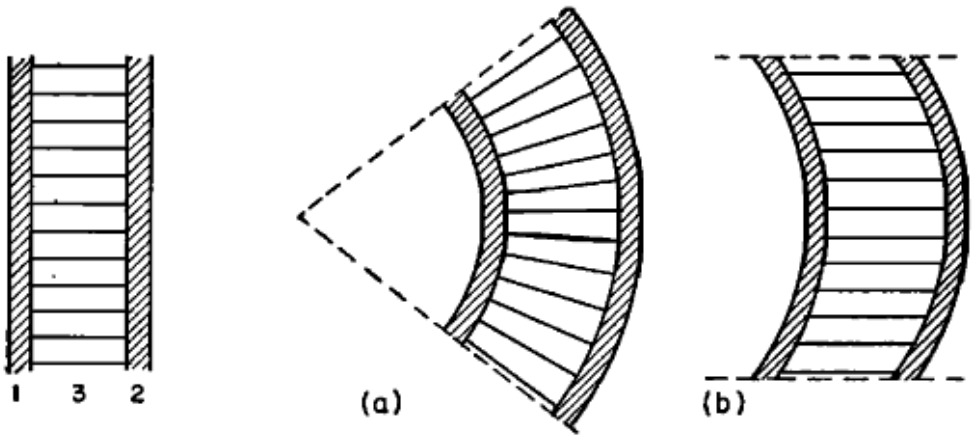

(a) Bending and (b) Shearing of the core layer

Figure 2.1 Bending of a sandwich panel [12]

Kurtze and Watters [12] found that the ratio of static to dynamic stiffness can be in excess of 1000:1 where this created a plateau region of constant wave speeds in its central region round the coincidence frequency, which increases with increasing core thickness. It was difficult to predict STL of the critical frequency region as small changes in bending stiffness could have a significant effect on the frequency range where this region occurred.

Kurtze and Watters [12] showed that the transverse wave speed in asymmetrical laminated panels changed from the bending speed of the laminated panel at low frequencies to the bending wave speed of a single skin panel loaded with half the mass of the core at higher frequencies. Equation 2.6 shows that the speed of bending waves is affected by the material properties and, ω the angular frequency of the propagating wave.

$$c_D = \omega^{\frac{1}{2}}(D/m)^{\frac{1}{4}} \tag{2.6}$$

where c_D is the velocity of the propagation of bending waves in isotropic materials, ω is the angular frequency, m is the mass per unit area and D is the bending stiffness. (Note: bending stiffness is noted as B after this section, throughout the thesis).

The velocity, c_s of the propagation of purely transverse shear waves and is given by equation 2.7 where μ is the shear modulus and ρ is the density of the material. A panel that favours the propagation of shear waves over bending waves provides better sound insulation as the shear waves are less than the speed of sound in the material.

$$c_s = (\mu/\rho)^{\frac{1}{2}} \tag{2.7}$$

Rindel [27] studied the propagation of sound through acoustically thick walled, light weight concrete and brick work. The constructions were sufficiently thick that wave speed was a function of frequency. The guide line for an acoustically thick plate is if the thickness is greater than $\lambda_B/6$. It was found that a cross over frequency, f_s where bending waves at low frequencies become dominated by shear waves at high frequencies (see equation 2.8).

$$f_s = \frac{c_s^2}{2\pi}\sqrt{\frac{\overline{m}}{D}} = f_c\left(\frac{c_s}{c}\right)^2 \tag{2.8}$$

From the cross over frequency, the phase speed or effective bending wave speed (c_{Deff}) can be calculated (see equation 2.9).

$$c_{Deff} = c_s\frac{f}{f_s}\sqrt{-\frac{1}{2}+\frac{1}{2}\sqrt{1+\left(\frac{2f_s}{f}\right)^2}} \tag{2.9}$$

In a recent study performed by Nilsson [28], the frequency dependency of lightweight sandwich panels used in the marine industry and comparison between measured and predicted STL was investigated. The types of sandwich panels considered in this study were symmetric with respect to the centreline and typically contained a lightweight core of 25-75mm. The laminate skin thickness varied between 3-8mm (see Figure 2.2). Young's modulus of the laminate skins was much higher than the core.

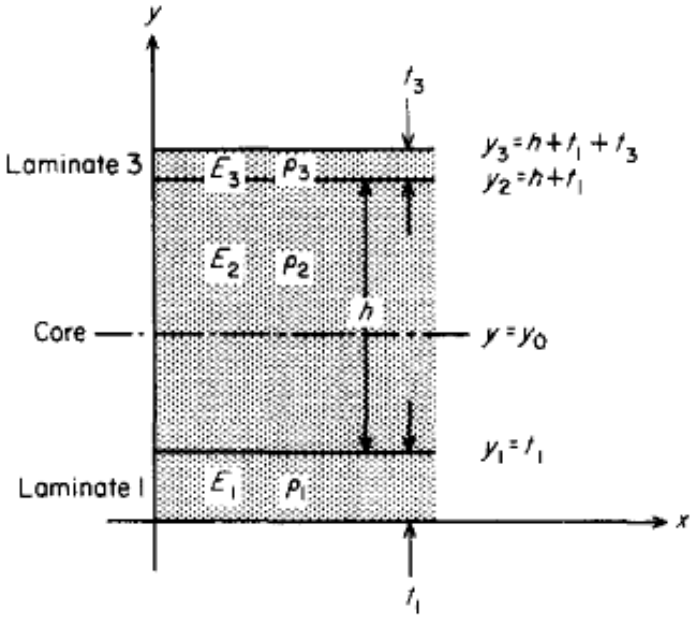

Figure 2.2 Geometry and material parameters for a sandwich panel [28]

The Bernoulli-Euler theory for the transverse motion of beams and the corresponding Kirchhoff theory were used to determine the response of sandwich plates. The plates considered had a bending wavelength compared to the thickness of the plates in order to satisfy the Kirchhoff's plate theory constraints. The bending stiffness D_0 at 31.5Hz for a sandwich plate is calculated using equation 2-9 where y_0 is the position of the neutral axis.

$$D_0 = E_3 t_3 (h - y_0)^2 + \frac{(h^3 - 3h^2 y_0 + 3h y_0^2)}{3} + E_1 t_1 y_0^2 \qquad (2.10)$$

$$y_0 = h(E_3 t_3 + E_2 h/2)/(E_1 t_1 + E_2 h + E_3 t_3) \qquad (2.11)$$

As frequency increases the lateral motion of a sandwich structure cannot be described as bending alone and the effective bending stiffness decreases. This occurs due to shear and rotation in the core that effects the deflection and apparent bending of the sandwhich plate.

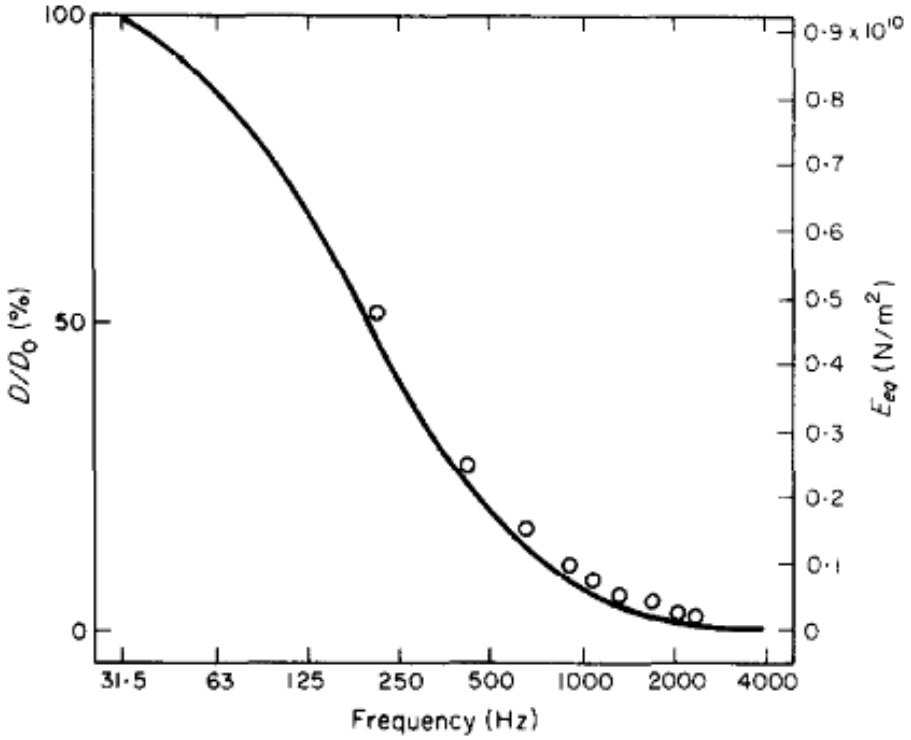

Key: —— is predicted and o o o is measured

Figure 2.3 Effective bending stiffness and equivalent Young's modulus as a function of frequency [28]

Predictions were obtained from individually measured skin laminates and core plates. These measurements entered into equations 2.12, 2.13 and 2.14 to obtain the predicted equivalent Young's modulus. An experimental Young's modulus was obtained from the complete sandwich plate construction and showed very good agreement with the calculated values. The vertical axis, D/D_0 displays the percentage of the bending stiffness at all frequencies, D relative to the bending stiffness at 31.5Hz, D_0 which is equal to $1.17 \times 10^5 Nm$.

It is apparent that the bending stiffness of the sandwich plate decreases with increasing Young's modulus and at frequencies above 1kHz the bending stiffness is only a few percent of the bending stiffness at 31.5Hz (see Figure 2.4). A good agreement is achieved by the inclusion of shear and rotation effects otherwise the predicted and measured bending stiffnesses would differ by approximately 50%.

The equivalent Young's modulus can be calculated from equations 2.12, 2.13 and 2.14 as

$$k_0 = k_N[f_{r+1}/f_r]^{0.5} \tag{2.12}$$

where k_0 is the wavenumber of the mode of interest in the interation f_{r+1} and k_N is the final wavenumber derived for the frequency, f_r.

$$D = \mu_{tot}\omega^2/k^4 = D_R(1 + i\delta_r) \tag{2.13}$$

$$E_{eq} = 12D\,(1 - \nu^2)/t_{tot}^3 \tag{2.14}$$

where μ_{tot} is the total mass per unit area, ω is the bending wave speed, δ is the loss factor of the structure, and D_R is the real part of the bending stiffness. The total thickness of the sandwich plate is t_{tot} and Possion's ratio, ν was assumed to be 0.3.

Further research by Nilsson [29] investigated Hamilton's principle [30] to derive dynamic properties of symmetric and asymmetric sandwich honeycomb cores beams. The apparent bending stiffness of the beams is strongly dependent on frequency. Which in turn is strongly dependent on the properties of the laminates where the bending stiffness decreases with increasing frequency. Timoshenko's model [25] on the apparent bending stiffness was applied to honeycomb core beams and was found to decrease steadily.

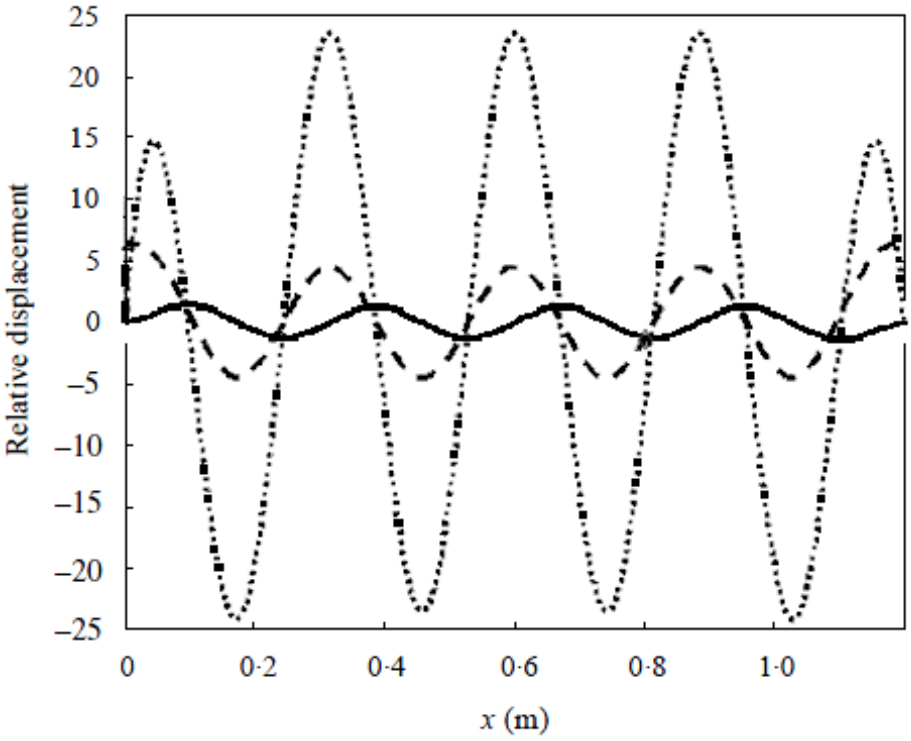

Key: —— is displacement, ···· is angular displacements and - - - is angular displacement caused by shear for mode 8

Figure 2.4 Displacement of a beam in the y-axis with fixed-fixed boundary condition at 1054Hz [29]

Nilsson [29] measured the bending stiffness of honeycomb beams using fixed-fixed and free-free boundary conditions and Hamilton's principle and found that the measured stiffness from fixed-fixed was lower than the free-free approach. For a clamped fixed beam, shear is introduced at the boundaries that make the beam more flexible compared to a beam with free edges. The effect is very pronounced close to the edges (see Figure 2.4).

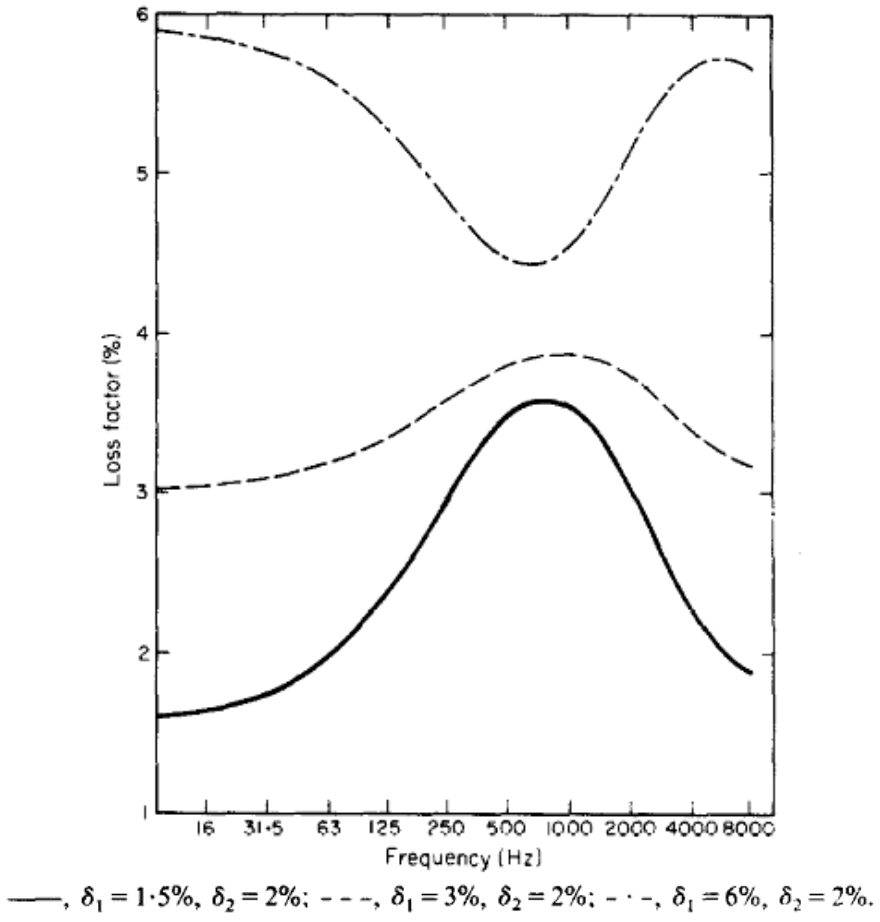

Figure 2.5 Predicted loss factors [28]

The loss factors [28] of free plates are much lower than for fixed plates in a large construction due to losses at junctions. Figure 2.5 shows the loss factors of a sandwich plate where the core's loss factor is kept constant at 2% while the skin's loss factors are varied from 1.5% to 6%. In the low frequency region lateral motion by pure bending dominates the loss factor and in the high frequency region is dominated by flexural waves in the laminate skins.

If the loss factor of the laminates is increased by a factor of two then the total loss factor increases by 10% since the loss factor of the core is unchanged. When the loss factor of the laminates are further increased, the total loss factor has a minimum in the frequency range 500Hz to 1kHz where shear and rotation in the core are the primary contributing factors.

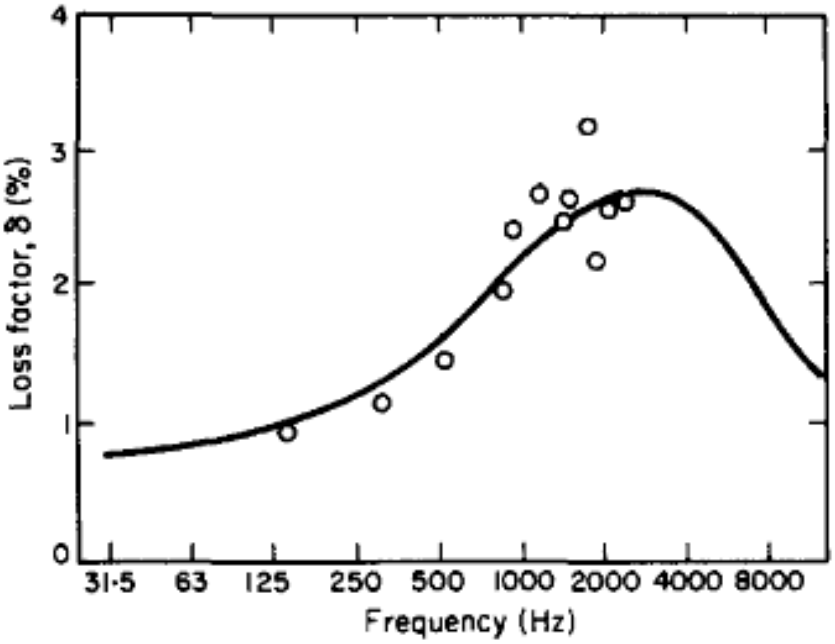

Key: —— is predicted and o o o is measured

Figure 2.6 Loss factor for a sandwich plate [28]

The loss factors over the frequency range of 31.5Hz to 10kHz were measured and compared with predicted results for a sandwich plate (see Figure 2.6). The predictions were based upon measurements of the individual skin and core material properties, with their respective loss factors assumed to be constant over the frequency range. When the structure is measured as a sandwich plate the overall loss factors agree relatively well with predicted results.

2.3 Methodology

Modal analysis is a method used to measure the dynamic properties of materials. For the laminate and core materials used in this study (see Table 2.1), the bending stiffness was not readily available. In order to determine the bending stiffness, two different boundary condition methods were used; fixed-free and free-free.

Table 2.1 Typical engine room roof/main saloon panel composite sandwich material composition

Skin material 1	Core material	Skin material 2
E-Glass Quadraxial 600g/m² × 3 layers of fibres (2.1mm)	Rigid PVC Foam Core (18.9mm)	E-Glass Quadraxial 600g/m² × 2 layers of fibres (1.8mm)

This followed the approach used by Phillips [31], Trevathan [32] and Anders [3] to obtain the material properties of sandwich, composite and multi leaf beams and measurements were performed according to the standardised test method, ASTM E756 [23].

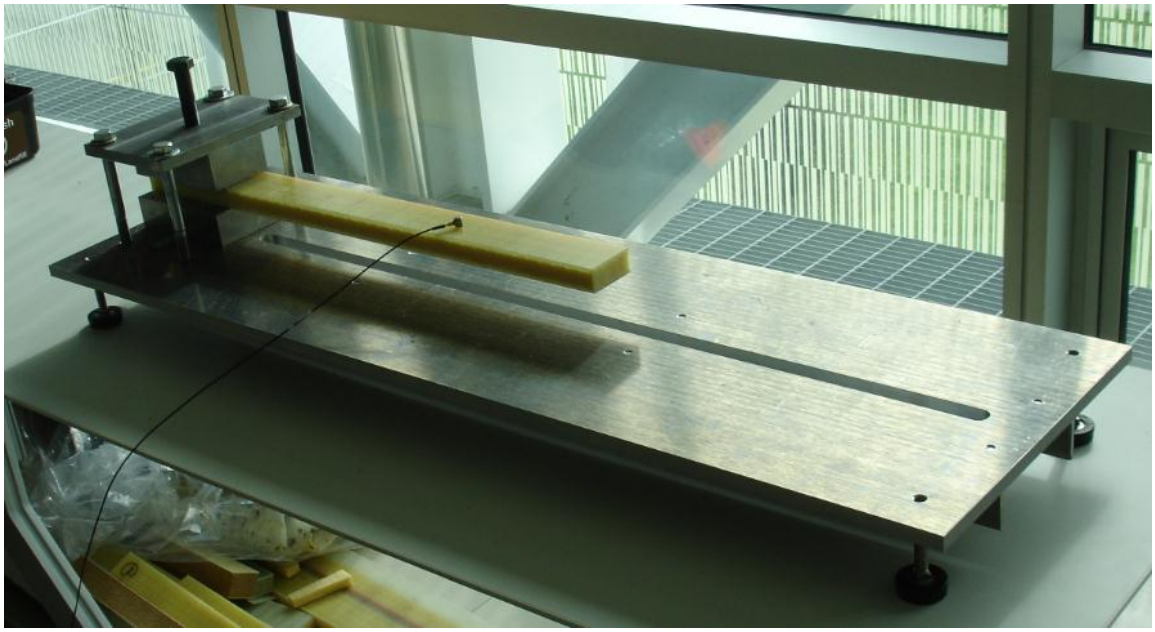

Figure 2.7 Fixed-free experimental setup

A purpose build cantilever test rig (see Figure 2.7) was constructed and verified by Phillips [31]. Three point bending tests with a MTS810 servo-hydraulic load frame was used to verify that the Young's modulus of steel and aluminium agreed with values obtained by the cantilever test rig of 200GPa and 70GPa respectively. ATSM E756 describes the procedure for Young's modulus and the loss factor. This method requires the excitation of beam samples while measuring the dynamic response.

Table 2.2 Equipment

Description	Manufacturer	Model	Serial Number
DAQ Chassis	National Instruments	cDAQ-9172	123B7F6
DAQ Module	National Instruments	9234	153CC17
Accelerometer	Brüel & Kjær	4519	4519-003 53413
Impact Hammer	PCB Piezotronics	T086C01	24883

The testing procedures specified by ASTM E756 were followed with the exceptions of:

1. Beam root section

ASTM recommends a well-defined root section including a block of material on the clamped end of the beam. Due to the type of construction of the composite sandwich beams used it was not possible to have a block at the clamping end. The overall dimensions of the beam were scaled up from the dimensions recommended but the aspect ratio was maintained as specified.

2. Beam excitation

ASTM recommends the use of non-contact transducers to excite the beam. Transducers powerful enough to produce a measurable response for the beams studied were not readily available. An impact hammer was used to excite the beam.

3. Environmental control

ASTM states that tests are to be performed inside an environmental chamber to control temperature and humidity. The appropriate equipment was not readily available and it was not deemed to be important within the scope of this project.

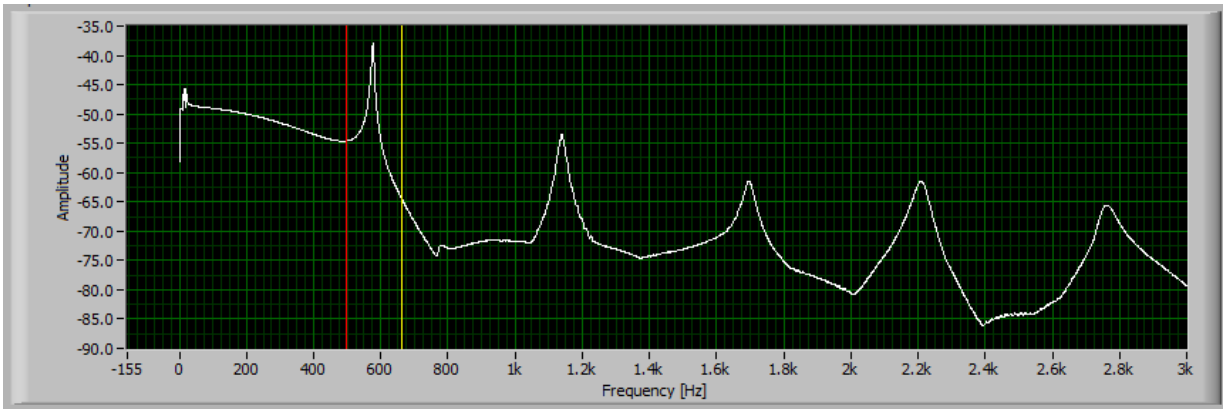

Figure 2.8 First five modes of a modal analysis

The beam samples were clamped in the headstock to a set torque for all measurements. An accelerometer (see Table 2.2) with a small mass to minimise the point mass effect was used to measure the response of each beam. The accelerometer was placed at a point in the centre of the beam at a non-modal point 15mm after the second mode point (see Figure 2.7). The beam was excited by an impact hammer at 20mm intervals across the entire beam to excite the first five modes (see Figure 2.8). The beam was excited perpendicular to the laminates, along the centreline to avoid twisting. Three different lengths from the same composite construction were used in order to obtain a wide range of frequencies. The unclamped beam lengths used for fixed-

free were: 0.47m, 0.235m and 0.118m. Each measurement was repeated three times and the beam was rotated 180° and the measurements were repeated. If a double hit occurred then that measurement was discarded and repeated.

The impact response was recorded using a National Instruments data acquisition system (see Table 2.2). The accelerometer was connected to the NI module and this provided a signal to a PC running Labview. Custom Labview code performed an FFT on the beam's response. The Young's modulus and loss factor was then calculated using equations 2.1 and 2.2 for the first five modes.

Figure 2.9 Free-free experimental setup

A free-free method was also used to determine the material properties of the sandwich composite beams (see Figure 2.9). A composite sandwich beam was hung from two points using string to reduce twisting on impact and an accelerometer was again placed at a non-modal point. The beam was excited by an impact hammer at 20mm intervals across the entire beam to excite the first five modes. The total beam lengths used for fixed-free were: 0.602m, 0.363m and 0.231m. As specified by ASTM E756 the first five are used to calculate the Young's modulus and loss factor (see equations 2.1, 2.2 and appropriate modal coefficients). The acquiring and processing of data was the same as described above.

The laminate skins were separated from the core. The fixed – free measurement procedure was then repeated separately out on each of the laminate skins and core. Three beam lengths were again used to obtain fifteen measurements over a range of frequencies.

2.4 Results and Discussion

Table 2.3 Material properties and dimensions of each component of a composite sandwich beam

Material	Thickness (mm)	Width (mm)	Density (kg/m^3)
Skin 1	2.1	50	1163
Skin 2	1.8	50	1163
Core	18.9	50	120
Total panel	22.8	50	374

2.4.1 Young's modulus

During the measurements it was discovered that the material properties were dependent not only on the physical properties but also on the frequency of excitation. This was not expected as previously tested isotropic beams had produced material properties constant over the frequency range. A literature search identified that other investigations had also reported this phenomena [24] [25] [26] [12] [27] [28] [29]. A modification was then implemented so that fifteen modal measurements using three different sized beams instead of one beam could be acquired over a frequency range from 53Hz up to 7161Hz. The Young's modulus and loss factors were found to change over the frequency of excitation.

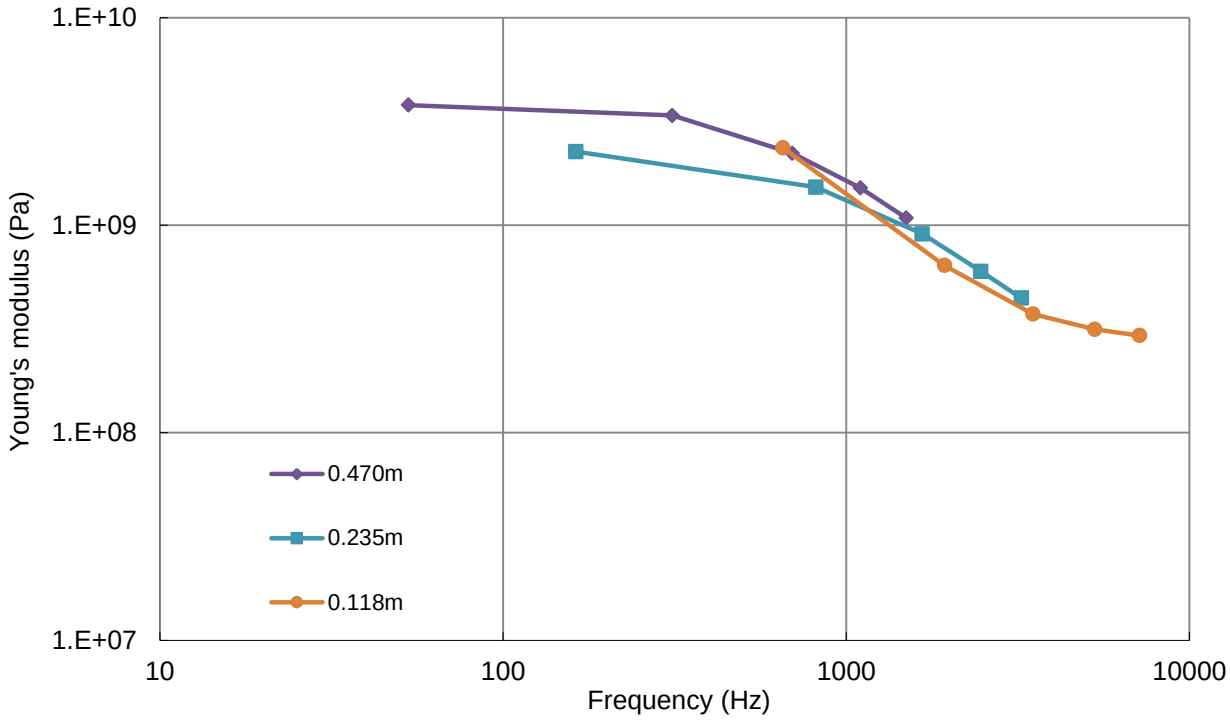

Figure 2.10 Fixed-free Young's modulus of a composite sandwich beam

In the low frequency range (<300Hz) the lateral motion of the sandwich construction is determined by pure bending as shown by the constant Young's modulus (see Figure 2.10). In the mid-high frequency range (>300Hz) the apparent bending stiffness is strongly dependent on frequency and is decreasing with frequency. These findings agree with research performed by Nilsson on sandwich plates [28] (see Figure 2.3).

The same analysis was performed using free-free boundary conditions (see Figure 2.11) where the same trend was observed with a decrease in Young's modulus with increasing frequency. The range of frequencies were not as great in Figure 2.11 as that obtained in Figure 2.10 because a much longer beam was required that was not readily available to achieve this low frequency region.

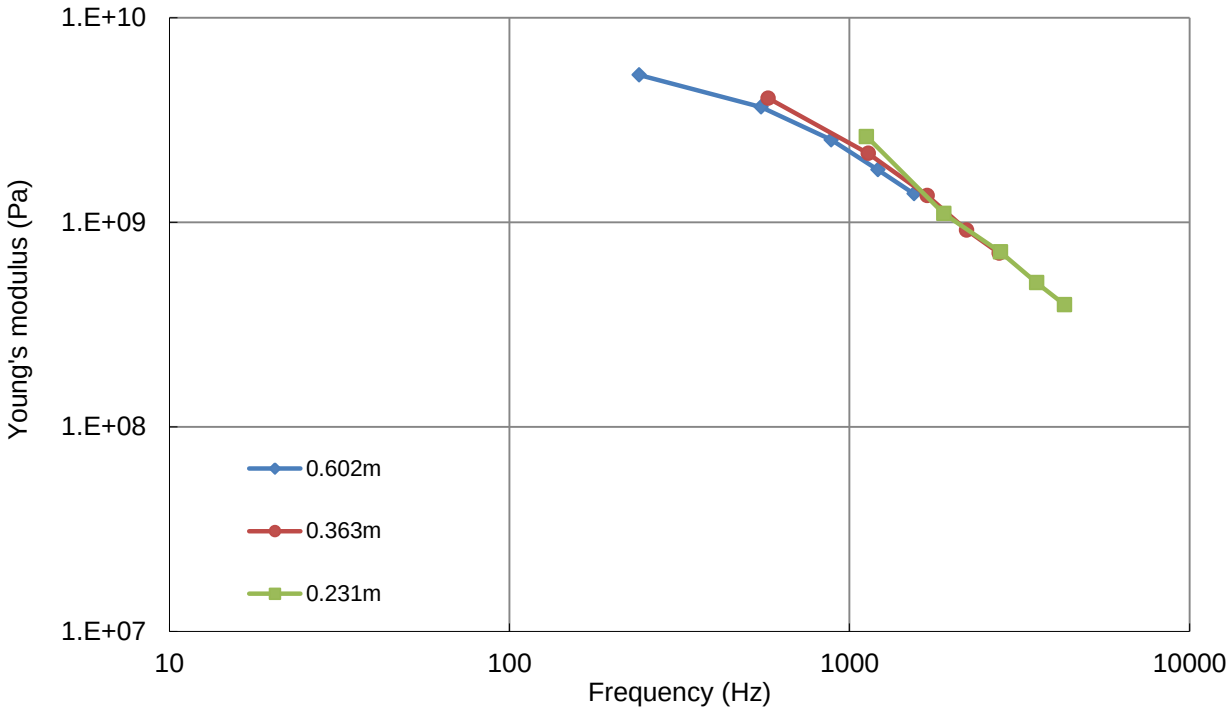

Figure 2.11 Free-free Young's modulus of a composite sandwich beam

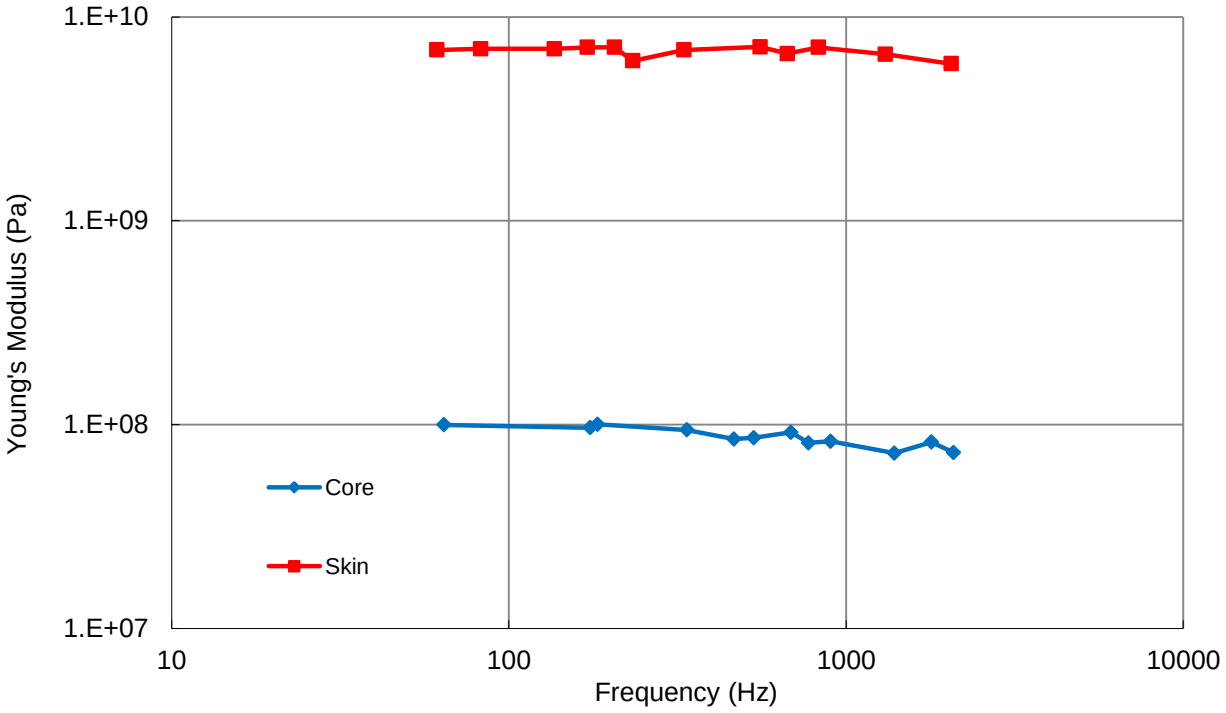

Figure 2.12 Experimental Young's modulus of core and skin beams using fixed-free boundary condition

The separated skin and core constructions demonstrated pure bending as the dominate factor over the frequency range from 64Hz to 2kHz. This is the same finding as Nilsson [28] described when a modal analysis was performed on the separated similar skin and core constructions.

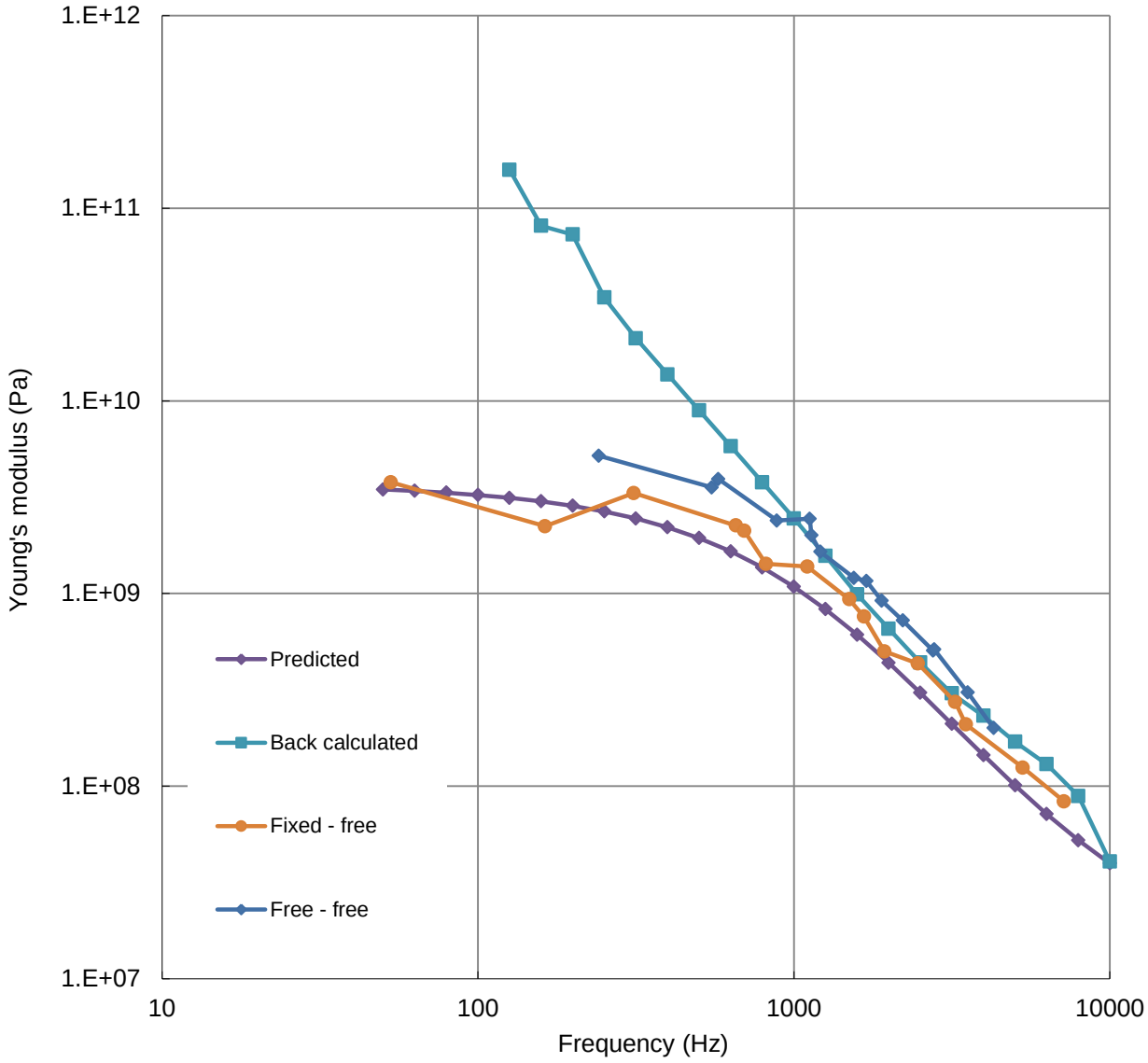

Figure 2.13 Experimental Young's Modulus of a composite sandwich beam using fixed-free, free-free boundary conditions and back calculated from experimental STL

Differences in the Young's modulus were identified between the free-free and fixed-free boundary conditions for the same beams. For a clamped (fixed) beam, shear is introduced at the boundaries and this results in a beam with greater flexibility compared to a beam with free edges. Thus a free-free beam produces a higher (and better) representation of a beam's material properties [29].

Back calculation of Young's modulus was made using Davy [1] and Cremer's model [4] for the STL of single leaf walls. The Young's modulus required to achieve perfect agreement with the experimental STL of the composite sandwich panel was calculated (see Figure 2.15) and see Chapter 3 for STL measurements.

A prediction of the Young's modulus was performed using measured material properties of the individual core and skin using theory from Kurtze and Watters [12] and Nilsson [28]. It can be seen that the predicted results agree reasonably well with the experimental Young's modulus of the entire sandwich structure over the frequency range from 50Hz to 10kHz for the fixed-free experiments.

2.4.2 Loss factor

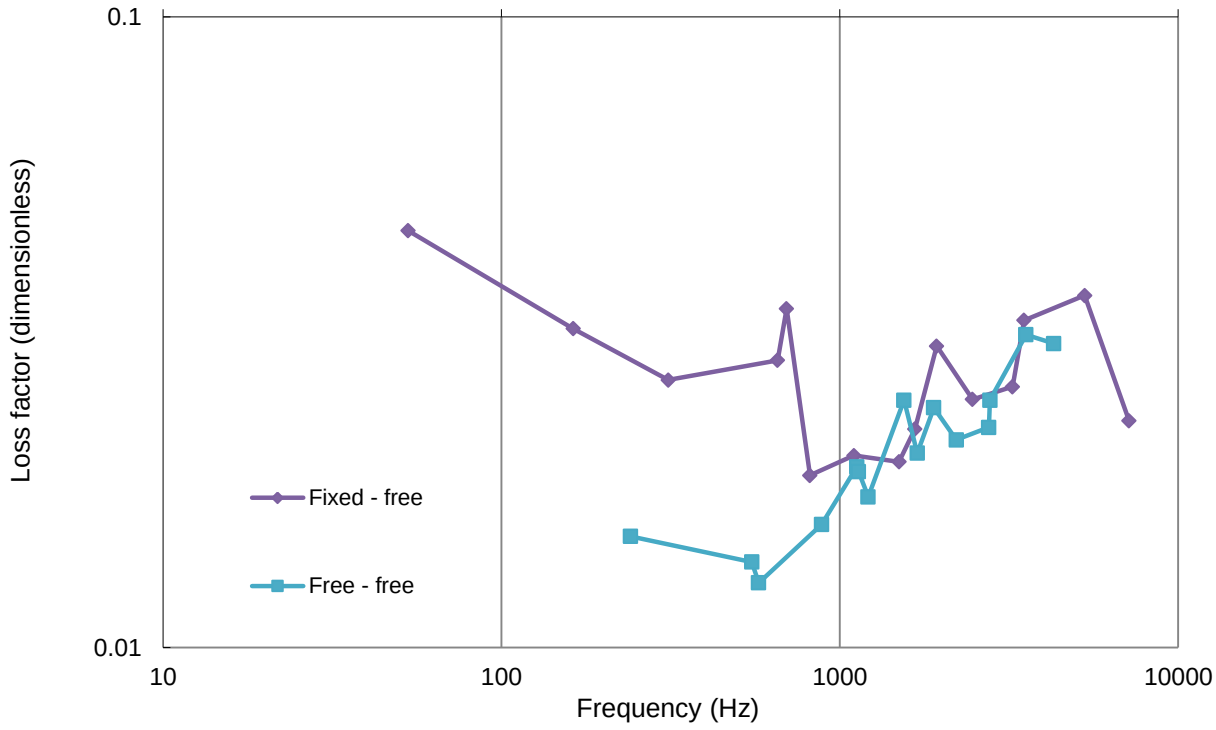

Figure 2.14 Fixed - free versus free-free loss factor

For the measurement of loss factor, the two boundary conditions give conflicting trends. The fixed-free arrangement decreases with frequency and the free-free increases with frequency. Nilsson [28] found that the loss factors of free plates are much lower than for fixed plates in a large construction due to losses at junctions.

Feng and Kumar [33] used a free-free boundary condition method with two corners freely hung to avoid introducing damping from the clamping arrangement. To obtain accurate STL

predictions around the critical frequency a loss factor plus theoretical radiation loss factor was included. The loss factor alone is often not good enough where the STL will be under predicted around the critical frequency. As the fixed-free is higher than free-free loss factor this may be sufficient to correctly predict the STL of the panel without a radiation loss factor according to Feng and Kumar.

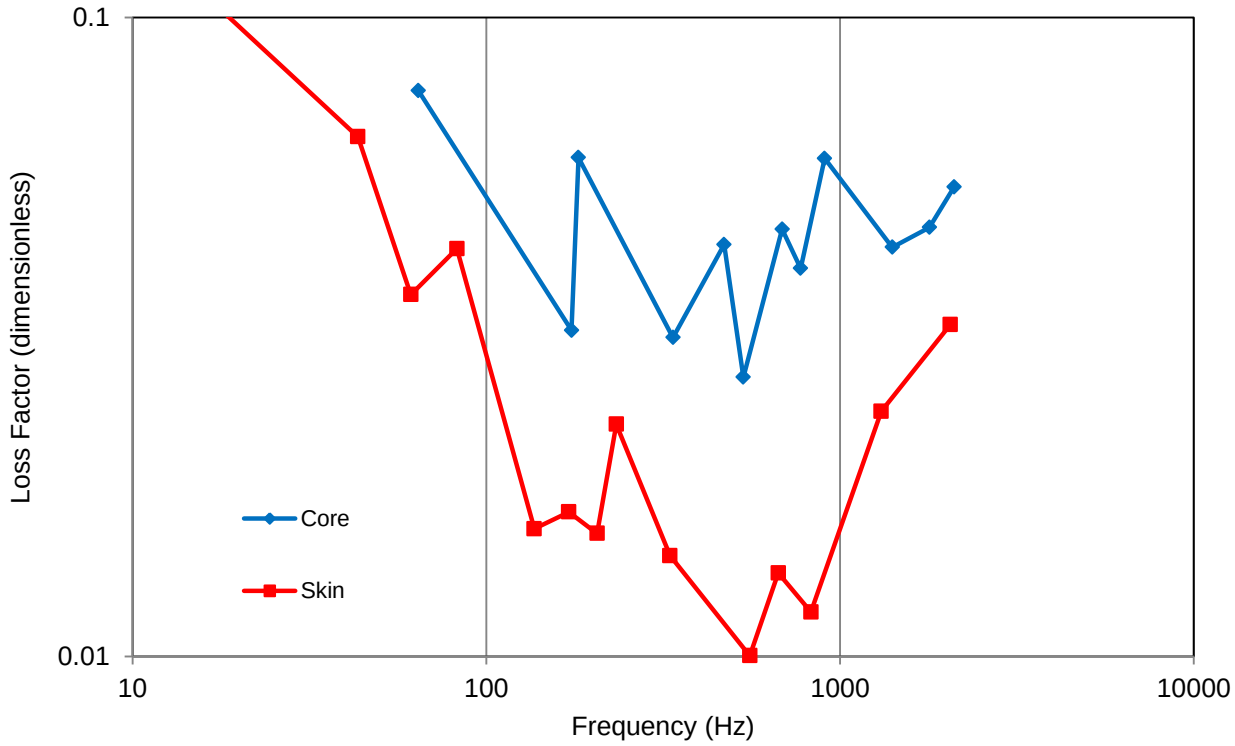

Figure 2.15 Experimental loss factor of core and skin beams using free-free boundary condition

According to Nilsson [28] the loss factor of a sandwich material is primarily determined by the losses of the skin in the high and low frequency ranges. The free-free boundary condition (see Figure 2.14 and 2.15) provides a somewhat conflicting result where the loss factor below 200Hz has not determined the loss factor of the sandwich beam, but from 200Hz to 1.4kHz in fact does have some agreement. The range of frequencies measured for the loss factors of the skin and core material (see Figure 2.15) does not extend to a high enough frequency to make a conclusion at high frequencies. The peaks that the 3dB down points were calculated from were not distinct in the high frequency region. In the mid-frequency range shear and rotational effects in the core dominate the loss factor for the lateral motion of the sandwich material according to Nilsson. The mid-frequency range for the core is 0.02 above the measured data from the sandwich material.

2.5 Conclusions

Experimental investigations were carried out on a range of composite sandwich panels to determine their material properties. The Young's modulus and damping ratio were found to be frequency dependent in these composite sandwich constructions.

There was good agreement between experimental and predicted Young's modulus of the composite sandwich beams.

Two methods for identifying these properties were investigated; fixed-free and free-free beam boundary condition modal analyses. There was disagreement between them which was identified as the clamping fixed nature that increased flexibility of the beam producing a lower Young's modulus than the free-free beam analysis.

Chapter 3

3 Theoretical Prediction and Measurements of Composite Sandwich Constructions

Summary

Methodologies for the analysis of measurements and predictions of the STL of composite sandwich constructions are described. Descriptions of the facilities, equipment, materials and models used are provided. The agreement between prediction and measurements is considered to be poor.

3.1 Introduction

In chapter two the bending stiffness was shown to reduce with increasing frequency which is in agreement with the literature. This decrease is attributed to the shear stiffness of the core becoming the primary mechanism over the bending stiffness for Sound Transmission Loss (STL) and is a well-known characteristic of laminated panels with stiff skins and lightweight cores.

Agreement between theory and experimental work is poor when using homogeneous isotropic panel theory. It is particularly poor in the coincidence frequency region as this region is regarded as being the most difficult to predict. The coincidence frequency region is highly sensitive to changes in bending stiffness.

3.1.1 Objectives

1. Investigate prediction models for homogeneous isotropic panels
2. Experimentally determine the STL of various composite sandwich panels
3. Predict the STL of composite sandwich panels and compare with experimental measurements

3.2 Prediction of STL

Predicting the STL of constructions and materials is very complex and requires sophisticated prediction programmes. There is always the issue of achieving agreement between experimental measurements and prediction. Correction factors are often added to prediction models to achieve this agreement. Whether the models are based on analytical, empirical or numerical calculations, there is no one model that is accurate with all constructions.

Insul® and ENC, Nilsson and numerical modelling are investigated. Cambridge [34] examined a range of analytical modelling programmes and described discrepancies between the predicted and measured values for low frequencies. He also looked at the calculations these programmes used to predict the STL.

3.2.1 Insul®

Insul® is an acoustic prediction package developed by Marshall Day Acoustics and (Ballagh [35]) used for sound reduction index of building elements such as walls, windows and ceilings. A range of features can be incorporated into wall constructions such as; studs, isolation mounts. Insul® is based on the mass law theory and critical frequency. Sewell's correction and edge dampening

correction can also be added for energy losses at the edges. For thin homogeneous materials, Insul® uses the modified mass law for below the critical frequency. These equations are based on Cremer's [4] work.

Since there are few materials provided in the Insul® library, customised material properties can be entered to calculate the STL. Properties that are required to be entered are density, mass per unit area, Young's modulus and loss factor. For the purposes of this study a composite sandwich panel can be modelled.

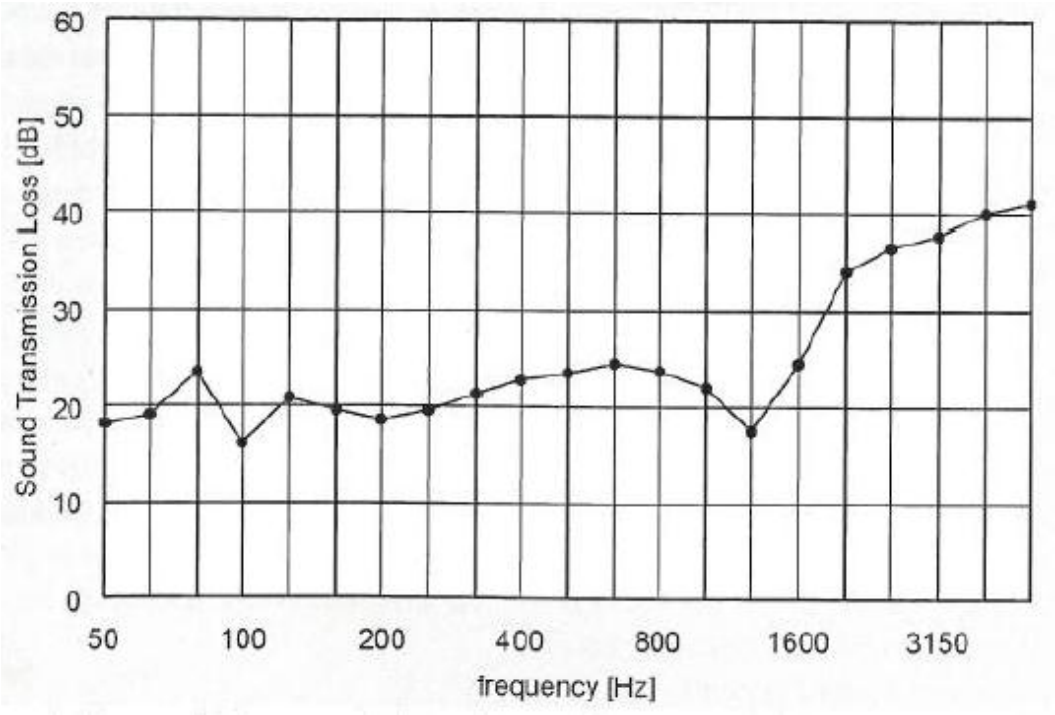

Figure 3.1 Sound transmission loss of typical foam core sandwich panel [6]

Ballagh [6] developed a method for predicting the STL of lightweight foam cored panels. A conventional isotropic model was modified to accommodate these constructions by introducing the transmissibility of a single degree of freedom resonant system. Reasonable agreement was found between experimental and predicted STL. These constructions modelled typically contained a high skin mass relative to the core. This introduced dilatational resonance into the frequency range of interest. Constructions with lightweight skins relative to the core material were not investigated as this would move the dilatational resonance outside the frequency range of interest.

3.2.2 ENC

ENC (Engineering Noise Control) is a modelling package that uses theory from the Engineering Noise Control text book, written by Bies and Hansen [2]. ENC spans basic approaches through to more complex models. Within the STL module, a range of models for isotropic and orthotropic panels are available. Isotropic panels typically contain one critical frequency while orthotropic panels can have more than one critical frequency depending on the direction of the incidence wave. The two isotropic models available in ENC are from Sharp's [22] and Davy's [36] models.

Cambridge [34] investigated these models and found that the important difference was the limiting angle θ_L which greatly affected the transmission coefficient. Sharp's model uses a constant limiting angle of between 78° to 85° while Davy's model uses a frequency dependent angle as shown in equation 3.1.

$$\theta_L = \cos^{-1}\sqrt{\frac{\lambda}{2\pi\sqrt{A}}} \tag{3.1}$$

where λ is wavelength and A is the area of the wall.

While theory assumes an infinite wall, a limiting angle must be introduced to provide agreement between experiments performed on finite wall constructions as true infinite wall measurements are impossible. The physical explanation for the incorporation of a limiting angle is that the radiation efficiency does not go to infinity as the angle of incidence and (and transmission) approaches 90° for a finite panel while the infinite panel theory predicts that the radiation does go to infinity as the angle of incidence approaches 90° [1].

Sharp's [22] model uses a constant value for angle of incidence of approximately 78° in the mass law range.

$$TL = \begin{cases} 20\log_{10}\left[\frac{\pi f m}{\rho c}\right] + 20\log_{10}\left[1-\left(\frac{f}{f_c}\right)^2\right] - 10\log_{10}\left[\log_e\left(\frac{1+a^2}{1+a^2\cos^2\theta_L}\right)\right] & f < 0.95f_c \\ 20\log_{10}\left[\frac{\pi f m}{\rho c}\right] + 10\log_{10}\left[\frac{2\eta\Delta_b}{\pi}\right] & 0.95f_c < f < 1.2f_c \\ 20\log_{10}\left[\frac{\pi f m}{\rho c}\right] + 10\log_{10}\left[\left(\frac{2\eta}{\pi}\right)\left(\frac{f}{f_c}-1\right)\right] & f \geq 1.2f_c \end{cases} \tag{3.2}$$

where 'a' can be calculated from equation 3.3 and Δ_b is the ratio of the filter bandwidth to the filter centre frequency of the filter used for measurements. For one third octave bands $\Delta_b = 0.236$, and 0.707 for one octave bands.

$$a = \left(\frac{\pi f m}{\rho c}\right)\left[1 - \left(\frac{f}{f_c}\right)^2\right] \tag{3.3}$$

Sharp calculates the sound reduction above the critical frequency using equation 3.2 using Cremer's [4] model. This model is also used in Insul® by Ballagh [35] and Davy [36].

According to [2] the Davy model is generally more accurate at frequencies below the critical frequency and the Sharp model is generally more accurate around the critical frequency. At high frequencies above the critical frequency, both models provide similar results. This suggests that the Davy model should incorporate the Sharp fixed limiting angle of 85° in the critical frequency region. The field incidence transmission coefficient is given by equations 3.4, 3.5 and 3.6.

$$\tau_f = \int_{cos^2\theta_L}^{1} \frac{d(cos^2\theta)}{1 + a^2 cos^2\theta} = \frac{1}{a^2} ln\left(\frac{1 + a^2}{1 + a^2 cos^2\theta_L}\right) \tag{3.4}$$

If $a >> 1$ then τ_f becomes

$$\tau_f \approx -\tau(0) ln[\tau(0) + cos^2\theta_L] \tag{3.5}$$

If $\tau(0) << cos^2\theta_L$ then τ_f becomes

$$\tau_f \approx -\tau(0) ln(cos^2\theta_L) \tag{3.6}$$

τ_f differs from $\tau(0)$ by a constant factor.

3.2.3 Nilsson's STL model

Nilsson [37] formulated a single panel STC model in 1974 that was further developed in 1990 by Nilsson [28] to accommodate for symmetric sandwich panels. The STL of a sandwich panel can be calculated by equations 3.7, 3.8, 3.9, 3.10 and 3.11.

$$f_c = (c/2\pi) k_{panel}^2 / k_{air} \tag{3.7}$$

For $f < f_c$

$$R_1 = 20\log(m) + 20\log(f) - 10log[\Gamma\Lambda + G] - 48 \tag{3.8}$$

For a simply supported panel

$$\Lambda = 1 + \frac{3 \times 10^4}{4\delta f^{0.5} f_c^{1.5}}\left(\frac{1}{b_1^2} + \frac{1}{c_1^2}\right) \tag{3.9}$$

For a clamped panel

$$\Lambda = 1 + \frac{3 \times 10^4}{\delta f^{0.5} f_c^{1.5}} \left(\frac{1}{b_1^2} + \frac{1}{c_1^2} \right) \tag{3.10}$$

For $f > f_c$

$$R_2 = 20 \log(m) + 30 \log(f) - 10 \log(f_c) + 10 log\delta + 5 log[1 - f_c/f] - 47 \tag{3.11}$$

where f is frequency, f_c is the coincidence frequency, G is the resonant transmission through the panel, Γ is a function of baffle and plate dimensions, Λ is a function of the boundary conditions for a plate with length and width equal to b_1 and c_1. At just above coincidence the STL is set equal to the maximum value $R_1(f_c)$ and R_2.

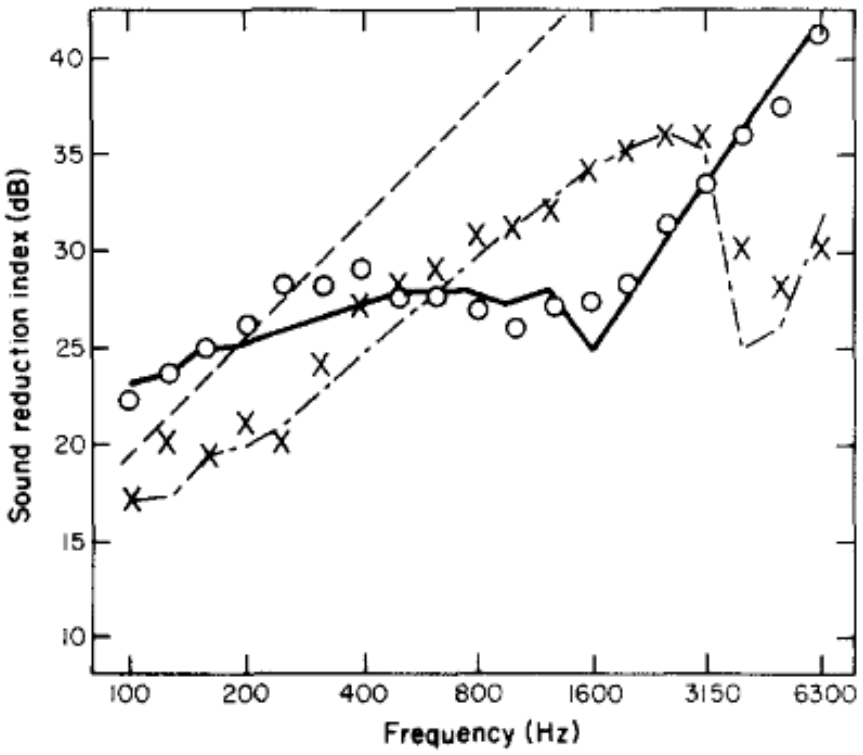

Key: —— is predicted sandwich panel, o o o is measured sandwich panel, – · – is predicted laminate, × × × is measured laminate and – – – is mass law for sandwich panel.

Figure 3.2 Comparison of measured and predicted sound reduction indices [28].

The prediction of STL for sandwich panels was compared to experimental measurements (see Figure 3.2). The sandwich composite panel performs well below a simple mass law prediction

suggesting that this material is a poor noise insulator. Nilsson's model agrees well with experimental data for a single leaf laminate and for sandwich composite materials.

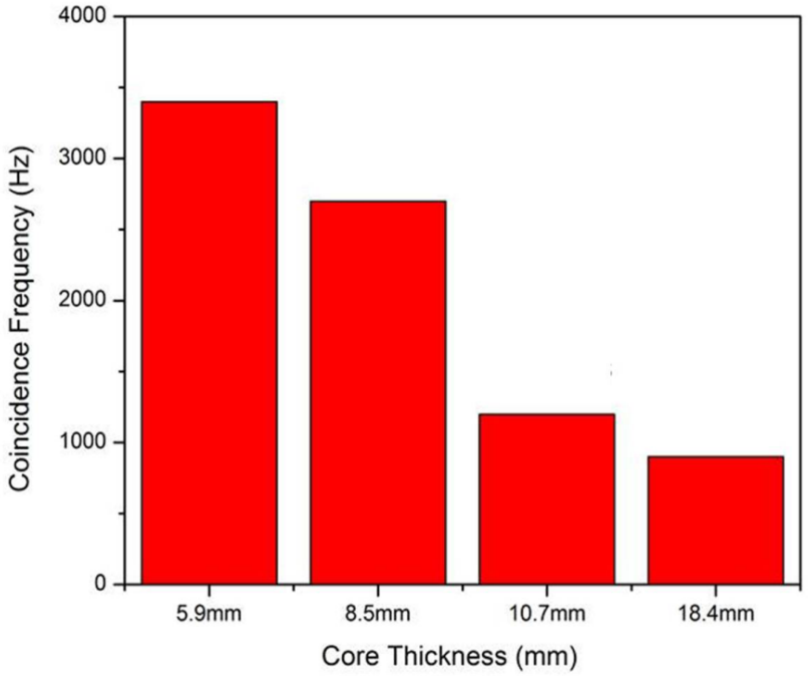

Figure 3.3 Coincidence frequencies of core thicknesses with carbon-fibre face sheets [18]

Sagianis and Suhr [18] investigated the coincidence frequency of various thicknesses of carbon fibre skinned sandwich panel constructions. They identified non-linear effects of the coincidence frequency as a function of core thickness (see Figure 3.3). This provides an explanation for the non-linear relationship of Young's modulus versus frequency (see Chapter 2). As the two outer skins are spaced further apart, shear and rotation effects increase the non-linearity.

3.2.4 Numerical modelling

Zhou [38] investigated the STL through composite sandwich panels using three different methods and showed that wave impedance analysis accurately predicts the STL of thin foam – filled honeycomb panels at frequencies above their first resonance frequency. Statistical energy analysis (SEA) accurately predicted the STL for sandwich panels when the measured radiation loss factor values near coincidence are used instead of the theoretical values for single layer panels. SEA is best used in high frequency predictions. The boundary element analysis accurately predicted STL for thick foam – filled honeycomb sandwich panels.

3.3 Methodology

3.3.1 Test Facilities

The tests were carried out in partial accordance with [39]. The tests were performed in the reverberation room and semi-anechoic room in the Department of Mechanical Engineering, University of Canterbury (see Figure 3.4) for the layout of this facility.

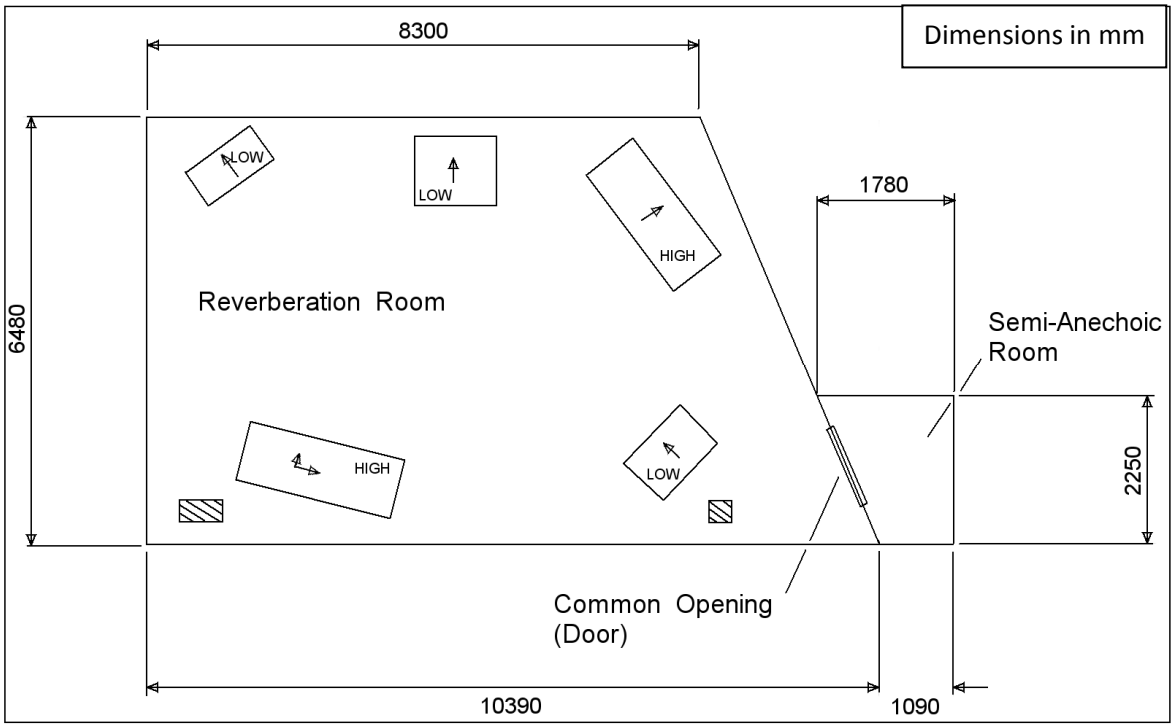

Figure 3.4 Test facility

The volume of the reverberation room is 216m³. A sufficiently diffuse sound field was established by the inclusion of six stationary diffusing panels of galvanized steel faced medium density fibreboard, each with a one-sided area of 2.88m² and suspended at random orientations. The total two-sided area of the diffusing elements is 13% of the total boundary surface area of the room. Previous tests carried out in the room have established that the diffusivity of the sound field within the room is acceptable. The total surface area of the room boundaries and diffusing elements is 305m².

Table 3.1 Equipment used during testing

Description	Manufacturer	Model	Serial Number
Analyzer	Brüel & Kjær	PULSE C Frame with 7539 5 Channel Module	2483932
Handheld Analysis	Brüel & Kjær	2260	1894145
Intensity Probe	Brüel & Kjær	3595	2680306
Acoustic Calibrator	Brüel & Kjær	4231	1934296
Dodecahedron Loudspeaker	Brüel & Kjær	OmniPower 4296	2071500
Dodecahedron Amplifier	Brüel & Kjær	2716	2301358
Microphones	Brüel & Kjær	4189-L	2573559 2573560 2573561 2573562 2573563

3.3.2 Generation of the sound field

The sound field was generated using Brüel & Kjær Pulse software and a Brüel & Kjær Pulse 3560-C data acquisition unit as shown in Figure 3.5. The signal was amplified by a Brüel & Kjær 2716 power amplifier and passed into the reverberation room to a Brüel & Kjær 4296 omnidirectional speaker.

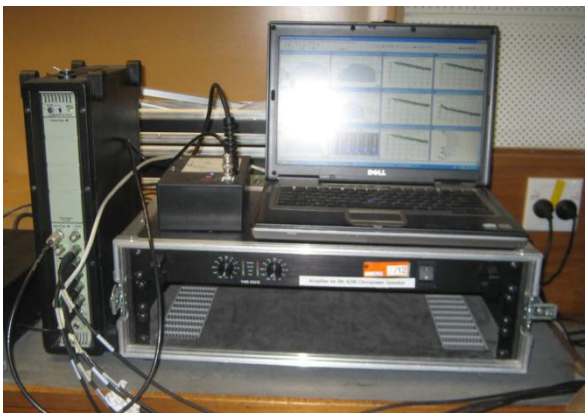

Brüel & Kjær Pulse 3560-C Pulse data acquisition unit (left) and Brüel & Kjær 2716 power amplifier (lower)

Figure 3.5 Signal generating laptop running Brüel & Kjær Pulse software

3.3.3 Receipt of signals

The sound pressure level in the reverberation room was measured according to ISO 15186-1 STL standard [39] using five Brüel & Kjær 4189 free field microphones connected to the Brüel & Kjær Pulse 3560-C data acquisition unit in the control room. Microphones were placed at locations in accordance with the ISO standard; distances from surrounding surfaces were a minimum of one meter.

Figure 3.6 Brüel & Kjær 2260 Investigator and intensity probe

In the semi-anechoic room, the surfaces of test samples were scanned according to the method described in [39] using a Brüel & Kjær 2260 Investigator as shown in Figure 3.6, analysed by Brüel & Kjær BZ7205 sound intensity software, and a Brüel & Kjær 3595 sound intensity probe kit. A set of three separate intensity measurements were taken for each test sample, each consisting of four scans of the surface shown in Figure 3.7 which were averaged in real time by the 2260. During scanning the probe was held at a distance of 100mm to 150mm from the sample surface. The measurement data was exported to a personal computer in the form of pressure and intensity levels for further analysis and calculation of the STL.

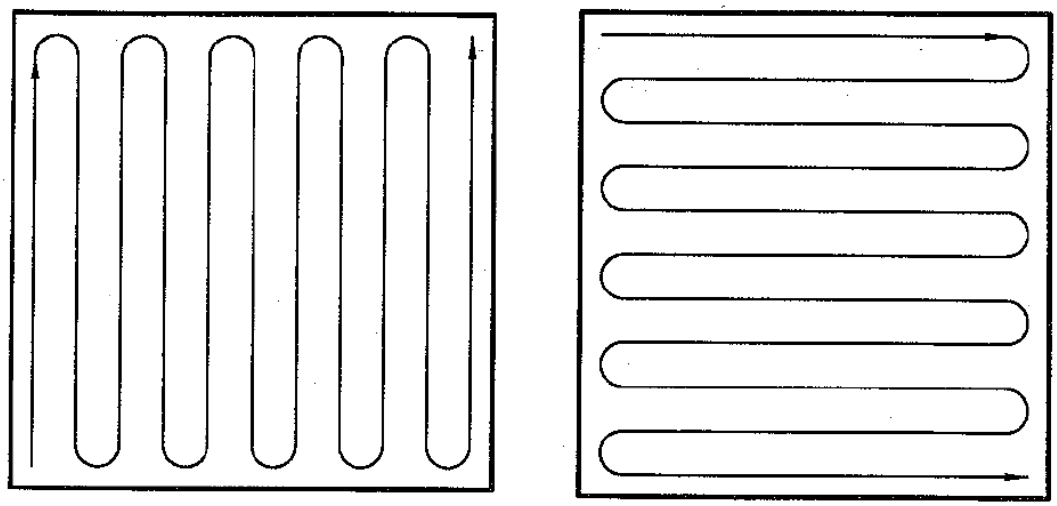

Figure 3.7 Sound intensity scan patterns

3.3.4 Calculations and background theory

The STL of each sample was calculated using:

$$\mathrm{STL} = \mathrm{L_{p(source\ room)}} - \mathrm{L_{I(receiving\ room)}} - 6 \tag{3.12}$$

where $\mathrm{L_{p(source\ room)}}$ is the average sound pressure level measured in the source room, and $\mathrm{L_{I(receiving\ room)}}$ is the average intensity measured using the 2260 in the receiving room. For each sample, average STL values were calculated by averaging the results from the three separate tests. Average values from five microphones $\mathrm{L_{p(source\ room)}}$ in the source room (5 microphones) were used to calculate the STL of each sample. For both of these cases energy averages of the sound levels were calculated as follows-

$$\mathrm{L_x} = 10\log_{10}\left[10^{\frac{\mathrm{L_{x1}}}{10}} + 10^{\frac{\mathrm{L_{x2}}}{10}} + \ldots + 10^{\frac{\mathrm{L_{x3}}}{10}}\right] \tag{3.13}$$

3.4 Results and Discussion

Three predictions models were computed and compared to the experimental results (see Figure 3.8 and 3.9). Two sandwich panels containing composite skins and PVC foam cores were investigated. As discussed in Chapter 2, the material properties are heavily frequency dependent, however the prediction models considered assume fixed material properties. An average Young's modulus and loss factor over the measured frequency range was used from the data described in Chapter 2 (see Table 3.2 and 3.3).

Table 3.2 Material properties of a 42mm sandwich construction

Density (kg/m³)	Thickness (m)	Poisson's ratio	Young's modulus (GPa)	Loss factor
86	0.042	0.3	0.14	0.039

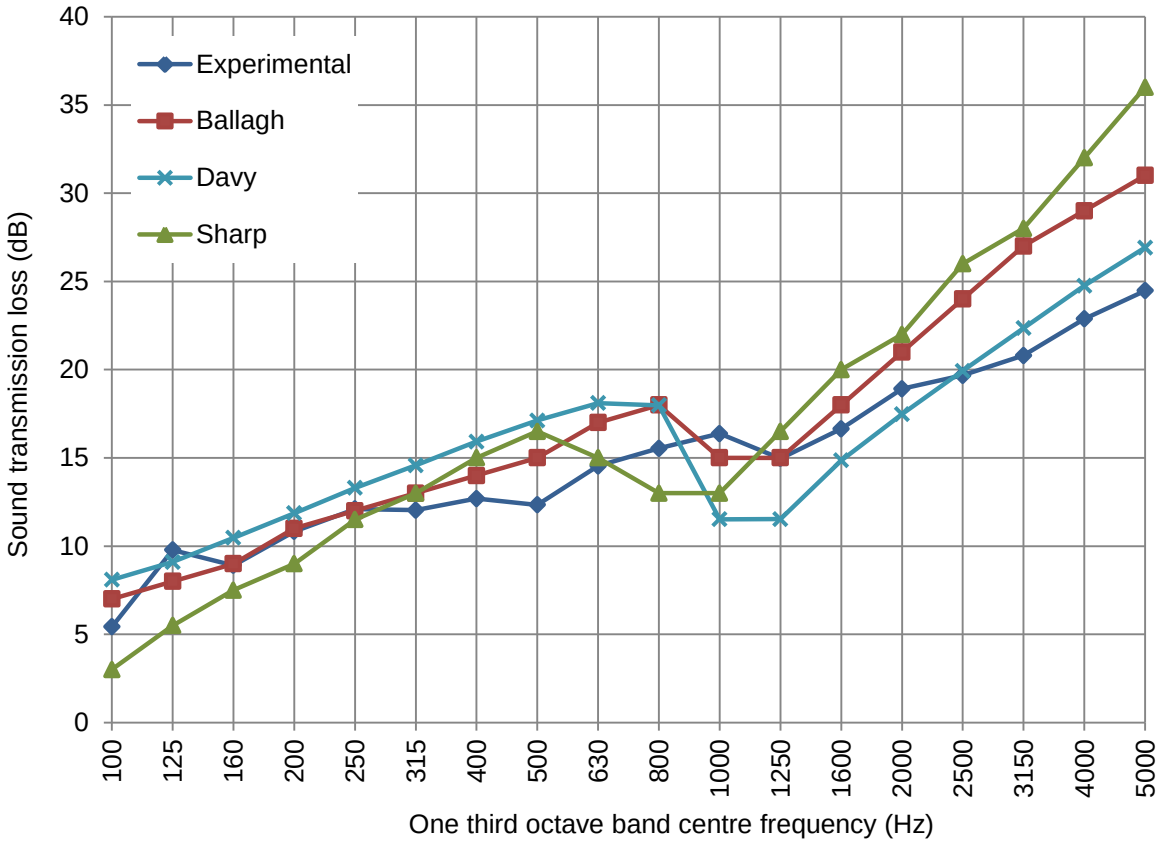

Figure 3.8 Experimental and prediction comparisons of the STL of a 42mm sandwich panel

There is a dip in the 1kHz one third octave band in the experimental data and all prediction models except Insul® which seems to only show the mass law prediction.

Table 3.3 Material properties of a 22.8mm sandwich construction

Density (kg/m^3)	Thickness (m)	Poisson's ratio	Young's modulus (GPa)	Loss factor
374	0.0228	0.3	1.3	0.028

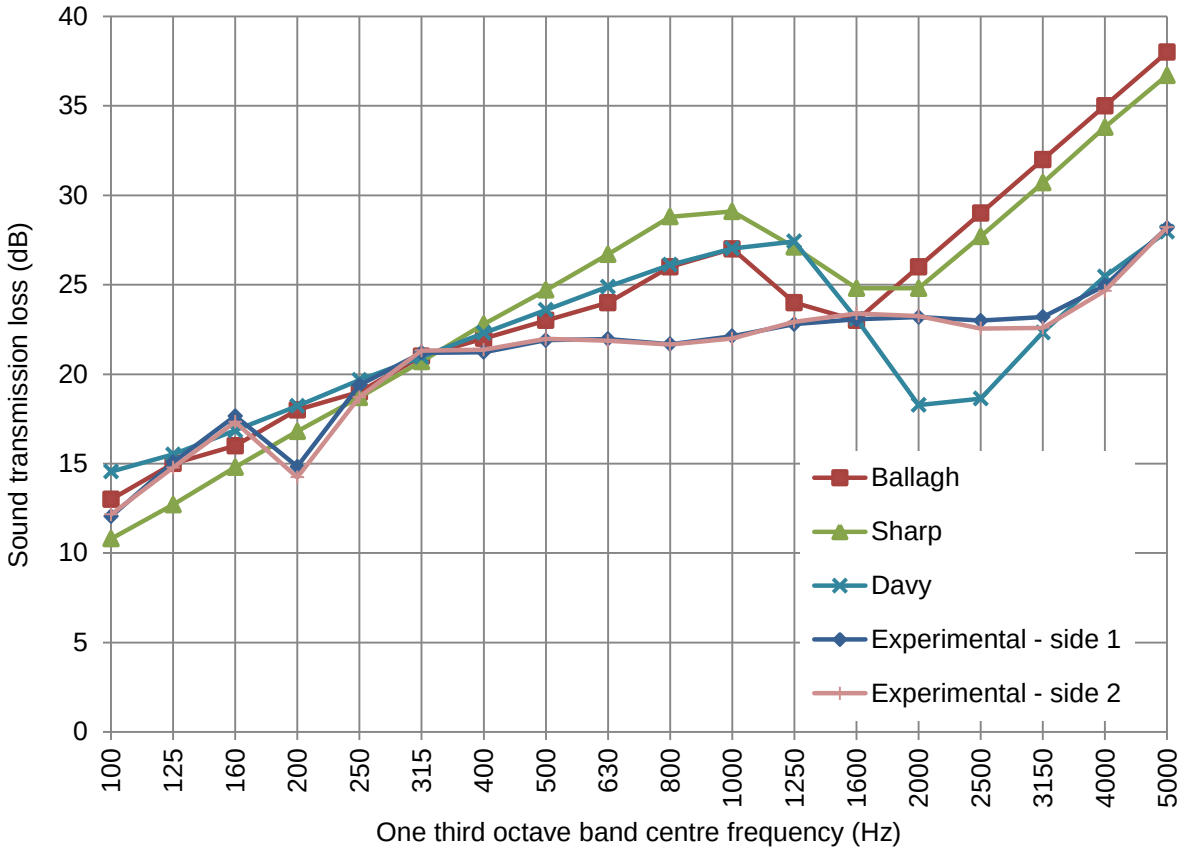

Figure 3.9 Experimental and prediction comparisons of the STL of a 22.8mm sandwich panel

The dilatational frequency was calculated as 11kHz for this construction which is well outside the frequency region of interest. It can be seen that none of the prediction models agreed with the experimental data over the entire frequency range of interest for a 22.8mm composite sandwich construction (see Figure 3.9).

The composite sandwich construction was experimentally tested in two positions as the skin thickness was different on each side at 2.1 and 1.8mm. Each side was placed on the source side and in turn in on the receiving side. There was no significant change in STL over the frequency range between the two orientations (see Figure 3.11).

All models accurately predicted the mass law region but all performed poorly in the coincidence region. Experimental results do not display a clear coincidence dip, but instead display a plateau in the STL from 315Hz to 3.15kHz . In chapter two the bending stiffness was found to reduce with increasing frequency consistent with the literature. This decrease is due to the shear stiffness of the core overcoming the bending stiffness of the laminated panel and is a well-known characteristic of laminated panels with stiff skins and lightweight cores. The agreement

between theory and experiment has been shown to be particularly poor in the coincidence region where it is often difficult to predict. The coincidence frequency region is sensitive to changes in bending stiffness.

The Ballagh and Sharp models are very similar and are based upon the Cremer and Sewell models which use a constant limiting angle of 78°. The main difference with the Davy model is that a variable limiting angle is used. The limiting angle is likely to describe the discrepancy between Davy, and Sharp and Ballagh. The Davy model was the only model to agree in the damping controlled region.

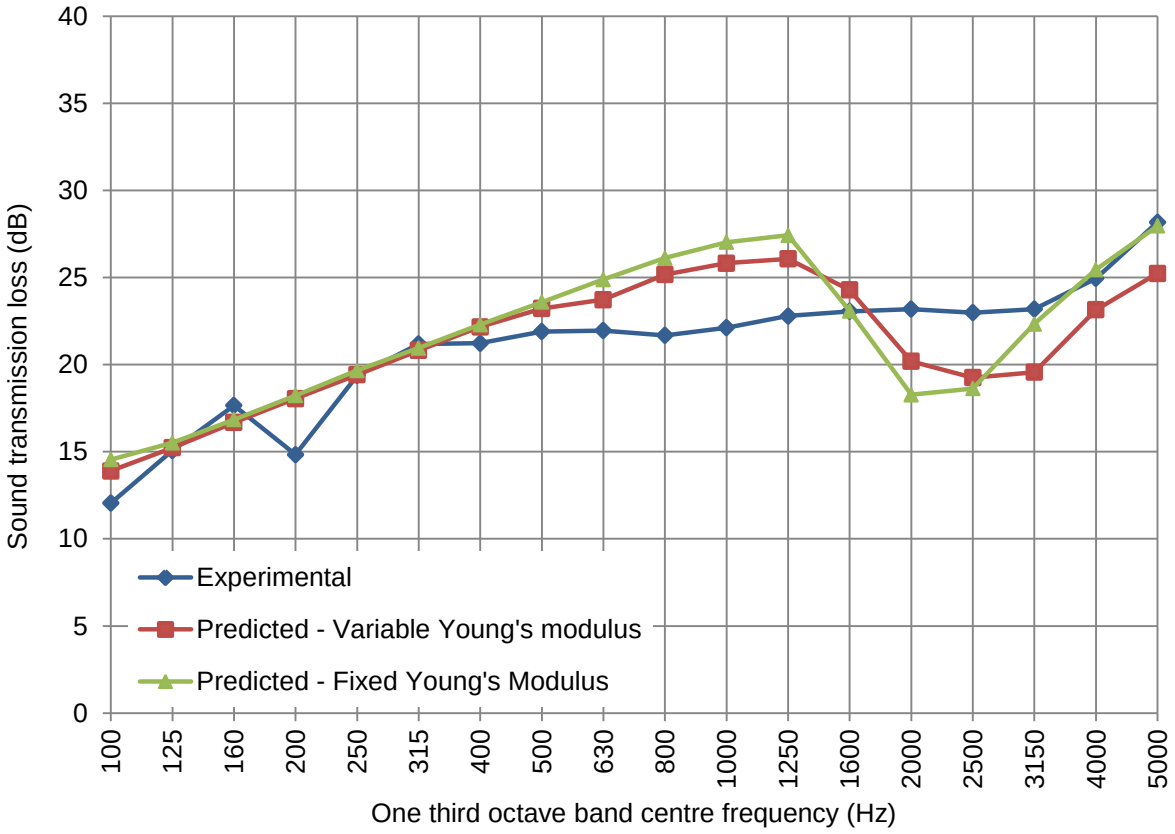

Figure 3.10 Experimental and prediction comparisons of the STL of a 22.8mm composite sandwich panel with a fixed and variable Young's modulus using theory from Davy [1]

In Chapter 2 it was shown that the Young's modulus decreases with increasing frequency. This is a characteristic of sandwich constructions with composite skins and PVC cores as shown in literature [28]. Prediction models considered in Figure 3.9 and 3.10 only had the ability to input a single value for Young's modulus. The Davy model was then modified by Davy to accommodate a variable bending stiffness in order to gain a better prediction comparative to experimental measurements.

The free-free boundary conditions measurement results in chapter 2 were used to represent Young's modulus in Figure 3.12. The mass law region appears to extend from 100Hz to 500Hz. It is apparent that the predictive model took into account variable stiffness and calculated the coincidence region at a third of an octave below the fixed stiffness. The coincidence region is between 500Hz and 3.15kHz which is the most difficult part of the STL curve to predict. A variable Young's modulus (or bending stiffness) provides slightly better agreement than a fixed Young's modulus.

The variable Young's modulus crosses over with the fixed Young's modulus at ≈ 2.5kHz. Above this cross over frequency a fixed Young's modulus provides the better agreement than a variable Young's modulus in the damping controlled region. In the damping controlled region a slope of 9dB/octave is observed. With a variable, decreasing with frequency Young's modulus the coincidence region becomes extended by one third of an octave compared with a fixed Young's modulus. The change in STL is not as significant as the change in Young's modulus with frequency because the bending wave speed is affected by a fourth root change in Young's modulus (see equation 2.6). A very large change in Young's modulus is required to achieve reasonable agreement in the coincidence region.

Limitations of the experimental work include the use of a finite panel with dimensions of 1550×950mm. The lowest frequency that can be accurately measured is the frequency with half the wavelength of the minimum dimension of the panel. Using equation 3.14 below it can be shown that this minimum frequency is 175Hz. Thus the one third octave bands below 175Hz may contain errors.

$$f = 0.5\frac{c}{\lambda} \tag{3.14}$$

The panel was clamped at fourteen positions evenly spaced at a torque of 1N/m against a thin foam strip recessed in the wall where it was assumed to be a fixed connection.

Kutrze and Watters [12] found that the ratio of static to dynamic stiffness can be in excess of 1000:1 and this created a plateau region of almost constant wave speed in the central region of the frequency range round the coincidence frequency, which increases with increasing frequency. The plateau region was observed (see Figure 3.12) and this region was not predicted well by Davy's model. It is difficult to predict STL of the critical frequency region as small changes in bending stiffness can have a significant effect on where this region occurs.

3.5 Conclusions

Due to the high level of variability no one model can predict the STL of all panel configurations. The prediction models investigated were poor at predicting the STL of either of the composite sandwich panels over mid-frequency range. This is because many of the prediction frequencies occur in the coincidence frequency dip due to the variation of the bending stiffness with frequency. However the Davy model was able to predict the STL accurately in the damping controlled and mass law regions. All models investigated, predicted the STL to within 3dB in the mass law region.

Chapter 4

4 Sorberbarrier® Noise Treatment Sound Transmission Loss Optimisation

Summary

A background and methodology for the optimisation of the noise treatment, Sorberbarrier® is presented. The results of optimisation of the Sorberbarrier® parameters using fractional factorial, design of experiments are presented. Fractional factorial design is a multi-variable analysis that identified the attachment method to produce the most significant effect on the performance of STC.

4.1 Introduction and Background

Sorberbarrier® is a product manufactured by Pyrotek Noise Control for use in engine rooms and enclosures. Pyrotek Noise Control develops and manufactures a range of noise control products applied in commercial and industrial buildings and the marine industry. Sorberbarrier® is expected to perform acoustically by increasing the sound transmission loss (STL) and sound absorption, meet fire regulations and resist decomposition in harsh conditions.

4.1.1 Objectives

1. Identify the significant parameters that affect the STL of Sorberbarrier®
2. Determine the optimal parameter settings that maximise STL
3. Evaluate the effectiveness of fractional factorial design as an optimisation technique for noise control materials

4.1.2 Sorberbarrier®

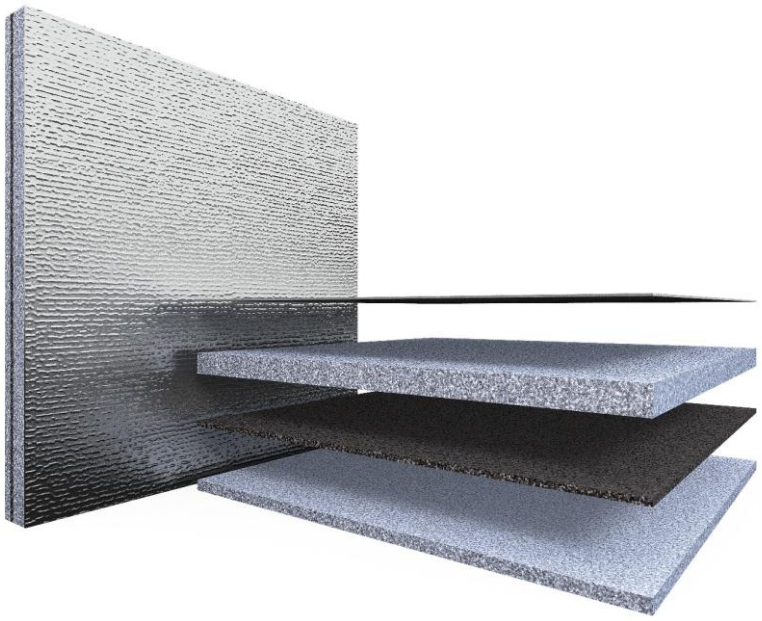

Figure 4.1 Sorberbarrier® [40]

Sorberbarrier® is an acoustic treatment applied to wall constructions that require improved performance. The material is also required to be flame resistant. Sorberbarrier® consists of a layer of polyurethane foam, a flexible mass barrier (Wavebar®), a second thicker layer of polyurethane foam and an aluminium film facing. Sorberbarrier® is typically attached to the noise source side of wall constructions and noise is reduced by the sound absorption of the

foam. The Sorberbarrier® product comes in a range of foam thicknesses and barrier weights (see Table 4.1), the product is selected based on space availability and performance required for the application.

Table 4.1 Sorberbarrier ® ALR product specifications [40]

Product name	Total thickness (mm)	Absorptive layer (mm)	Mass barrier (kg/m²)	Decoupling layer (mm)
Sorberbarrier ALR20/4.5	20	12	4.5	6
Sorberbarrier ALR25/4.5	25	12	4.5	12
Sorberbarrier ALR32/4.5	32	25	4.5	6
Sorberbarrier ALR32/8.0	32	25	8	6
Sorberbarrier ALR50/4.5	50	25	4.5	25
Sorberbarrier ALR50/8.0	50	25	8	25
Sorberbarrier ALR75/4.5	75	50	4.5	25
Sorberbarrier ALR75/8.0	75	50	8	25

4.1.3 Sorberbarrier® attachment methods

Sorberbarrier® has no structural properties and is a limp material. Sorberbarrier is commonly attached to wall constructions by pinning or pressure (or contact) adhesive. Depending on the environment surface pins can be either adhered or stud-welded. In this study the adhered pin will be investigated. The recommended adhesive for attaching Sorberbarrier® is either a pressure or contact adhesive. In this study contact adhesive is investigated.

The pins used by this study have a perforated base (see Figure 4.2) but a solid base is also available. The bases are 50×50mm and are made out of mild steel, stainless steel or aluminium. Two types of clips are used to fix Sorberbarrier® to the pins as shown in the Figure 4.2. Domes are used to improve the aesthetic finish and to cover the ends of the sharp pin. Flat rectangular clips are an alternative.

Figure 4.2 Pins specified by Pyrotek [40]

Pins are specified to be spaced 50-80mm from the edges and 280mm between centres (see Figure 4.3). The recommendation is based on the structural load pins can carry without failure. This layout can vary depending on the barrier mass used and foam thickness.

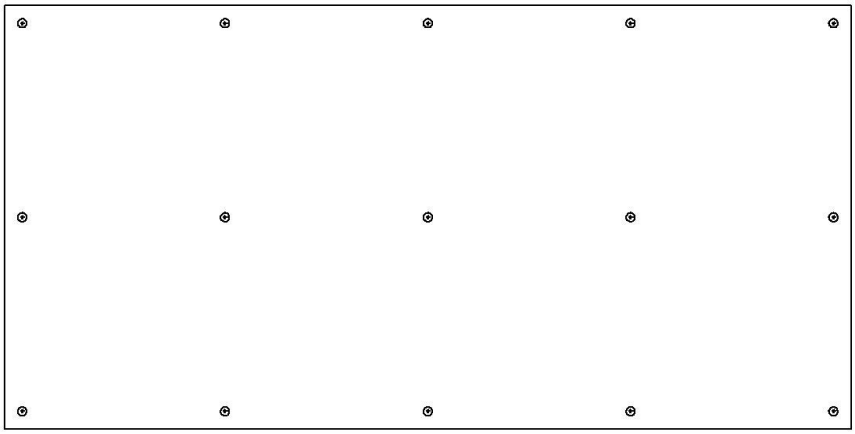

Figure 4.3 Typical pin layout as specified by Pyrotek [40]

4.1.4 Bonded versus unbonded

Pyrotek don't specify any acoustic advantage related to the bonding method. It is important to understand the acoustic system as a whole as well as break the system down into its individual components as minimising structural paths and increasing impedance mismatch has been well documented to increase STL performance. The primary mechanism for STL improvement is reflection due to impedance mismatch and sound reflection. Bonding or gluing noise treatments onto wall constructions creates a structural connection where the impedance mismatch is less

advantageous than pinning. The stiffness of the construction varies depending on the attachment method and this may also affect the STL.

Bolton [41] investigated polyurethane foam multi-panel structures (0.762mm and 1.27mm thick face sheets with 27mm thick polyurethane foam) and compared the performance of bonded versus unbounded. A simple system of one aluminium sheet attached to polyurethane foam was evaluated using experimental and predictive methods and good agreement was found between the two approaches. A significant difference was found between the systems depending on how the aluminium was bonded to the polyurethane foam.

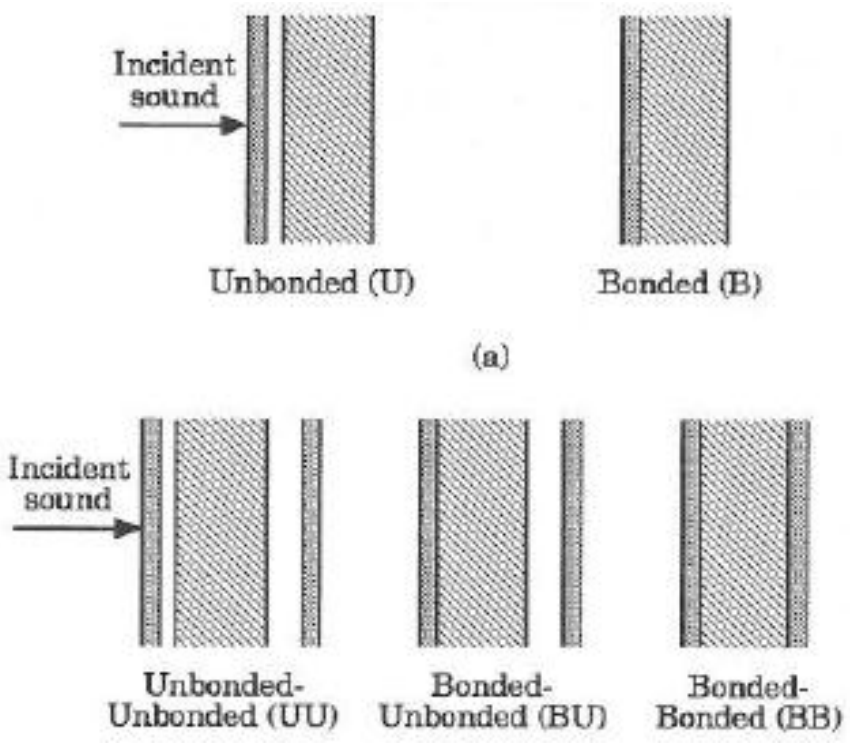

(a) single panel (b) double panel

Figure 4.4 Cross-sectional view of lined panel configurations [41]

STL testing was performed on one sheet of aluminium inclusive and exclusive of polyurethane foam on the transmitted side. It was found that the unbonded configuration produced a higher STL than the aluminium sheet with the aluminium sheet simply following the mass law of 6dB/octave (see Figure 4.4). Below 1kHz bonded performs better than unbonded. Stiffness is increased in the bonded configuration by the applied foam layer which moves the coincidence dip into the frequency range of interest at 2kHz.

The double leaf configurations investigated contained layers of aluminium, foam and aluminium (see Figure 4.5). It is important to note in this study that in the unbonded and unbounded-unbonded configurations there is an air gap of 2mm on the incident side and in the double wall, a 6mm gap on the transmitted side. In the BU configuration there is a 14mm gap on the transmitted side.

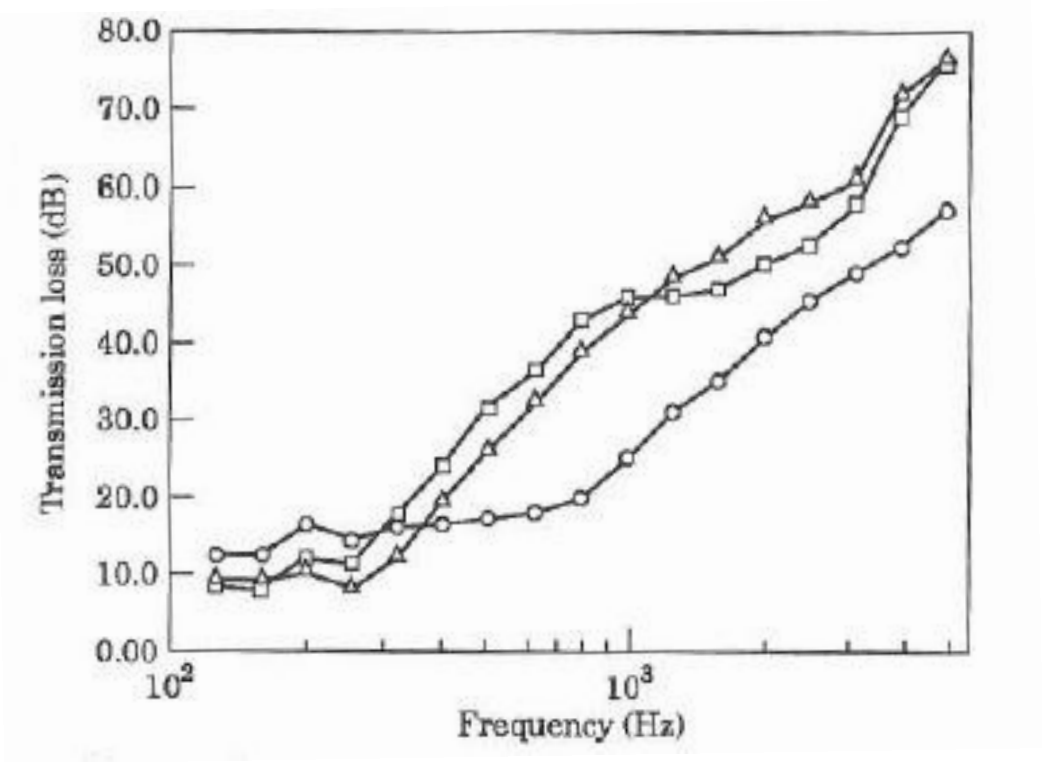

Key: UU (▲), BU (■), BB (●)

Figure 4.5 Summary of measured results [41]

Bonded-bonded gives the highest STL below 400Hz where the panel behaves as a single leaf (see Figure 4.5). Unbonded-unbonded behaves as a double leaf panel without structural connections and has a double panel resonance at 250Hz. The mechanism for this resonance is the outer masses vibrating against the cavity filled with foam as a mass-spring-mass system. After the double panel resonance the STL curve has an 18dB/octave slope. STL of both bonded-unbonded and unbounded-unbonded show the same trend due to the isolation of the structural connections between the panels. Bonded-unbonded shows a higher STL up to 1kHz, then above 1kHz unbounded-unbonded is greater. It can be concluded from this study that double leaf wall constructions provide a better STL per mass than single leaf wall constructions assuming appropriate design and construction.

4.1.5 Design of Experiments

For development of products it is essential to understand the behaviour of the system, the amount of design, manufacture and installation variability and the effect each variable has on the overall performance of the system. It is often important to explore the relationship between the key variables and the total performance of the product.

Experiments are often conducted with a series of tests that produce a quantifiable outcome. A common approach used today is One-Variable-At-a-Time (OVAT), where one variable is changed leaving all other variables constant. This approach investigates a multi-parametric space by sampling along the axes of each variable and may include important combinations or interactions of variables. This approach requires luck, experience, intuition and often guesswork. OVAT is often unreliable, time intensive, inefficient and may not produce optimum conditions. The application of design of experiments (DOE) is wide and can be used to reduce development time, manufacturing costs and increase the understanding of key interactions between inputs and outputs. Below are the outcomes achieved by using DOE method [42].

- Determine the design parameters or product variables that affect the mean product performance
- Determine the design parameters or product variables that influence performance variability
- Determine interactions between variables
- Determine the design parameters that yield the optimum performance
- Determine whether further improvement is possible

It is important to know how much effect each variable has on the overall performance. Interactions between variables are important to determine if there is in fact no interaction, synergistic interaction or antagonistic interaction. A specific combination of variables may work together to produce a negative effect where the opposite is also possible which is why the ability to determine interaction effects is so valuable.

Fractional factorial design is used when a large number of parameters are investigated and where time and cost is limited. The downside is that confounding effects during low resolution tests can make it difficult to draw clear conclusions. To remove confounding effects a full factorial design can be implemented. Full factorial design can be very time and cost intensive unless a small number of parameters are investigated. Chapter 5 investigates and implements a full factorial design.

4.2 Methodology

See Chapter 2 for details of the STL experimental method

4.2.1 Fractional factorial design

Six design parameters were chosen for this project. 2-levels of design parameters were used instead of 3-levels as information was readily available to 2-levels. Each of the design parameters were chosen because STL theory suggested possible gains. See Figure 4.7 and Table 4.2 for the changes made to Sorberbarrier®.

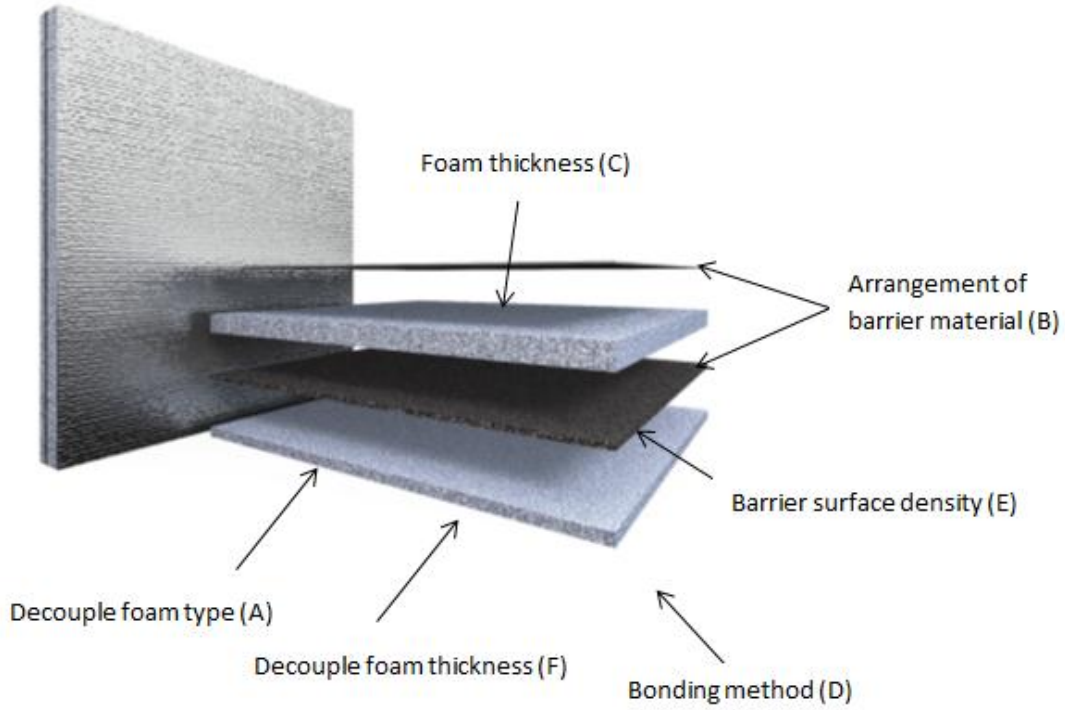

Figure 4.6 Design parameters

Table 4.2 List of factors of interest at two levels

Factor	Label	Low level	High level
Decouple foam type	A	Flat	Dimples
Arrangement of barrier material	B	Between foam	Outer side of foam
Outer foam thickness	C	23mm	46mm
Bonding method	D	Pinned	Glued

Barrier surface density	E	4.5kg/m²	8kg/m²
Decouple foam thickness	F	23mm	46mm

The composite sandwich panel that was studied in Chapters 2 and 3 was used as the base panel on which Sorberbarrier® was attached and tested. The panel represented a typical construction used in deckheads and bulkheads of marine craft. The STL of sixteen panels (1550×950mm) were measured at The University of Canterbury as an array of arrangements of Sorberbarrier® (see Table 4.2). The STC was recorded for each run.

Apart from analysis of the main effects there were also important interaction effects that were analysed. In order to minimise error, each experiment was performed under the same conditions (temperature, humidity and when background noise level was less than 40dB). The trial order of experiments was randomised to reduce errors. Each experiment was repeated three times and averaged.

Six main factors and three interaction effects were of interest. The total degrees of freedom were eight. For fractional factorial design 2^(k-p) was used where k is the number of variables and p is the fraction of a full factorial design. The number 2 corresponds to the number of levels investigated which is two in this case. This experiment used 2^(6-2) which is a quarter replicate of a full factorial experiment. The design matrix is shown in Table 4.3.

4.3 Results and Discussion

4.3.1 Design matrix

Table 4.3 shows the results for each experimental run as a single number, Sound Transmission Class (STC). For design of experiments a single number must be used. STC is often used to describe the STL performance of wall constructions. The highest STC was obtained in run 8 and the worst was in run 13.

Table 4.3 Design matrix of a 16-run experiment with 6 factors

Run	Decouple foam type (A)	Arrangement of barrier material (B)	Outer foam thickness (C)	Bonding method (D)	Barrier surface density (E)	Decouple foam thickness (F)	STC (dB)
1	-1	-1	-1	-1	-1	-1	34
2	1	-1	-1	-1	1	-1	37
3	-1	1	-1	-1	1	1	43
4	1	1	-1	-1	-1	1	40
5	-1	-1	1	-1	1	1	39
6	1	-1	1	-1	-1	1	39
7	-1	1	1	-1	-1	-1	41
8	1	1	1	-1	1	-1	43
9	-1	-1	-1	1	-1	1	32
10	1	-1	-1	1	1	1	38
11	-1	1	-1	1	1	-1	34
12	1	1	-1	1	-1	-1	35
13	-1	-1	1	1	1	-1	31
14	1	-1	1	1	-1	-1	34
15	-1	1	1	1	-1	1	36
16	1	1	1	1	1	1	39

Note: See Appendices for the STL curve of each run.

4.3.2 Pareto plots

To identify and analyse the main effects and interactions of the performance of Sorberbarrier® a Pareto plot was constructed (see Figure 4.7). The Pareto plot displays the absolute value of standardised values. Significant levels show that the effect is unlikely to be due to pure chance. Low significance levels indicate a possible random effect which should be ignored.

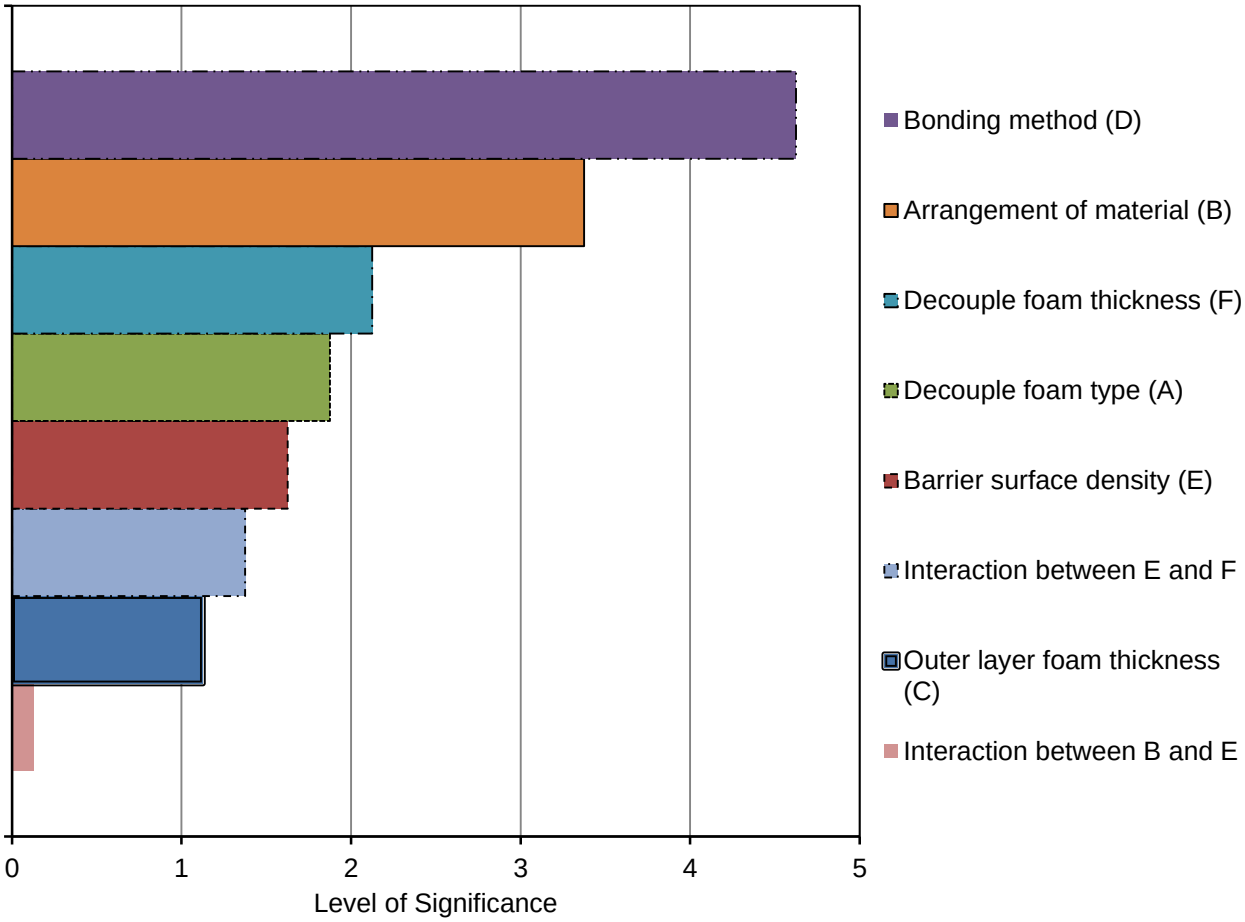

Figure 4.7 Pareto plot of the effects and interactions using STC

Figure 4.7 demonstrates that the bonding method had the greatest influence on STC. By using pinning rather than glued bonding, the structural connection is reduced which increases low frequency performance. Increasing low frequency performance is often favourable when designing for a high STC due to the curve fitting technique used.

Gluing and pinning also have a significant effect on stiffness of the wall system. It is possible to work backwards from experimental data to estimate the difference in stiffness between pinned and glued configurations. This will not be investigated in this project but is an important consideration for future work.

Arranging the material effectively changes the decoupling layer thickness which is also the same as changing parameter F. Increasing the decouple layer increases the cavity between the two masses of the double leaf wall system. This foam decouple layer reduces resonances or dips in the frequency range of interest occurring between the mass layer and wall construction the Sorberbarrier® is attached to. It is interesting that the barrier surface density has a low level of significance. It would be expected the mass law would increase the sound insulation over the frequency range resulting in a much greater level of significance. Fractional factorial design is limited by 2-levels where the change in the 2-levels of one parameter may out weight or over shadow a change in another parameter. For example if the barrier surface design was increased by a factor of ten instead of two, the level of significance of other parameters be would greatly be over shadowed and distort the representation of the interactions. The outer layer of the foam produced the least significant effect. This was expected as the outer layer of foam's primary function is noise reduction inside the room/enclosure due sound absorption. Sound absorption is investigated in Chapter 5.

The mass-air-mass resonance frequency f_0 used by Davy in his double leaf model [1] and shown in equation 4.1 causes a dip in the STL curve with double wall constructions where the air acts as a spring between the two wall masses.

$$f_0 = \frac{1}{2\pi}\sqrt{\frac{\rho c^2}{d m_r}} \tag{4.1}$$

where m_r is the reduced mass of the two panels, ρ is the density of air, c is the speed of sound in air and d is the cavity depth or in this project, the decouple thickness.

The ratio of masses of the composite sandwich panel and the mass loaded barrier are combined to give the reduced mass (m_r). This affects the normal incidence mass-air-mass resonance frequency, f_0 of a double leaf panel (see equation 4.1). The reduced mass is calculated from equation 4.2 where the mass per unit surface area of the composite sandwich panel was 8.5kg/m², where m_1 and m_2 are the mass per unit areas of each panel.

$$m_r = \frac{m_1 m_2}{m_1 + m_2} \tag{4.2}$$

The 8.5kg/m² barrier has a resonant frequency of 90Hz whereas the 4.5kg/m² barrier has a resonance frequency of 108Hz. Both have a cavity depth of 0.1m. After the resonance frequency, the STL curve gradient typically increases at 18dB/octave. A high reduced mass gives a low resonance frequency which is beneficial to achieving the 18dB/octave gradient increase

compared to 6dB/octave below the resonance frequency. Figure 4.11 displays a 14dB/octave increase from 100Hz to 315Hz with the 8kg/m² barrier.

Figure 4.8 shows the effect of the barrier mass per unit area (m_2) on the reduced mass where the composite sandwich panel (m_1) remains constant. Figure 4.8 shows that large a difference between the two mass per unit area leads to a smaller change in the reduced mass.

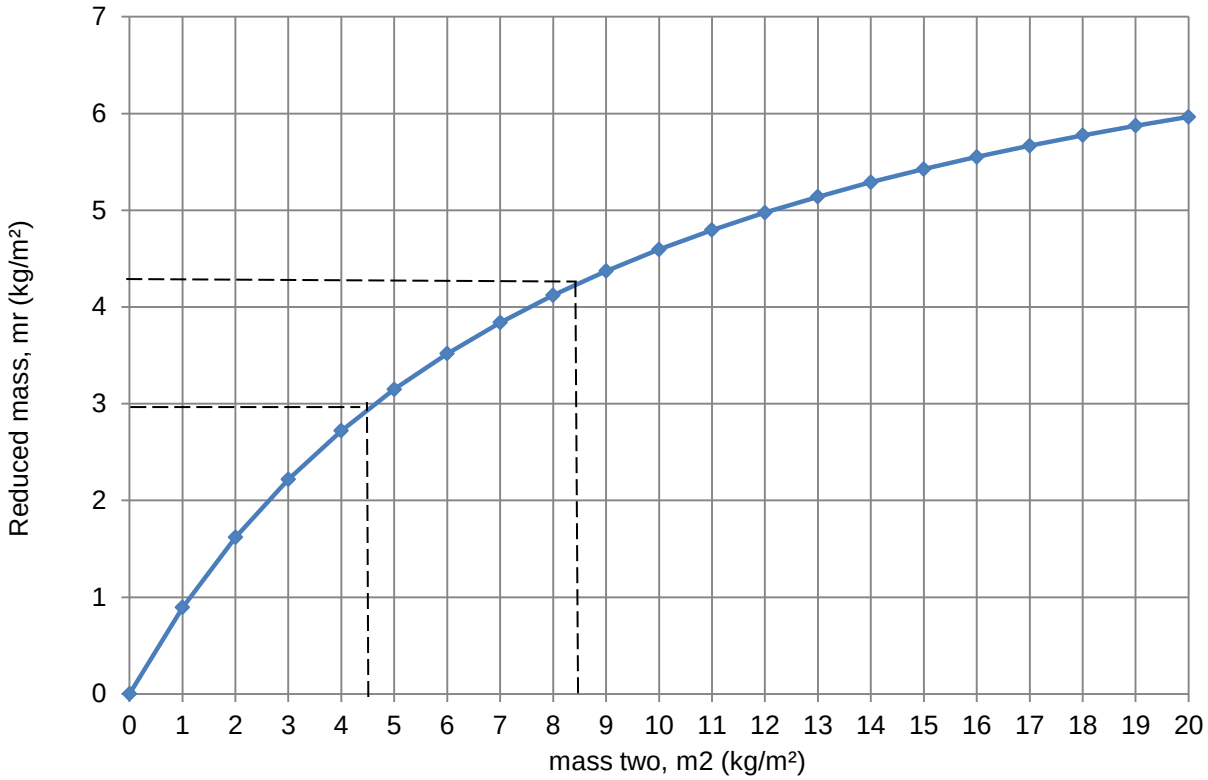

Figure 4.8 Effect of mass 2 on reduced mass

Two interactions were considered in this experiment. The first was between barrier surface density (E) and decoupling foam thickness (F). The second interaction considered was the arrangement of material (B) and barrier surface density. Both interactions had a low level of significance so were not working together or against each other. It is important to identify interactions between variables and establish whether they are synergistic (two factors working together) or antagonistic (two factors cancelling each other out).

Another means of obtaining a single performance number over a greater frequency range than STC is to simply subtract the sum of the STL values over the frequency range of interest for the sandwich panel without noise treatment from the same sum for the composite sandwich panel inclusive of the noise treatment. The significance of the parameters is shown in Figure 4.9 for this single number rating. It can be seen that all parameters have remained similarly

proportioned except the significance of bonding method has dropped. This is because only low frequencies are affected and this is less important with the new measure where higher frequency performance becomes more important.

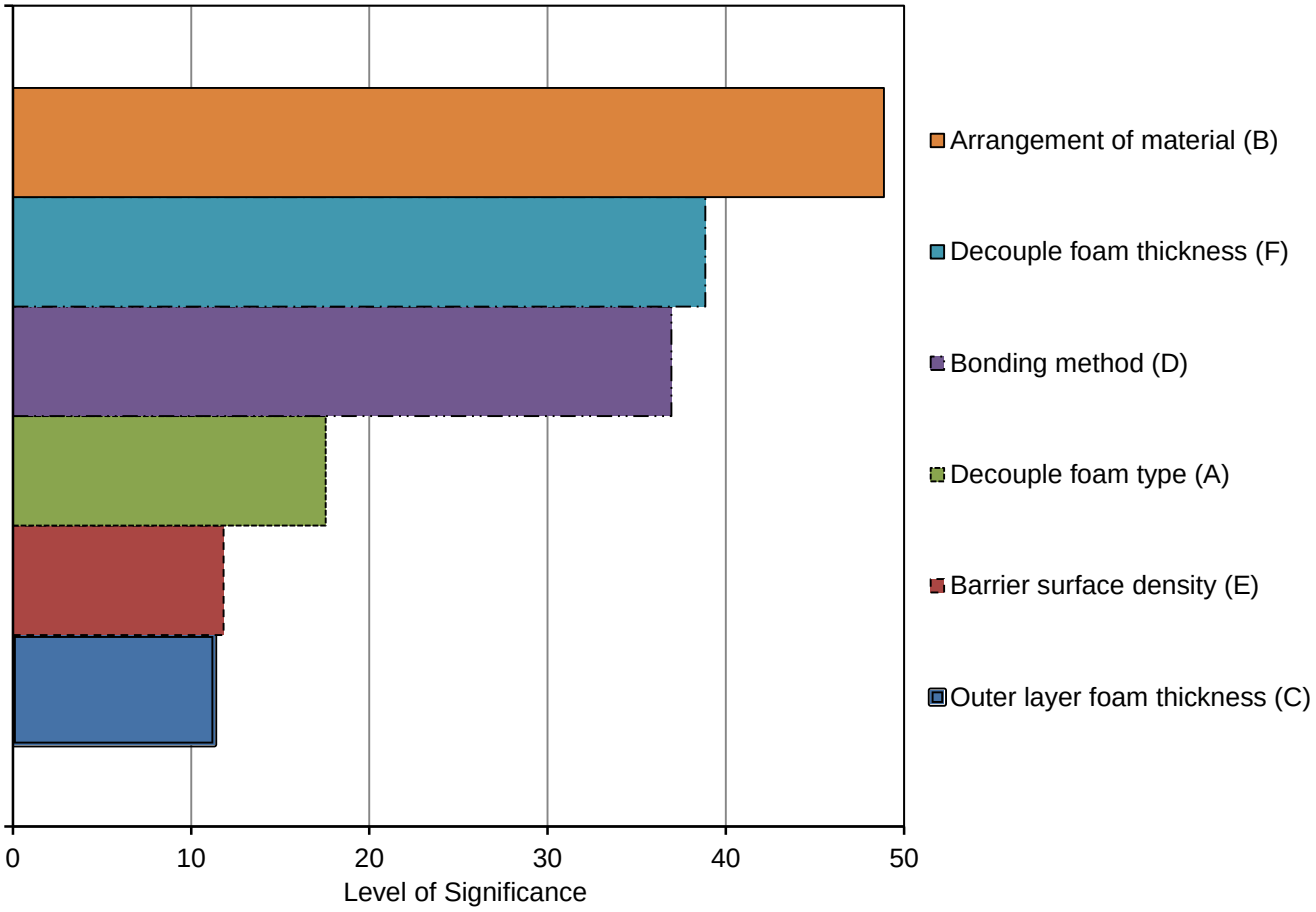

Figure 4.9 Pareto plot of the effects and interactions using the difference in the sums of the STL values

Table 4.4 Optimal parameters

Design Factor	Setting
A	Dimpled foam (high level)
B	Outer side of foam (high level)
C	46mm outer foam thickness(high level)
D	Pinned (low level)
E	8kg/m² (high level)
F	46mm decoupling layer thickness(high level)

The optimal parameter settings to maximise the STC are shown in Table 4.4. These are used later in this chapter to predict the optimal STC rating.

Figure 4.10 shows the effects of each design factors. The dotted line is the average STC obtained across all the tests. The likely STC rating that would be obtained is shown by the line plots for each parameter. The most significant parameters are the bonding method, then arrangement of barrier material and the decouple foam thickness.

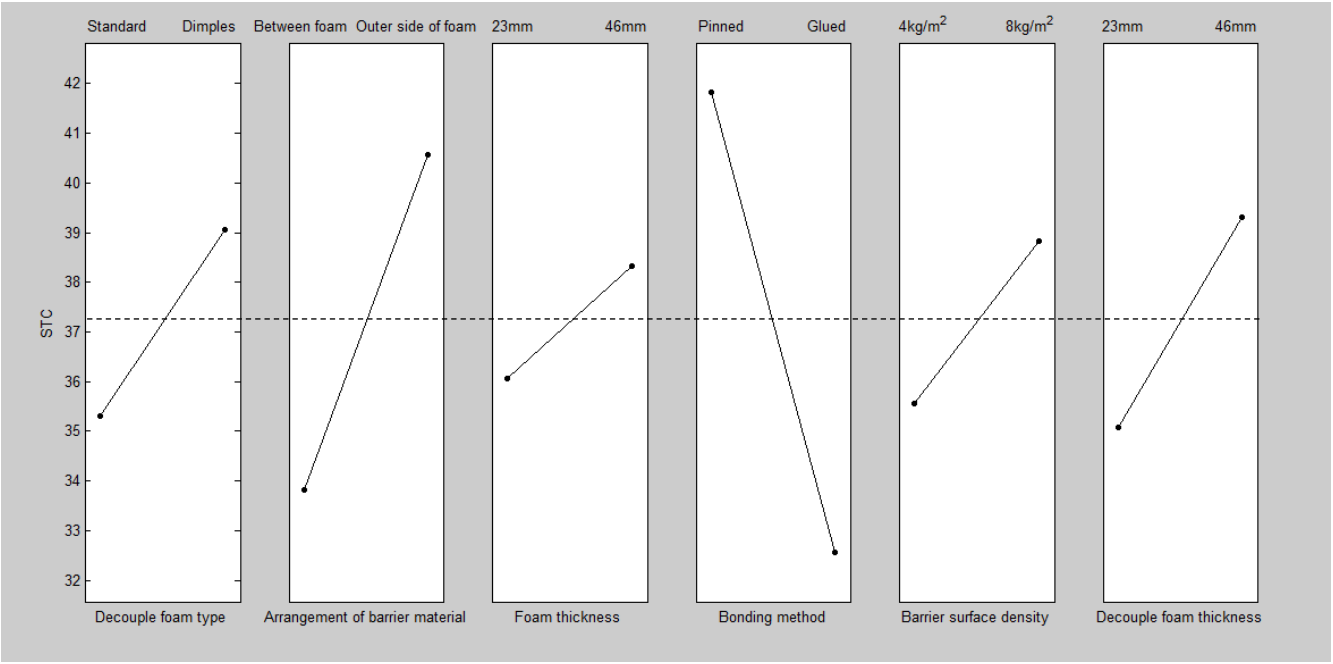

Figure 4.10 Main effects plot of the design parameters

4.3.3 Prediction model

Having identified the significant main and interaction effects which influence the STC, it was considered important to develop a simple regression model which provides the relationship between STC and the critical effects. The use of this model is to predict the STC for the different factors at their best levels. It is important to note that the regression coefficients are half the estimates of the effects. The regression model for the STC as a function of significant main and interaction effects is given by equation 4.3.

$$\hat{y} = \beta_0 + \beta_1(A) + \beta_2(B) + \beta_3(C) + \beta_4(D) + \beta_5(E) + \beta_6(F) \qquad (4.3)$$

where β_0 = overall mean STC, β_1 is the regression coefficient of factor A (decouple foam type), β_2 is the regression coefficient of factor B (arrangement of barrier material), β_3 is the regression coefficient of factor D (bonding method), β_4 is the regression coefficient of factor F (decoupling

foam thickness). Factors B, C and E are not significant enough to incorporate into the model. The predicted model for STC is calculated in equation 4.4, 4.5 and 4.6.

$$\hat{y} = 37.19 + \beta_1(A) + \beta_2(B) + \beta_3(D) + \beta_4(F) \quad (4.4)$$

$$\hat{y} = 37.19 + (0.94 \times 1) + (1.69 \times 1) + (-2.315 \times -1) + (1.065 \times 1) \quad (4.5)$$

$$\hat{y} = 43 \quad (4.6)$$

The best model Figure 4.11 below displays the measured STL where the STC was calculated as 44, providing very good agreement between experimental and predictive models.

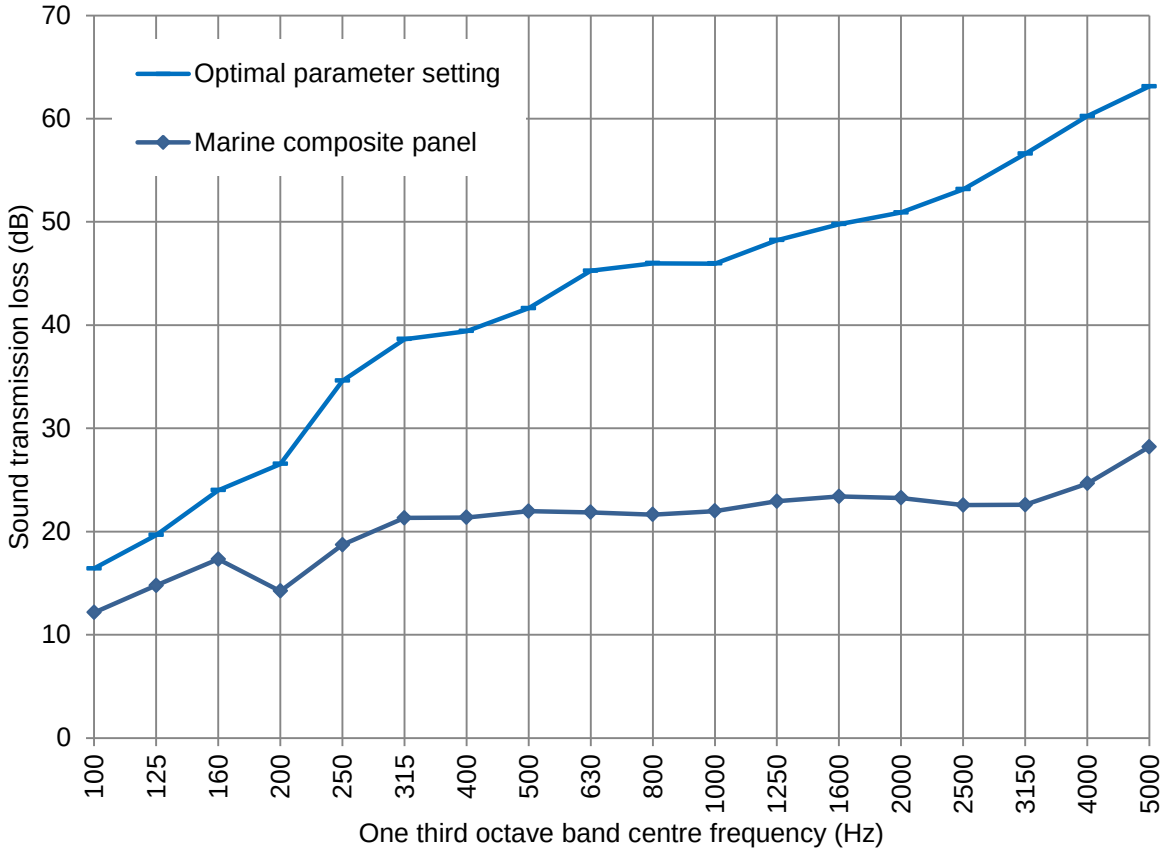

Figure 4.11 Experimental data with optimal configuration of parameters

4.3.4 Confounding pattern of factor effects

In factorial designs, the main effects will be confounded and it can be difficult to make a clear conclusion during low resolution interactions. To avoid this high resolution fractional factorial design can be used. The downside of using a high resolution fractional factorial design is time and cost and a balance must be found depending on the need for optimal results.

4.4 Conclusions

The most significant parameters that affect the STC of Sorberbarrier® are the decoupling layer foam thickness and the bonding method. The pinned bonding method provided the most significant increase in STC performance compared to gluing. The second most significant factor was the arrangement of material that yields a thicker decoupling layer thickness. Increasing the decoupling layer thickness increases the STC rating.

The optimal settings to maximise the STC are listed below.

- High level (Dimples)
- High level (Outer side of foam)
- High level (46mm)
- Low level (Pinned)
- High level (8kg/m²)
- High level (46mm)

Fractional factorial design was effective as a STL optimisation technique when used as a pilot in an optimisation study. Although exact optimal setting cannot be reached since only two levels are examined, this study does identify the factors most likely to be significant in achieving an optimal design.

Chapter 5

5 Sound Absorption Optimisation of a Noise Treatment Product

Summary

A background and methodology for the optimisation of sound absorbing coefficients of the noise control material, Sorberbarrier® is presented. The results of optimisation of the Sorberbarrier® parameters using full factorial, design of experiments are presented. Full factorial design is a multi-variable analysis that identified the outer foam layer to produce the most significant effect on the sound absorption. The effects of a face foil and barrier thickness are investigated. These are shown to have a significant effect on the sound absorption coefficients.

5.1 Introduction and Background

Sorberbarrier® is a product manufactured by Pyrotek Noise Control for marine engine rooms and enclosures. This material absorbs sound and increases sound transmission loss (STL) as well as meeting fire regulations and resisting decomposing in harsh conditions.

The previous chapter investigated optimisation of the sound transmission loss (STL) using a method from the Design of Experiments (DOE) (fractional factorial design) and this method proved successful at identifying the significant parameters that affect STL. DOE was performed to identify significant parameters affecting sound absorption in this chapter. A full factorial design is used in this chapter, in contrast to the fractional factorial design used for STC, to produce a higher resolution of significant parameters.

In the previous chapter it was demonstrated that the outer layer of foam had an insignificant effect on STL. Pyrotek's reasoning for attaching the outer layer of foam to their product, Sorberbarrier® is to provide sound absorption.

5.1.1 Objectives

1. Identify the differences between the experimental reverberation time (RT) and Sabine's equation for RT
2. Identify the significant parameters that affect the absorption performance of Sorberbarrier®
3. Determine the parameter settings that produce the optimal absorption performance
4. Identify the effect of covering the open pores of foam with (i) thin aluminium foil and (ii) a relatively thick mass loaded barrier
5. Evaluate the effectiveness of a full factorial design as an acoustic optimisation technique

5.1.2 Sound absorption coefficient

The sound absorption coefficient is the factor by which the intensity of sound energy decreases when reflected from a material. Sound is absorbed by visco-thermal shearing which converts sound energy into heat. Methods to determine the absorption coefficient include the reverberation room method, flow of resistivity method, the impedance tube method and theoretical models. The reverberation method was used in this study.

5.1.3 Reverberation time (RT)

Sabine's equation is applicable when the average sound absorption coefficient is less than 0.1 which is typically the case in reverberation rooms. The absorption coefficient of painted concrete walls, columns and steel diffusers were used (with their respective areas) to calculate the RT in each one octave band frequency.

$$RT = \frac{55.3V}{\alpha Sc} \tag{5.1}$$

where RT is the reverberation time in seconds, V is the volume of the empty reverberation room, α is the average sound absorption coefficient, S is the absorbing surface area of the room and c is the speed of sound in air.

5.1.4 Experimental reverberation time

The reverberation method measures the RT of an empty reverberation room or reference room configuration which is then subtracted from the RT of the same room with absorption material mounted in an appropriate way.

$$A_T = 55.3V\left(\frac{1}{c_2 RT_2} - \frac{1}{c_1 RT_1}\right) - 4V(m_2 - m_1) \tag{5.2}$$

$$\alpha = \frac{A_T}{S} \tag{5.3}$$

where A_T is the equivalent sound absorption area, subscript 1 denotes the conditions of an empty reverberation room and subscript 2 denotes the conditions of a reverberation room containing the test specimen, c is the speed of sound in air and m is the power attenuation due to propagation of sound through air in the room.

5.1.5 Material mounting

If an acoustically transparent material is mounted very close or glued to a wall the fibrous or porous material absorbs 0% - 20% of the incident sound energy. Sound absorption provided by a material over the frequency range depends primarily on the distance mounted from the wall, number of folds, flow resistivity and weight of the fabric [43]. An air cavity generally increases the absorption performance up to an optimal distance. An optimal flow resistance of 1235 MKS Rayls was found for ¼ wavelength cavity depths [44]. The absorption coefficient over the frequency range is very

sensitive to cavity depth. At a quarter of the wavelength of the sound in air the particle velocity is maximised hence maximising the visco-thermal shearing. The process of visco-thermal shearing converts sound energy into heat.

5.1.6 Porous liner covered with a limp impervious layer

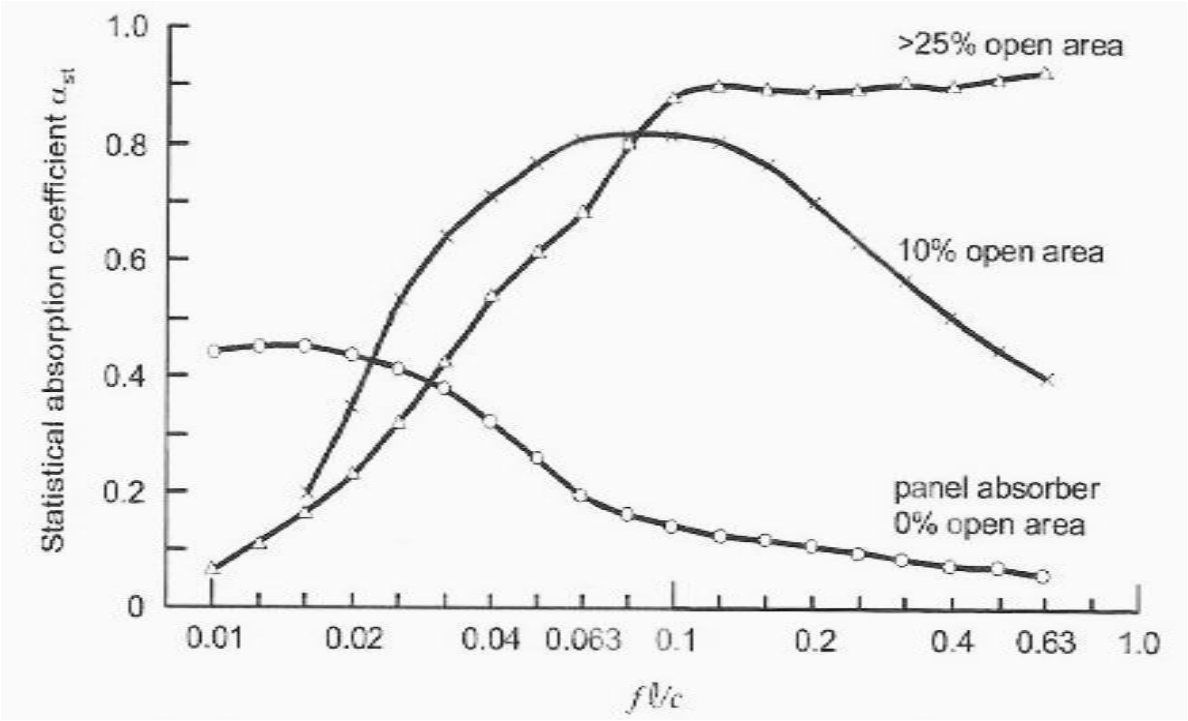

Figure 5.1 The effect of perforations on the sound absorption of a panel backed by a porous liner [2]

Sorberbarrier® is a porous liner covered with a mass loaded barrier, another porous liner then a limp impervious layer. The limp impervious layer protects the porous liner from dust, oil, chemicals and fire.

The statistical absorption coefficient of a panel with surface weight of 2.5kg/m² and a thickness of 3mm is used in the study by Bies and Hansen [2] (see Figure 5.1). The porous liner is 50mm thick and has a flow resistance of $5\rho c$. The x-axis label is frequency, multiplied by the effective length of each of the porous holes at high frequency and the speed of sound in air c. A trend is shown that at higher percentages of open area, the absorption coefficient is higher. When a limp impervious layer covers a porous liner, the high frequencies cannot pass through and are reflected. Low frequency absorption performance increases because of a resonance between the mass of the limp layer and the stiffness of the air cavity behind it. Once the open area is greater than 25% the absorption performance flattens at high frequencies and very little gain is achieved by increasing the open area

further. Maximum absorption occurs at the first resonance of the coupled panel-cavity system. If a foil is sufficiently thin (20µm), the effect is not measurable and foil can be assumed to be acoustically transparent. The effective normal impedance at the outer surface of the material, Z_{NB} can be calculated by equation 5.4.

$$Z_{NB} = Z_N + j2\pi f\sigma' \tag{5.4}$$

Where f is the frequency of the incident sound, tone or centre frequency of a narrow band of noise, σ' is surface density, Z_N is the normal impedance of the porous material and j is $\sqrt{-1}$. Table 5.1 lists the properties of aluminium foil similar to that used in Sorberbarrier®.

Table 5.1 Material properties of aluminum foil

Material	Density (kg/m³)	Typical thickness ($10^{-6}m$)	Surface density $\sigma'(kg/m^2)$	Speed of sound in material (approx.) (m/s)
Aluminium	2700	2-12	0.0055-0.033	5150

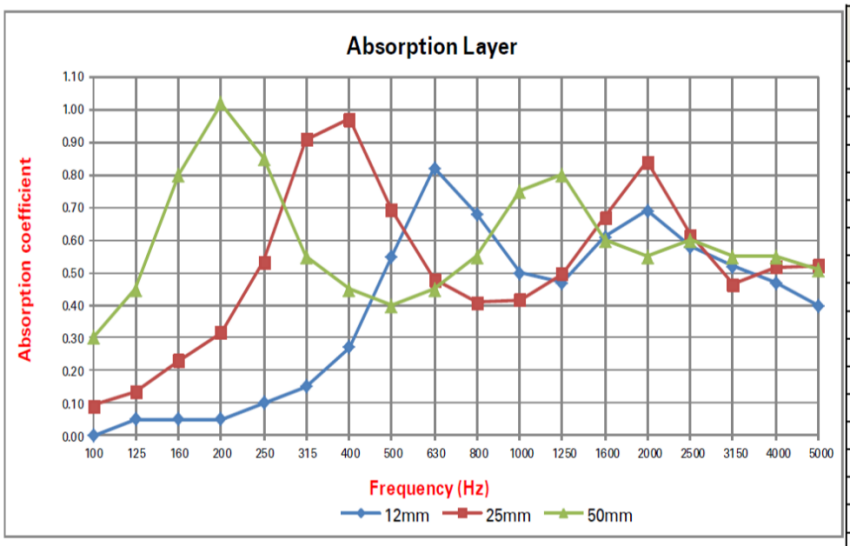

Frequency (Hz)	12 mm	25 mm	50 mm
100	0.00	0.09	0.30
125	0.05	0.14	0.45
160	0.05	0.23	0.80
200	0.05	0.32	1.02
250	0.10	0.54	0.85
315	0.15	0.91	0.55
400	0.27	0.97	0.45
500	0.55	0.69	0.40
630	0.82	0.48	0.45
800	0.68	0.41	0.55
1000	0.50	0.42	0.75
1250	0.47	0.50	0.80
1600	0.61	0.67	0.60
2000	0.69	0.84	0.55
2500	0.58	0.61	0.60
3150	0.52	0.47	0.55
4000	0.47	0.52	0.55
5000	0.40	0.52	0.51
NRC	**0.50**	**0.60**	**0.65**

Figure 5.2 Absorption coefficients of various foam thicknesses [45]

Figure 5.2 shows the absorption coefficients of three thicknesses of Sorberbarrier® foam with a thin foil attached to the face side. The results shown in Figure 5.2 do not agree with Bies and Hansen [2] as the foil is sufficiently thick or thin that acoustically it should be transparent. A cause for this discrepancy could be due to the adhesive used to attach the foil to the porous foam. An adhesive

may increase the effective mass per unit area of the thin foil layer which increases the impedance, hence reduces absorption performance.

The lower frequency sound absorption coefficient peaks occur at the resonant frequency due to mass of the foil and the stiffness of the air cavity filled with porous foam. At high frequencies the absorption coefficient decreases because of reflections from the fireproof foil. At lower frequencies, noise passes through the fireproof foil and into the porous foam as the foil is effectively transparent.

5.1.7 Flow resistivity

Acoustical transparency is a measure of the passage of sound through a material and depends primarily on the amount of open area of the material. A material that provides very little reflection is an effective absorber.

Table 5.2 Flow resistivity [46]

Foam (see Figure 5.3)	Flow resistivity (MKS Rayls/m)
A	18000 – 26000
B	28000 – 35000
C	26000 – 44000

Kim [46] investigated the sound absorption performance of foam and the effects of a film facing applied to the foam surface. Table 5.2 lists three types of foam with different ranges of flow resistivity. The thickness of foam was 12.3mm. The sound absorption coefficient was measured from 200Hz-3kHz (see Figure 5.3). Foam A with the lowest flow resistivity had the lowest absorption coefficient where sample B and C had significantly higher. When a film facing is applied, foam A produces the highest sound absorption at frequencies above 800Hz (see Figure 5.4). Below 800Hz foam B and C perform slightly better and produce a similar result over the entire frequency range considered.

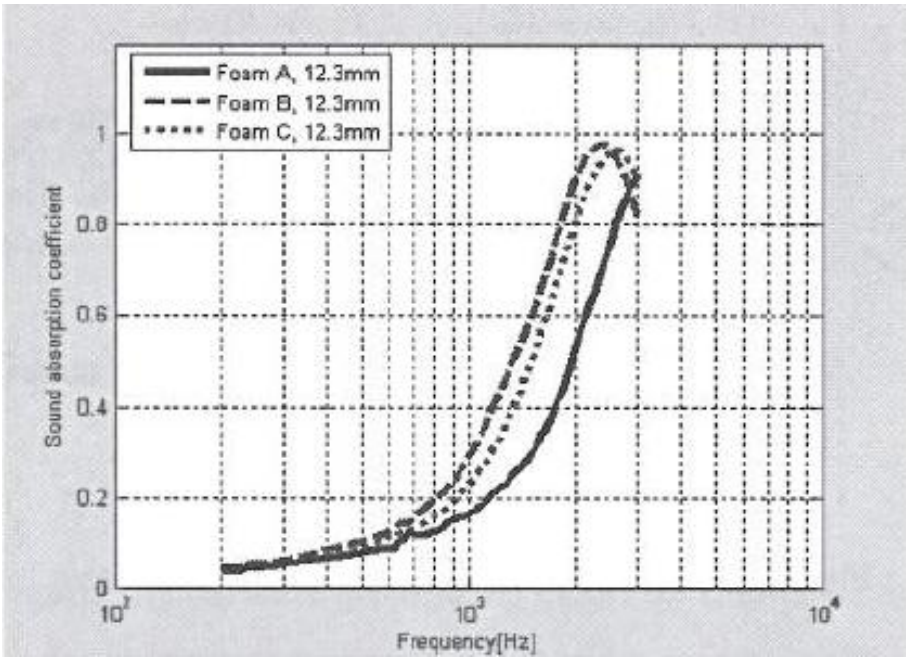

Figure 5.3 Experimental sound absorption coefficients for materials in Table 5.2 [46]

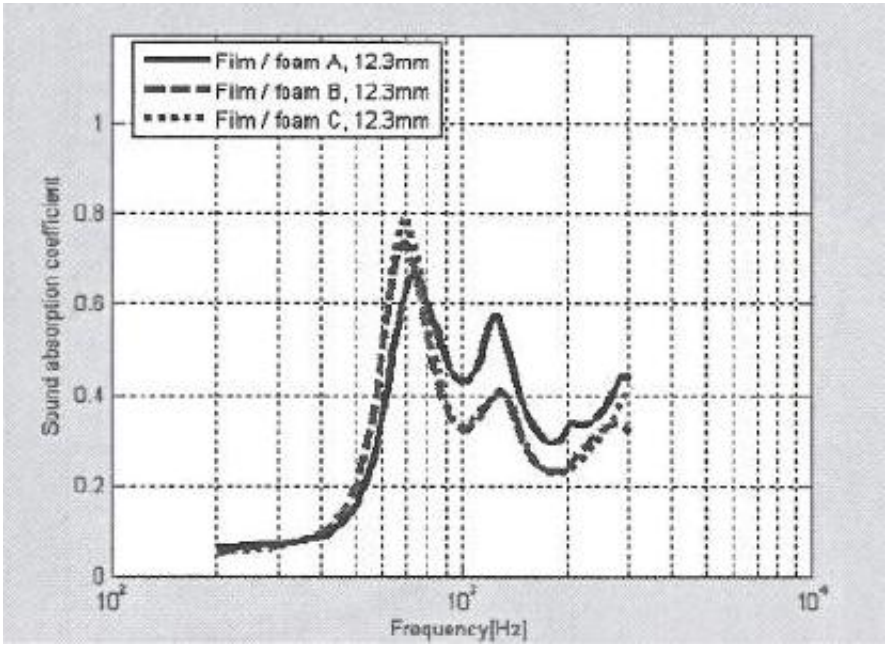

Figure 5.4 Experimental sound absorption coefficients for a range of flow resistivity in film faced foams [46]

5.2 Methodology

5.2.1 Full factorial design

Chapter 4 describes One-Variable-At-a Time (OVAT) and fractional factorial design theory. In this chapter a full factorial design was be implemented. Figure 5.5 shows changes made to Sorberbarrier® and Table 5.3 defines the high and low variable settings.

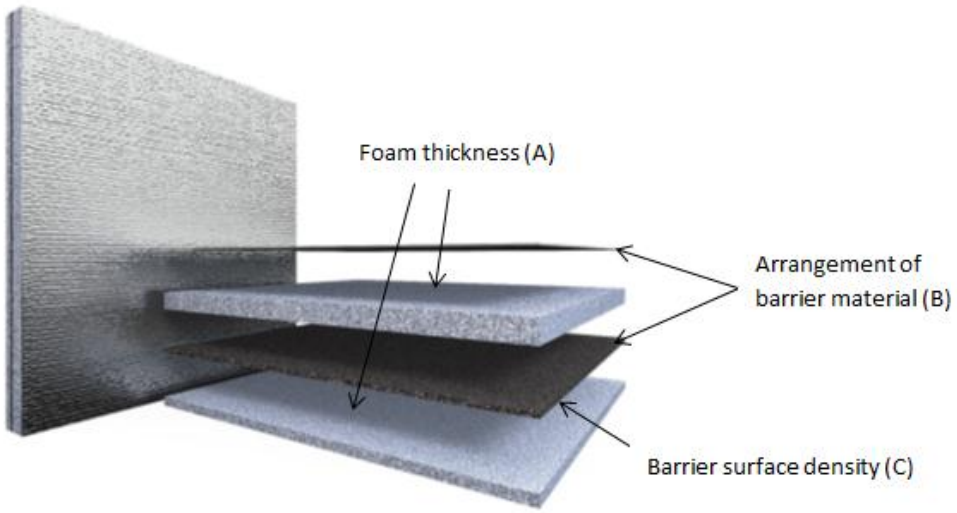

Figure 5.5 Design parameters

Full factorial design is often used when the number of variables is less than or equal to four. To investigate a trial with more than four factors using full factorial design becomes very time and resource intensive where 2^5 or more runs must be investigated and a fractional factorial design would normally be implemented in this case. The advantage of using full factorial design is that all possible combinations for all levels of variables are investigated which removes all confounding effects [42].

Table 5.3 List of factors of interest at two levels

Factors	Labels	Low level	High level
Foam thickness	A	46mm	92mm
Arrangement of barrier material	B	Between foam	Outer side of foam
Barrier surface density	C	4.5kg/m²	8kg/m²

Three design parameters were chosen for this experiment based on absorption theory suggesting possible gains. In order to make the experiment achievable, 2-levels of design parameters were used instead of 3-levels. Figure 5.5 and Table 5.3 shows the high and low level variables for each factor. In this analysis a linear response was assumed over the range for each variable.

5.2.2 Experimental procedure and equipment

According to ISO354:2003 [47] a reverberation room must be at least 150m³.The RT was measured with microphones placed at a height of 1.5m around the room in random positions at least 1m from any diffusers, walls and 2m from the sound source as specified in [47] (see Figure 5.6). A B&K dodecahedron loudspeaker produced pink noise at a sound level of about 95dB, the signal to background noise ratio was very large. A Pulse system was used to record and analyse the results. Eight different microphone positions and two speaker positions were used to determine the RT of the reverberation room. Each measurement with set speaker and microphone positions were repeated three times and averaged. The temperature and humidity was recorded to verify they complied with [47]. The equipment used is listed in Table 5.5.

Table 5.4 Reverberation room dimensions

Walls	116.1m²
Floor	60.1m²
Ceiling beams	85.2m²
Concrete columns	9.2m²
Volume	217.0m³
Total surface area of the room	305.1m²

Table 5.5 Equipment used during testing

Description	Manufacturer	Model	Serial Number
Analyzer	Brüel & Kjær	PULSE C Frame with 7539 5 Channel Module	2483932
Dodecahedron Loudspeaker	Brüel & Kjær	OmniPower 4296	2071500
Amplifier	Brüel & Kjær	2716	2301358

Microphones	Brüel & Kjær	4189-L	2573559 2573560 2573561 2573562 2573563

The empty room RT was measured first then the material was laid out on the floor as shown in Figure 5.7 and the measurement repeated. Eight absorption tests were performed with the eight configurations of Sorberbarrier® provided in the Table 5.3. The Noise Reduction Coefficient (NRC) was calculated for each test. Apart from the main effects analysed, there were also important interaction effects that will be analysed. In order to minimise error, each experiment was performed under the same conditions (temperature, humidity and when background noise level is low). The experimental trial order was randomised.

5.2.3 Test facilities

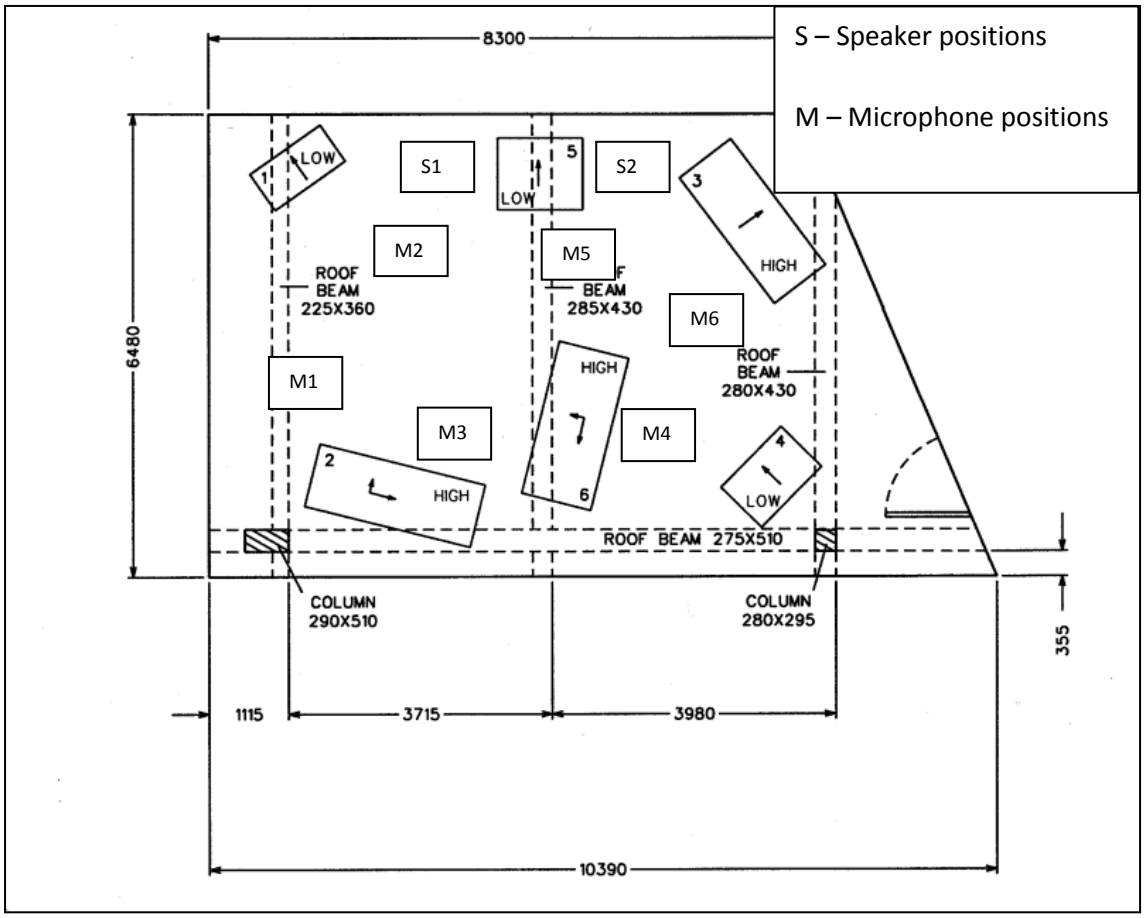

Figure 5.6 Test facility

Figure 5.7 Material mounted in reverberation room with foil face sheet

5.3 Results and Discussion

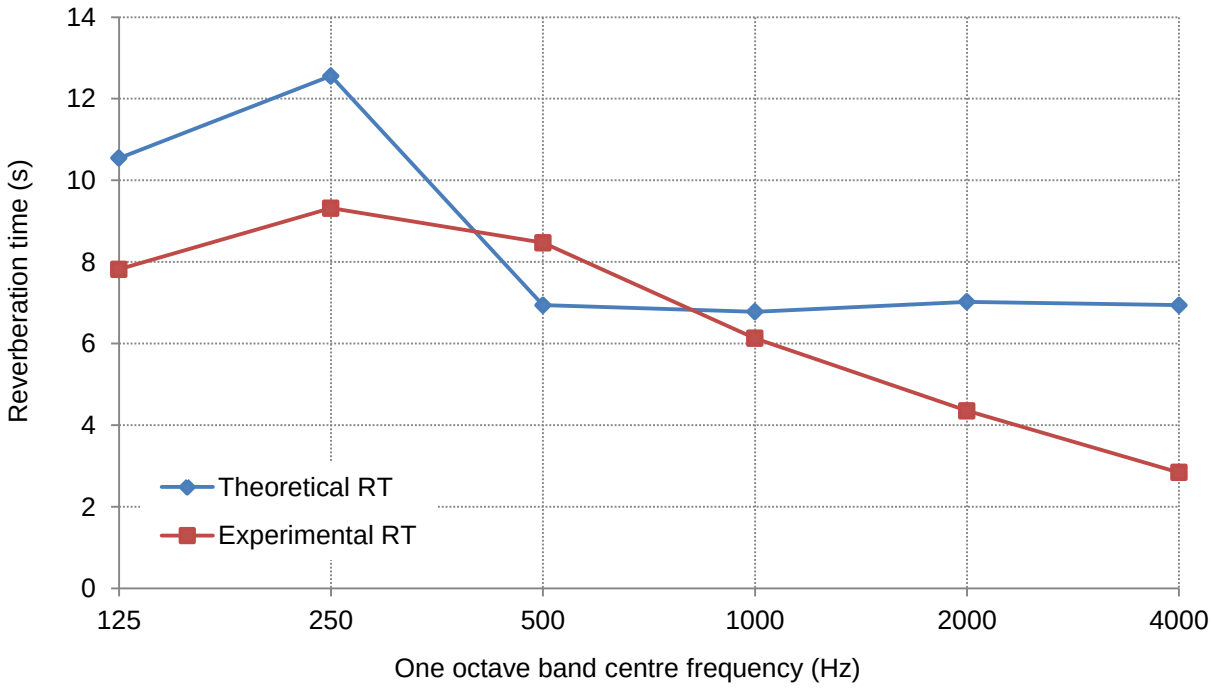

Figure 5.8 Predicted and experimental empty reverberation room RT

Figure 5.8 compares the theoretical and experimental RTs in the University of Canterbury's reverberation room and shows good agreement in the 500-1kHz one octave bands. The other octave band centre frequencies differ by 2.5-4s. Discrepancies at low frequencies are probably due to the fixed room dimensions. Absorption of a room is not solely determined by the materials inside as air absorption at high frequencies can be significant. Air absorption is most likely to explain discrepancy at the higher frequencies.

5.3.1 Design matrix

Table 5.6 shows the NRC results for each experimental run (a single number must be used). NRC is typically used to simplify the description of the sound absorption performance of materials allowing easy comparisons between absorbers. NRC averages the absorption coefficient over four octave band frequencies; 250Hz, 500Hz, 1000Hz and 2000Hz to obtain a single number. The best performance was obtained in run 2 and the worst in run 7.

Table 5.6 Design matrix of an 8-run experiment with three factors

Run	A	B	C	NRC
1	-1	-1	-1	0.74
2	1	-1	-1	0.94
3	-1	1	-1	0.20
4	1	1	-1	0.23
5	-1	-1	1	0.73
6	1	-1	1	0.93
7	-1	1	1	0.22
8	1	1	1	0.23

5.3.2 Pareto plots

To identify and analyse the main effects and interactions of the performance of Sorberbarrier® material, a Pareto plot was used. A Pareto plot displays the absolute value of the standardised values.

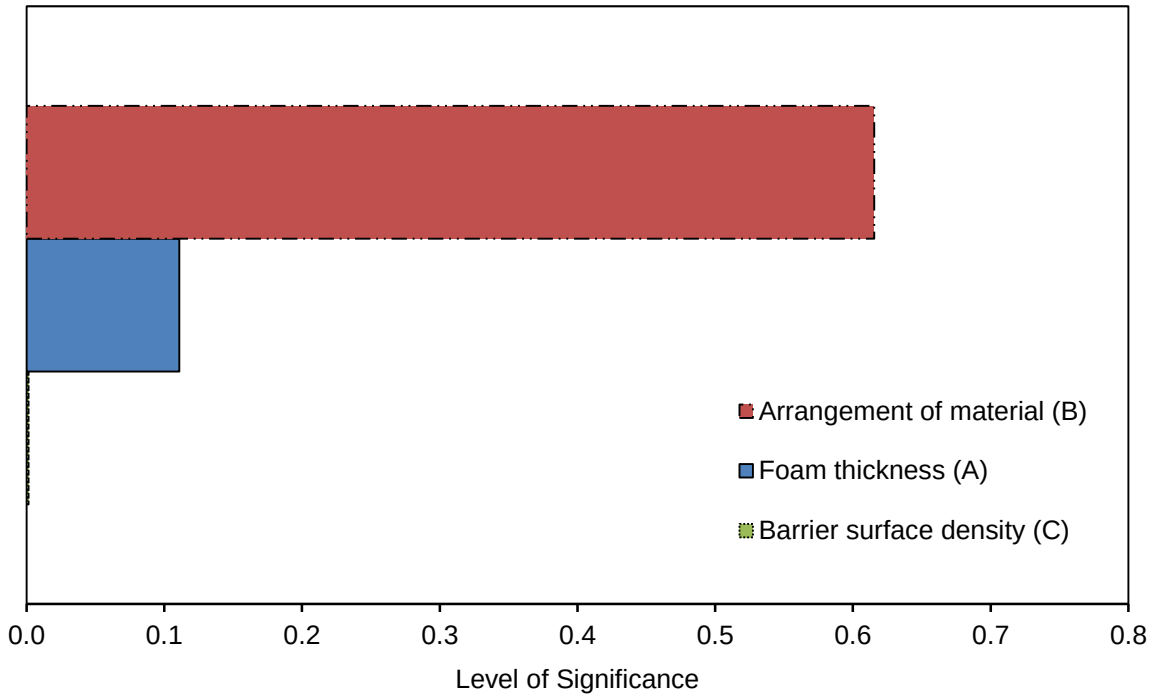

Figure 5.9 Pareto plot of main effects

The most significant effect on NRC is the arrangement of material. An outer layer of foam provides greater performance gain than when the foam is inside the barrier where essentially the face sheet is changed from a thin foil to a thick mass loaded barrier. The effect of a face sheet on foam is investigated later in this chapter.

The thickness of the foam material has a significant effect on the NRC. As the thickness increases, more of the porous material is in a higher acoustic particle velocity region. The absorption coefficient increases across the frequency range but the greatest effect occurs at low frequencies.

The barrier surface density had no effect on NRC of Sorberbarrier® as would be expected. The optimal settings to maximise the NRC are listed in Table 5.7.

Table 5.7 Optimal parameters

Design Factor	Setting
A	96mm (high level)
B	Outer side of foam (low level)
C	Barrier surface density (no effect)

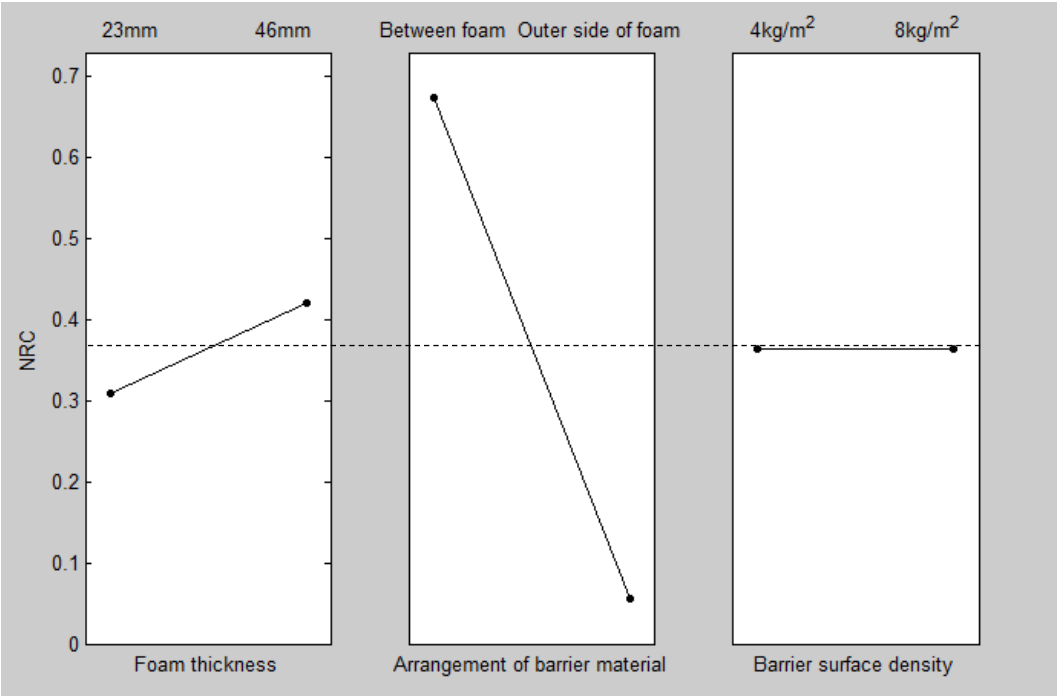

Figure 5.10 Main effects plot of design factors

Figure 5.10 shows the effects of each design factor. The dotted line is the average NRC obtained across all the tests. The likely NRC rating that would be obtained is shown by the line plots depending on the variable used assuming no interaction effects between the variables. The most significant parameters were the arrangement of the barrier material and the foam thickness. The barrier surface density had no effect on NRC.

5.3.3 Face sheets

The thickness of the aluminium foil was 18µm. This was laid flat over the foam but not glued. Above 2kHz the absorption coefficient decreases from 0.95 to 0.49 at 10kHz. The thickness of the mass loaded barrier was much greater than the foil which significantly decreased the absorption performance (see Figure 5.11). The thicker the face sheet, the greater the reflection and less noise is able to pass into the foam, where the absorption occurs. The sound absorption coefficient of the mass loaded barrier and foil is likely to be very low (~0.1).

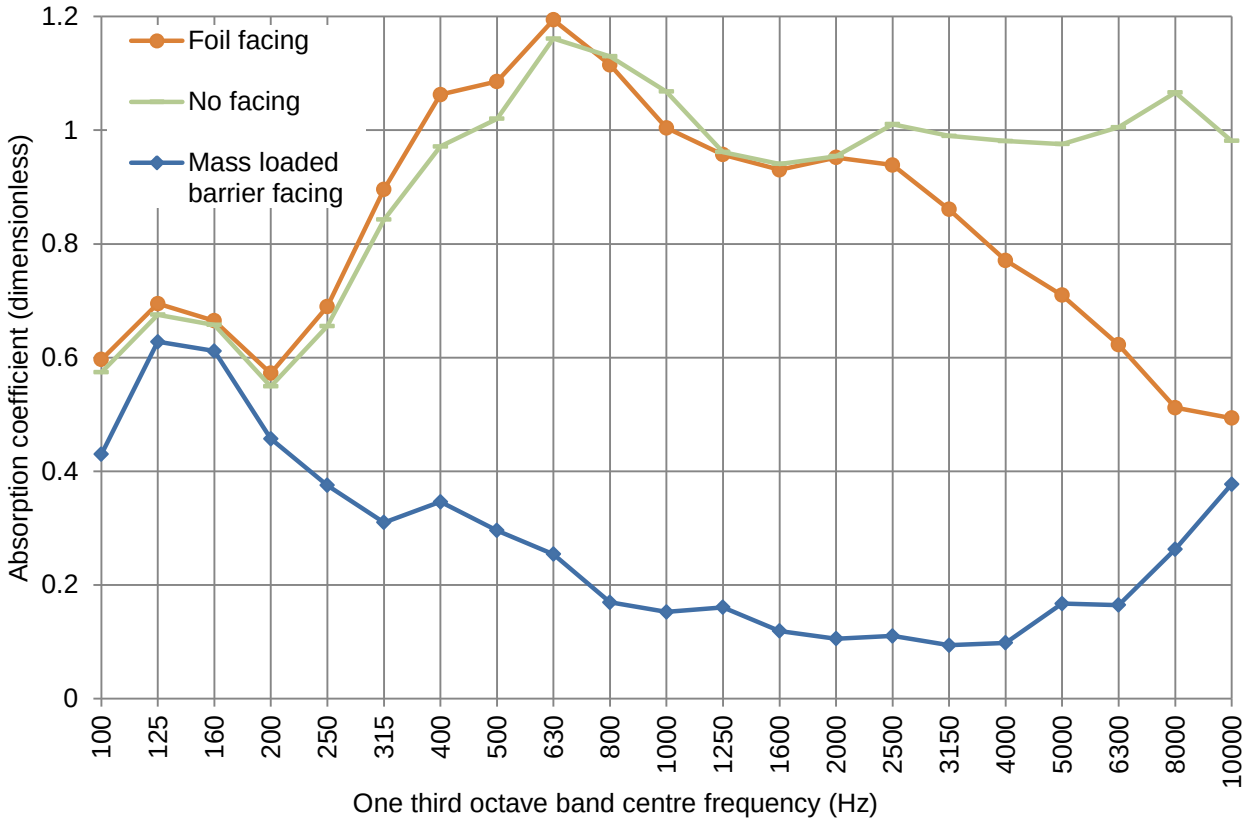

Figure 5.11 Effect of face sheets in sound absorption

To achieve a high absorption coefficient or maintain the foam absorption coefficient while achieving protection from dust, oil, chemicals and maintaining fire regulations a porous mesh material should be used. There are currently products in the market that meet this specification. An acoustic advantage can be achieved by using a mesh instead of a facing. Results obtained at RMIT [48] show a gain in performance with a facing (see Appendices, Figure 7.9)

5.3.4 Full factorial design versus fractional factorial design

Full factorial design should be used over fractional factorial design whenever possible. One major limitation of using full factorial design is the large number of experiments required to consider all factors at a multitude of levels. The main advantages were that both methods produce a powerful analysis and graphical representation of the significance of variables studied. Results obtained from DOE can be used to build a model to predict the response at different levels of factors.

5.4 Conclusions

Above 2kHz, the sound absorption coefficient of foam without foil maintains a constant coefficient of about 1. The absorption coefficient of foam with foil above 2kHz steadily drops to 0.5 at 10kHz. The sound absorption coefficients both with and without foil are the same up to 2kHz. When a thick mass loaded barrier was mounted on top of the foam there was a significant decrease in absorption. The thicker the face sheet the greater the reflection.

The significant design parameters that influence the NRC of Sorberbarrier® and the optimal settings to maximise the NRC are shown below.

- High level (94mm of foam)
- Low level (Outer layer of foam)

Full factorial design as an optimisation technique for acoustic absorption is found to be limited since the single number, NRC must be used. A means to find out the significant parameters in achieving an optimal sound absorption is very valuable. The optimal setting for these parameters would require further investigation using the OVAT method.

Chapter 6

6 Conclusions and Future Work

6.1 Introduction

The first section of this chapter draws together the main results and conclusions from this research and the second section proposes avenues for future investigations.

6.2 Conclusions

The aim of this project was to develop a fundamental understanding of how sound is transmitted through single leaf walls. Focussing on lightweight composite sandwich panels in the marine industry, this was accomplished by investigating each region of the STL curve and the lightweight noise treatments that maximised STL.

The material properties of composite sandwich panels were reviewed. It was concluded that material behaviour is not only dependent on physical properties but also on frequency. The two methods used to measure these properties were 'fixed-free' and 'free-free' beam boundary condition modal analyses. The disagreement between them was due to the fixed clamping increasing the flexibility of the beam to produce a lower Young's modulus than the 'free-free' method. There were also smaller discrepancies between loss factor measurements based on the method used.

Much of the work in the literature on STL through single leaf panels makes the assumptions of isotropy and homogeneity. Although a lot is understood about the transmission of sound through single leaf panels, an analytic method of accurately predicting the STL of composite sandwich panels is not currently available. Some methods give reasonable estimates over a restricted frequency range, generally in the mass law and damping controlled regions, but not in the coincidence region as this becomes extended due to the decrease in Young's modulus with increasing frequency.

A better understanding of how changes to a noise treatment product (Sorberbarrier®) affects the STL of the overall system is studied using a statistical model called fractional factorial design. It was found that the bonding method, and increasing the decouple layer of foam had the greatest impact on sound transmission class (STC). It was concluded that the addition of Sorberbarrier® to the composite sandwich panel increased the STC by up to double in the optimal case. This changed the characteristics of STL from that of a single leaf panel to a double leaf wall system. Fractional factorial design is effective as a STL optimisation technique when used as a pilot in an optimisation study. Although a perfect result cannot be guaranteed as only two levels are examined, the factors most likely to be significant are identified.

The statistical analysis of this work increased to full a factorial design to provide a better understanding of the factors involved in the sound absorption coefficient of Sorberbarrier®. The analysis clearly illustrated that a thicker foam and acoustically transparent facing of the foam layer produced the most significance increase in the noise reduction coefficient (NRC).

6.2.1 Optimal parameters

The primary aim of the project was to deliver an experimental analysis of the acoustic performance of composite sandwich panels with treatments to improve the sound transmission loss (STL). From testing existing constructions, literature review, analytical modelling and other statistical tools, a recommendation for a new panel with greater acoustic performance can be made.

The construction with optimal STL and absorption performance has been identified and compared with previous constructions. The design of absorption and STL for Sorberbarrer® require different parameters to be maximised therefore it must be established whether absorption or STL are more important in each application. Factor settings that maximise the STC are as follows-

- High level (Dimples)
- High level (Outer side of foam)
- High level (46mm)
- Low level (Pinned)
- High level (8kg/m²)
- High level (46mm)

Factor settings that maximise the NRC are as follows-

- High level (94mm of foam)
- Low level (Outer layer of foam)
- No effect (mass loaded barrier)

6.3 Future Work

The project used an analytical model to describe the STL through a composite sandwich panel which did not provide agreement with experimental STL in the coincidence region. More work should be performed to better describe the coincidence region of composite sandwich panels which have frequency dependent material properties.

Independent optimisation studies have been performed for STC and NRC with conflicting results. A more complex optimisation study should be performed to assess these two objectives simultaneously (perhaps weighted for their relative importance) to produce a single solution. A heavier weighting on the STL is proposed, this was suggested to be the more important in investigations of acoustics in the marine industry. Such a study should also include the constraints of mass and space as this is also important in the marine industry.

The effect that gluing and pinning have on the stiffness should be quantified as it is still unknown why pinning increases the STC compared to gluing. Since the protective facing had a negative effect on the absorption, further work should be done on a protective facing that increases the absorption as studies suggested. This was not carried out due to the resources available, but a recommendation for a particular mesh material was provided.

References

1. Davy, J.L., "Predicting the Sound Insulation of Single Leaf Walls: Extension of Cremer's model," *Journal of the Acoustical Society of America*, vol. 126, p. 1871-1877, 2009.
2. Bies, D.A. and C.H. Hansen, *Engineering Noise Control: Theory and Practice*, 4th edition, Spon Press, 2009.
3. Anders, S., "Sound Transmission Loss of Sandwich Panels," *Department of Mechanical Engineering*, University of Canterbury, Master's Thesis, Christchurch, New Zealand, 2010
4. Cremer, V.L., "Theorie der Schalldammung dunner Wande bei schragem Einfall," *Akustische Zeits*, p. 23-29, 1942.
5. Beranek, "Noise and Vibration Control," McGraw-Hill, 1971.
6. Ballagh, K.O., "Adapting Simple Prediction Methods to Sound Transmission of Lightweight Foam Cored Panels," *New Zealand Acoustics*, vol. 24, p. 24-28, 2010.
7. Moore, J. and Lyon, R.H., "Sound Transmission Loss Characteristics of Sandwich Panel Constructions," *Journal of the Acoustical Society of America*, vol. 89, p. 777-791, 1990.
8. Pollock, C.J., "Sound Transmission Loss of Alternative Construction Panels," *Department of Mechanical Engineering,* University of Canterbury, Master's Thesis, Christchurch, New Zealand, 1999.
9. Fahy, F., "Sound and Structural Vibration, Transmission and Response," Academic Press, 1985.
10. Lang, M.A. and Dym, C.L., "Optimal Acoustic Design of Sandwich Panels," *Journal of the Acoustics Society of America*, vol. 57, p. 1481-1487, 1975.
11. Wang, T., Li, S., and Nutt, S.R., "Optimal Design of Acoustical Sandwich Panels with a Genetic Algorithm," *Applied Acoustics*, vol. 70, p. 416-424, 2008.
12. Kurtze, G. and Watters B.G., "New Wall Design for High Transmission Loss or High Damping," *Journal of the Acoustical Society of America*, vol. 31, p. 739-738, 1959.
13. Wennhage, P., "Weight Optimization of Large Scale Sandwich Structures with Acoustic and Mechanical Constraints," *Journal of Sandwich Structures and Materials*, vol. 5, p. 253-265, 2003.
14. Bootten, R*., Yachting Developments Limited*, Personal interview, 2012, March.
15. Goujard, B., Sakout, A., and Valeau V., "Acoustic Comfort on Board Ships: An Evaluation Based on a Questionnaire," *Applied Acoustics*, p. 1063-1072, 2005.
16. Kim, H.M., Hong, S.Y., Kil, H.G., Song, J.H., Jung, J.D., Kim, N.S., "Using a Small-Scale Reverberation Chamber to Improve a Ship's Double Sandwich Panel Noise Attenuation Performance," *Noise Control Engineering Journal*, vol. 58, p. 636-645, 2010.

17. Naify, C.J., “Lightweight Acoustic Treatments for Aerospace Applications,” *Faculty of the USC Graduate School*, University of Southern California, PhD Thesis, p. 136, 2011.
18. Sagianis, J. and Suhr, J., “Vibration and Wave Number Characterization in Carbon-Fiber Sandwich Composite Structures,” *SPIE*, vol. 8342, p. 1-9, 2012.
19. Fuller, C.R. and Harne, R.L., “Passive Distributed Vibration Absorbers for Low Frequency Noise Control,” *Noise Control Engineering Journal*, vol. 58, p. 627-635, 2010.
20. Fuller, C.R. and Cambou, P., “An Active-Passive Distributed Vibration Absorber for Vibration and Sound Radiation Control,” *Journal of the Acoustical Society of America*, vol. 104, 1988.
21. Rajaram, S., Wang, T. and Nutt, S., “Inherently Quiet Honeycomb Sandwich Panel,” *International SAMPE Symposium and Exhibition*, vol. 50, p. 3001-2008, 2005.
22. Sharp, B.H., “Prediction Methods for the Sound Transmission of Building Elements,” *Noise Control Engineering*, vol. 11, p. 53-63, 1978.
23. “ASTM E756-05 Standard Test Method for Measuring Vibration - Damping Properties of Materials,” 2005, (Reapproved 2010).
24. Timoshenko, S.P., “On the Correction for Shear of the Differential Equation for Transverse Vibrations of Prismatic Bars,” *Philosophical Magazine*, vol. 6, p. 744-746, 1921.
25. Timoshenko, S.P., “On the Transverse Vibrations of Bars of Uniform Cross-Section,” *Philosophical Magazine*, vol. 6, p. 125-130, 1922.
26. Kaneko, T., “On Timoshenko's Correction for Shear in Vibrating Beams,” *Journal of Physics: Applied Physics*, vol. 8, p. 1927-1936, 1975.
27. Rindel, J.H., “Dispersion and Absorption of Structural-Borne Sound in Acoustically Thick Plates,” *Applied Acoustics*, vol. 41, p. 97-111, 1994.
28. Nilsson, A.C., Wave Propagation in and Sound Transmission through Sandwich Plates. Jornal of Sound and Vibration, 1990. 138(1): p. 22.
29. Nilsson, E. and Nilsson, A.C., “Prediction and Measurement of some Dynamic Properties of Sandwich Structures with Honeycomb and Foam Cores,” *Journal of Sound and Vibration*, vol. 251, p. 409-430, 2002.
30. Fung, Y.C., “Foundations of Solid Mechanics,” Englewood Cliffs, 1965.
31. Phillips, T., “Sound Transmission Loss of Sandwich Panels,” *Department of Mechanical Engineering*, University of Canterbury, Christchurch, Master’s Thesis New Zealand, 2012.
32. Trevathan, J., “Sound Transmission in Marine Craft,” *Department of Mechanical Engineering,* University of Canterbury, Christchurch, New Zealand, 2002.

33. Feng, L. and Kumar, S. “On Application of Radiation Loss Factor in the Prediction of Sound Transmission Loss of Honeycomb Panel,” *Acoustical Analysis of a General Network of Multi-port Elements*, Stockholm, Sweden, 2011.
34. Cambridge, J.E., “An Evaluation of Various Sound Insulation Programs and their use in the Design of Silent Rooms,” *Department of Civil and Environmental Engineering,* Chalmers University of Technology, Master’s Thesis, 2006.
35. Ballagh, K.O., “Accuracy of Prediction Methods for Sound Transmission Loss,” *International Congress and Exposition on Noise Control Engineering*, 2004.
36. Davy, J.L., “A Model for Predicting the Sound Transmission Loss of Walls,” *Australian Vibration and Noise Conference* 1990, p. 23-27, Canberra, Australia, 1990.
37. Nilsson, A.C., “Sound Transmission through Single Leaf Panels,” *Chalmers University of Technology*, Goteborg, Sweden, 1974.
38. Zhou, R., “Sound Transmission Loss of Composite Sandwich Panels,” *Auburn University*, p. 210, PhD Thesis, Auburn, 2009.
39. “ISO 15186-1 Acoustics - Measurement of Sound Insulation in Buildings and of Building Elements using Sound Intensity,” *Part 1: Laboratory Measurements*, Switzerland, 2000.
40. “Sorberbarrier ALR Information Page,” *Pyrotek Noise Control*, 2012.
41. Bolton, J.S., Shiau, N.M. and Kang, Y.L., “Sound Transmission through Multi-Panel Structures lined with Elastic Porous Materials,” *Journal of Sound and Vibration*, vol. 191, pp. 317-346, 1996.
42. Mathews, P.G., *Design of Experiments*, American Society for Quality, Tony, W.A., 2005.
43. White, R., “Fabrics for Acoustic Control,” *Technical Textiles*, Unpublished work, 1993.
44. Parkinson, J.P., “Acoustic Absorber Design,” *Department of Mechanical Engineering*, University of Canterbury, Master’s Thesis, Christchurch, p. 102, 199.
45. “Sorberbarrier ALR Data Sheet,” *Pyrotek Noise Control*, 2012.
46. Kim, J., “Flow Resistivity Effect on Sound Absorption and Sound Transmission of Film-faced Foam,” *Noise-Con*, Nevada, 2007.
47. “ISO 354-2003 Acoustics - Measurement of Sound Absorption in a Reverberation Room,” 2003.
48. “Soundmesh® G8,” *Megasorber*, http://www.megasorber.com/soundproofing-products, 2011

7 Appendices

PRODUCT SPECIFICATIONS

PRODUCT NAME	TOTAL THICKNESS (mm)	CONSTRUCTION Absorptive layer(mm)/Mass barrier(Kg)/Decoupler(mm)	SHEET SIZE ** (metres)	OPERATING TEMPERATURE RANGE (°C)	THERMAL CONDUCTIVITY (K)
Sorberbarrier ALR20/4.5	20	ALR12/4.5/06	1.3 x 1.0 and 1.3 x 2.2	-40 to100 (Continuous) -40 to 120 (Intermittent)	0.033W/mK*
Sorberbarrier ALR25/4.5	25	ALR12/4.5/12	1.3 x 1.0 and 1.3 x 2.2		
Sorberbarrier ALR32/4.5	32	ALR25/4.5/06	1.3 x 1.0 and 1.3 x 2.2		
Sorberbarrier ALR32/8.0		ALR25/8.0/06	1.3 x 1.0		
Sorberbarrier ALR50/4.5	50	ALR25/4.5/25	1.3 x 1.0 and 1.3 x 2.2		
Sorberbarrier ALR50/8.0		ALR25/8.0/25	1.3 x 1.0		
Sorberbarrier ALR50/4.5	75	ALR50/4.5/25	1.3 x 1.0		
Sorberbarrier ALR50/8.0		ALR50/8.0/25	1.3 x 1.0		

Tolerances: Weight: +/- 0.5Kg; Thickness: +/- 3mm ; Length and Width: -0 to +5mm
* Typical value for Polyurethane foam - Polyurethane handbook: Chemistry, Raw Materials, Processing, Application, Properties 2nd edition
**Useable width is specified. Some surface coverings such as foils, films or fabric may overhang the useable width.

SELF ADHESIVE TAPES SPECIFICATIONS

CODE	DESCRIPTION	OPERATING SERVICE TEMPERATURE °C
Alpha – **A**	Premium high performance transfer tape suitable for most applications.	-10 to 110
Alpha - **A1**	Versatile, resilient, high tack adhesive with excellent bonding strength to a wide range of substrates.	-10 to 80
Alpha - **A2**	Scrim reinforced acrylic backing for extra strength and high durability.	-10 to 60

Under extreme temperature conditions or where the substrate surfaces cannot be free from contaminants, mechanical fixing will be required on vertical surfaces. For all inverted installations including ceiling installations, mechanical fixing must be done in addition to PSA adhesion.

When ordering products with adhesive backing, please specify your choice of tape with the appropriate code **A, A1** or **A2** as Sorberbarrier ALR32**A**/4.5, Sorberbarrier ALR32**A1**/4.5 or Sorberbarrier ALR32**A2**/4.5. Unless otherwise stated, the standard adhesive backing supplied is premium grade (Alpha - **A**)

FLAMMABILITY PROPERTIES

TEST METHOD	INDEX	RESULTS	DESCRIPTION
AS 1530.3 1999 (Report No. 7-564774-CV)	Ignitability Spread of Flame Heat evolved Smoke Developed	0 0 0 1	Method for fire tests on building materials, components and structures. Complies
ISO 4589.2 - 1996 (Report No. 7-547912-CV)	Limiting Ambient Oxygen Index (LOI)	24.9% *	Oxygen Index in accordance with ISO-4589-2 plastics determination of burning behaviour by oxygen index-part 2 ambient temperature.
BS EN ISO 4589.3 - 1996 (Report No. 192822)	Limiting Elevated Oxygen Index (LOI)	21.5%	Oxygen Index in accordance with ISO-4589-3 plastics determination of burning behaviour by oxygen index-part 3 elevated temperature @ 60°C.
EN ISO 9094-1:2003 (Report No. 192822) Summary Report	Classification/Compliance	Complies	Complies to Directive 94/25/EC and EN ISO 9094-1:2003
FMVSS-302	Burn Rate - mm/min	Self Extinguishing	Automotive burn rate test. Complies

* Results for Sorberfoam ALR

Figure 7.1 Sorberbarrier® product specification [45]

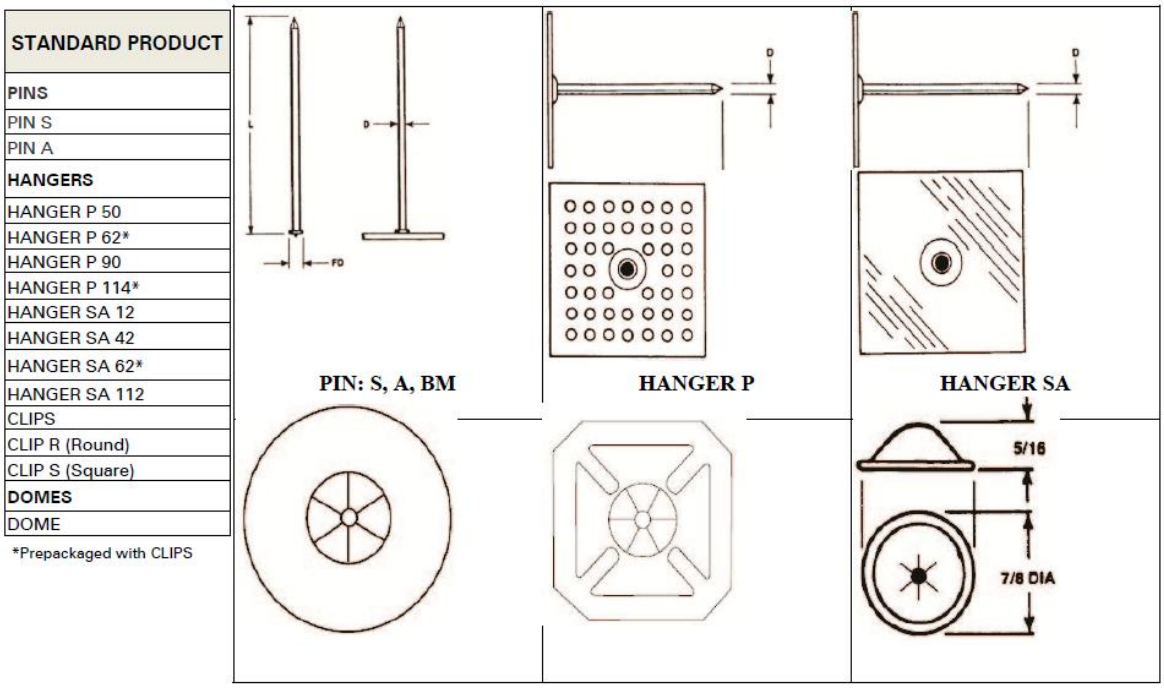

Figure 7.2 Pin drawings [45]

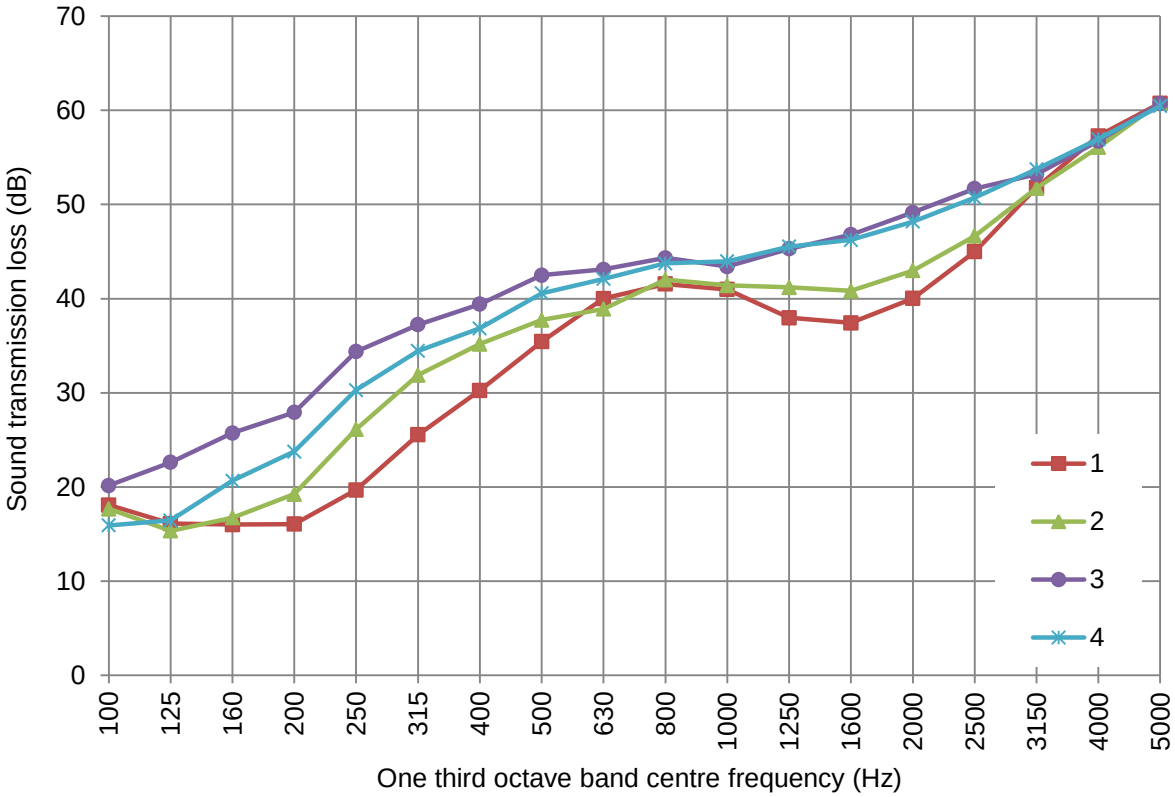

Figure 7.3 DOE STL runs 1 to 4

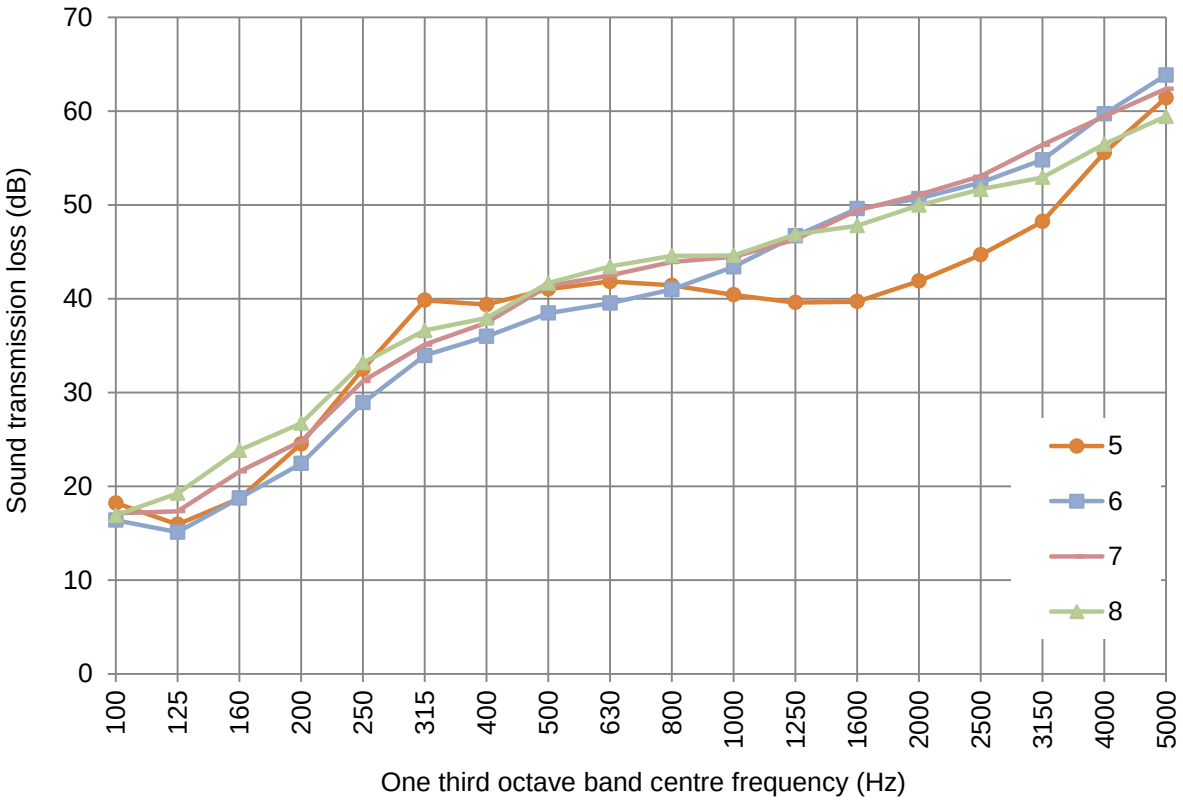

Figure 7.4 DOE STL runs 5 to 8

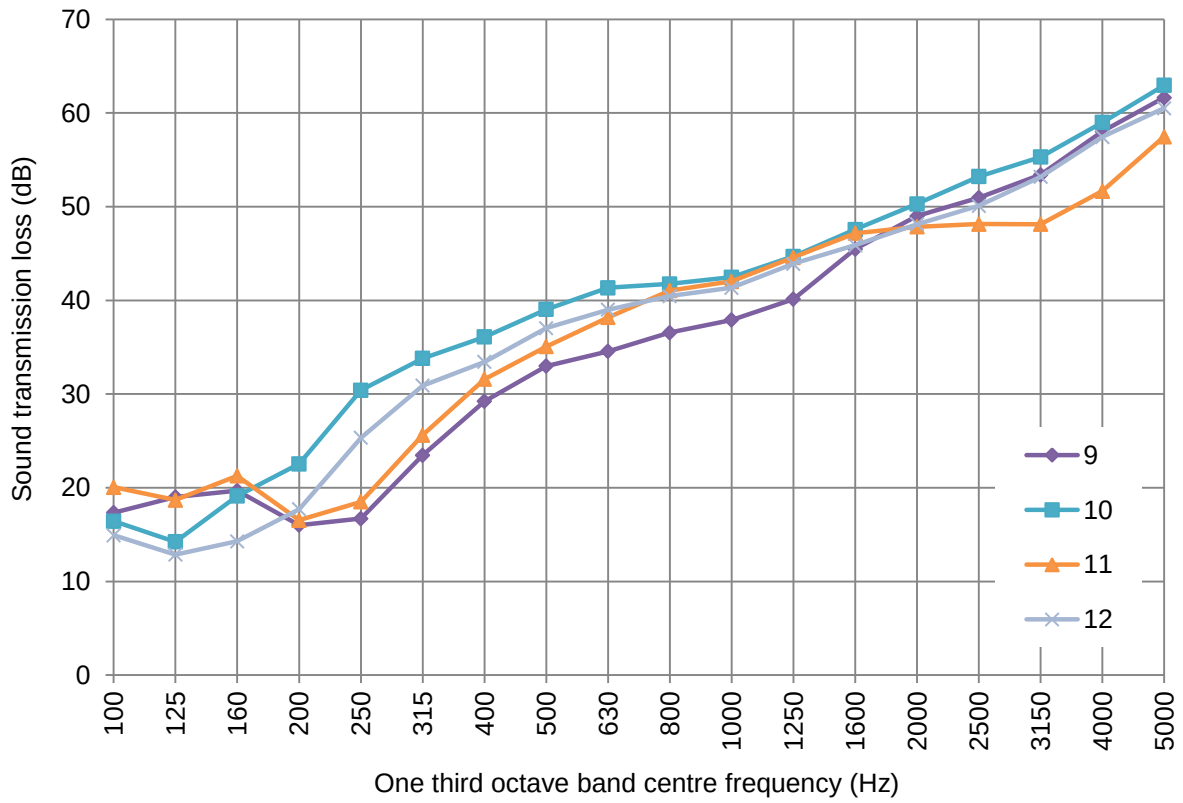

Figure 7.5 DOE STL runs 13 to 16

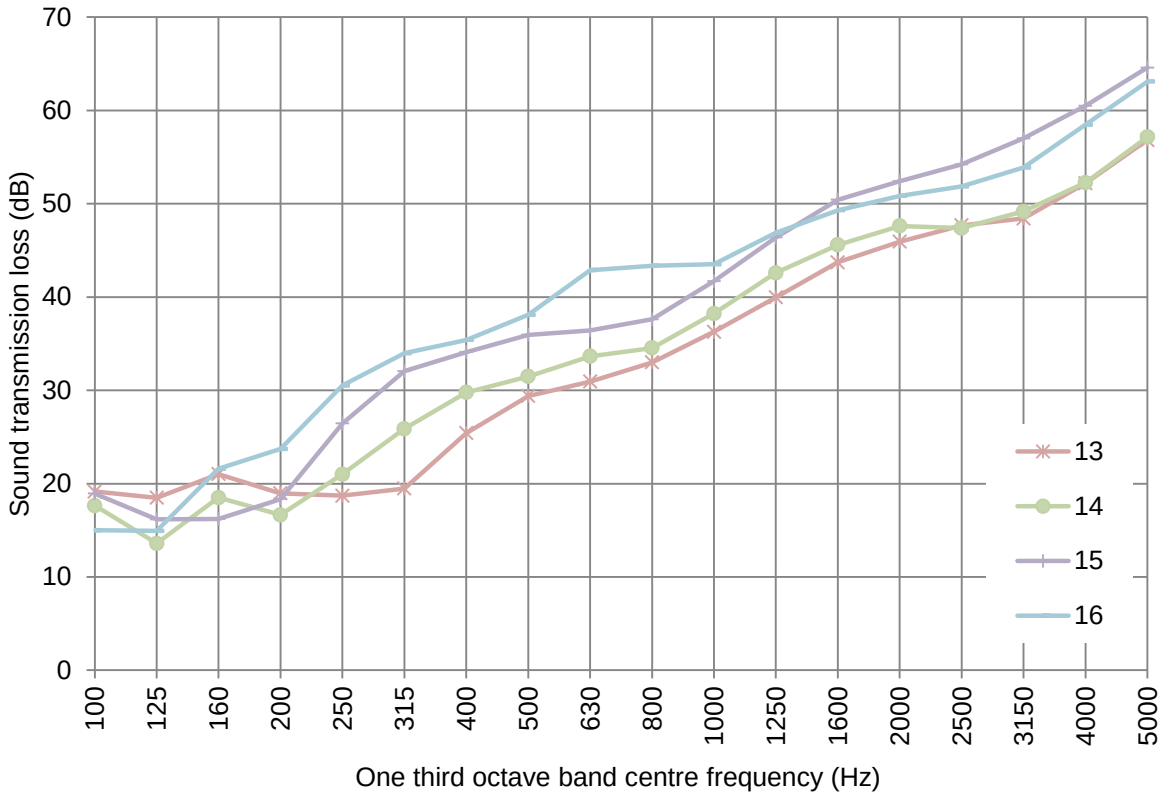

Figure 7.6 DOE STL runs 9 to 12

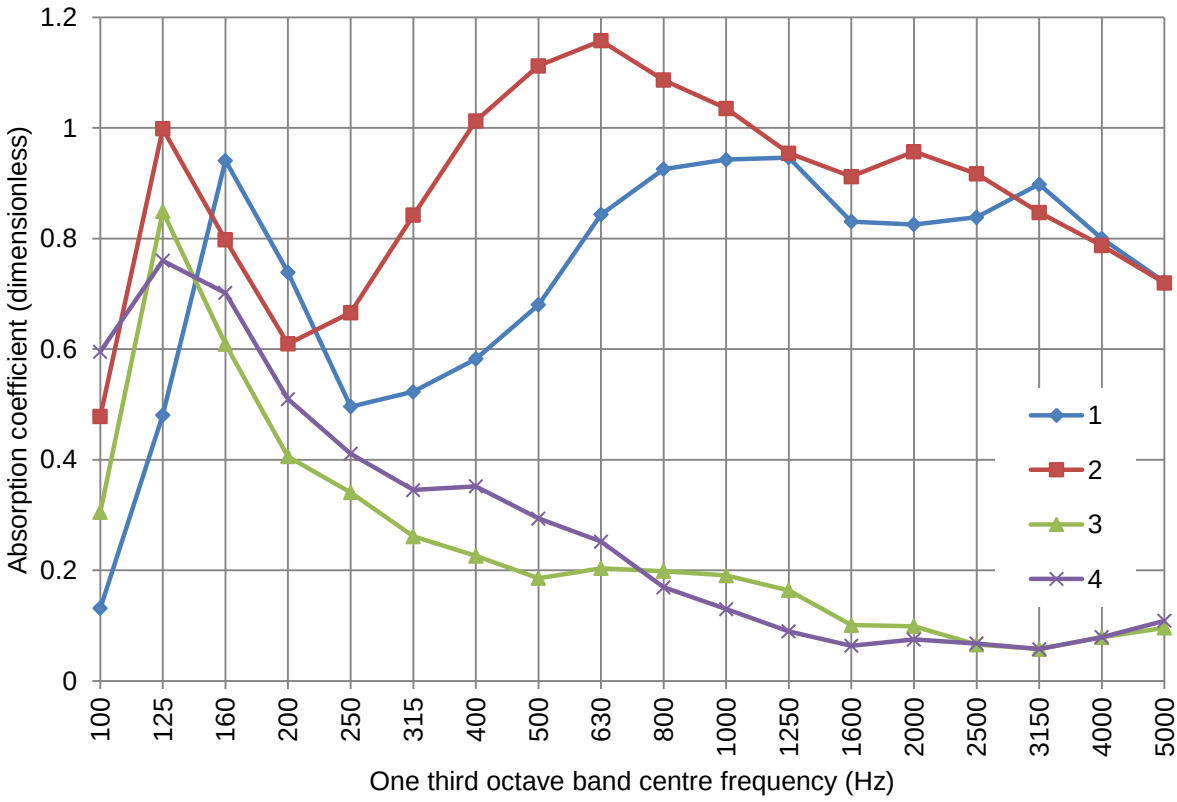

Figure 7.7 DOE sound absorption runs 1 to 4

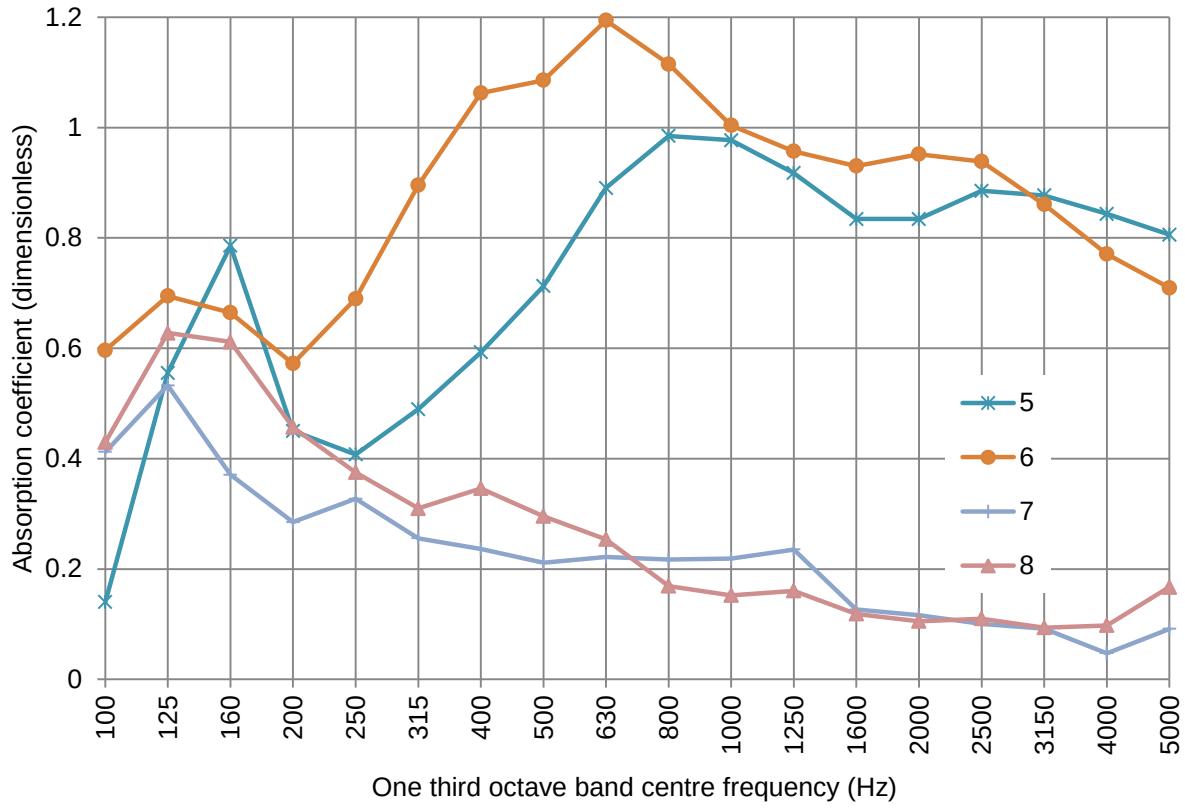

Figure 7.8 DOE sound absorption runs 5 to 8

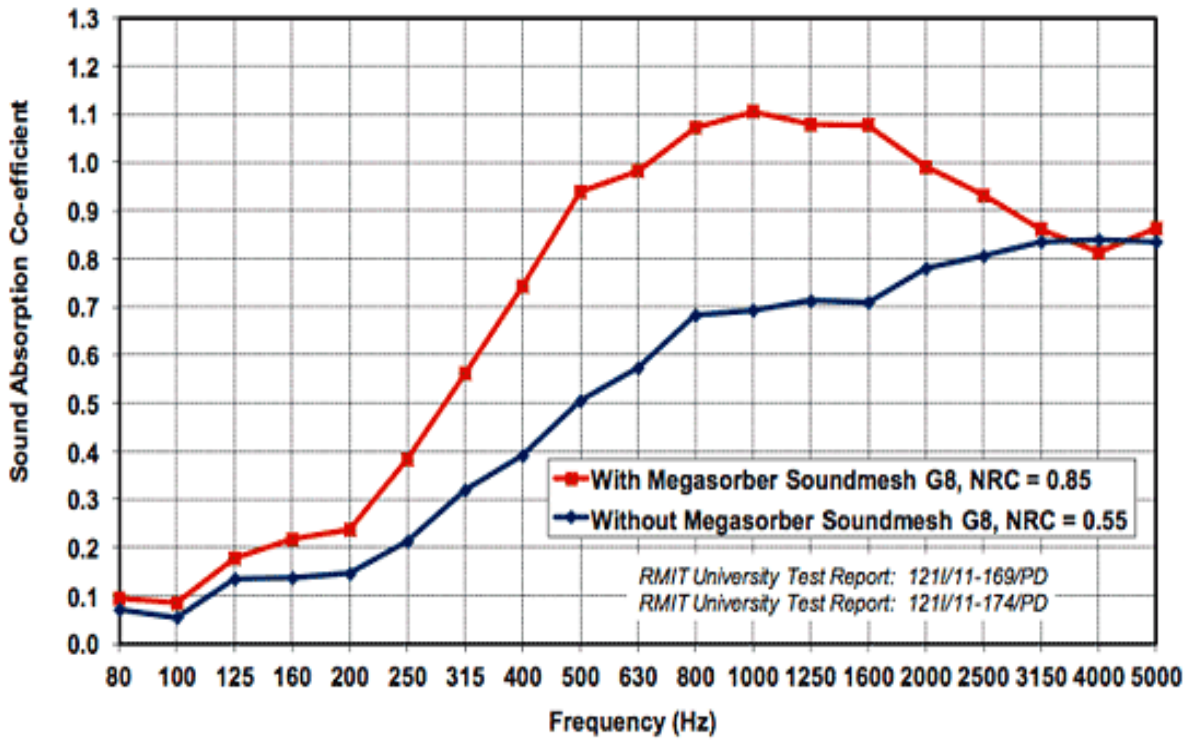

Figure 7.9 Sound absorption coefficient of 25mm thick acoustic foam with and without Soundmesh® [48]

Figure 7.10 Acoustic face mesh - Soundmesh® [48]